ROLES OF THE MITOCHONDRINAL SINGLE-STRANDED DNA-BINDING PROTEIN AT THE MITOCHONDRIAL DNA REPLICATION FORK

By

Marcos Túlio Oliveira

A DISSERTATION

Submitted to
Michigan State University
in partial fulfillment of the requirements
for the degree of

DOCTOR OF PHILOSOPHY

Genetics

2011

ABSTRACT

ROLES OF THE MITOCHONDRIAL SINGLE-STRANDED DNA-BINDING PROTEIN AT THE MITOCHONDRIAL DNA REPLICATION FORK

By

Marcos Túlio Oliveira

The mitochondrion is one of the most important and versatile eukaryotic organelles, responsible for the bulk of energy production in the cell, and involved in apoptosis, signaling, cellular differentiation, and control of cell cycle and cell growth. It possesses its own genome, the mitochondrial DNA (mtDNA), which encodes polypeptides that are essential subunits of the complexes that form the energy-producing respiratory chain. mtDNA replication is thus an important process that maintains proper mitochondrial function, accomplished by the coordinated action of three main protein components that work directly at the mtDNA replication fork: DNA polymerase γ (pol γ), which catalyzes DNA synthesis *per se*; mtDNA helicase (also known as Twinkle), which unwinds double-stranded DNA to provide a single-stranded DNA (ssDNA) substrate for pol γ; and mitochondrial single-stranded DNA-binding protein (mtSSB), which binds ssDNA to protect it against damage and to coordinate the functions of pol γ and mtDNA helicase. The general aim of my thesis work was to examine the roles of mtSSB at the mtDNA replication fork by investigating the biochemical and physiological performance of a group of mtSSB variants bearing alanine substitutions or deletions of amino acid residues conserved across animal species. We purified 9 recombinant human mtSSB (*Hs*mtSSB) proteins, which maintained their homotetrameric state and bound ssDNA with only slightly different affinities. However, they exhibited very distinct capacities to stimulate the DNA polymerase activity of human pol γ (*Hs*pol γ) and the DNA unwinding activity of human mtDNA helicase

(*Hs*mtDNA helicase) *in vitro*. Whereas the variants *Hs*mtSSBΔN (Δ1-9), ΔC (Δ126-132) and ΔNΔC (Δ1-9, Δ126-132) stimulated *Hs*pol γ ~2-fold higher than *Hs*mtSSBwt (wild type), the variants *Hs*mtSSBloop23 (Δ51-59), α1 (Y83A/Q84A) and loop45-1 (Y100A/G101A/E102A) exhibited an ~40% reduction as compared to *Hs*mtSSBwt. We developed a molecular model of mtSSB-pol γ interaction that explains these and other biochemical data published previously, and that suggests how a group of *Hs*pol γ mutations associated with various human diseases may disturb such interactions. Interestingly, the variants *Hs*mtSSBloop12 (E33A/G34A/K35A) and loop45-2 (K106A/N107A/N108A), which did not exhibit altered capacity to stimulate *Hs*pol γ, were indeed defective in stimulating *Hs*mtDNA helicase, presumably by failing to interact with its C-terminal tail. We also evaluated mtSSB in *Drosophila* S2 cells by knocking down the endogenous protein (*Dm*mtSSB) and expressing variants of *Dm*mtSSB equivalent to those of *Hs*mtSSB. Endogenous *Dm*mtSSB knockdown and overexpression of *Dm*mtSSB variants caused reduction of mtDNA copy number under conditions of mitochondrial homeostasis, and impeded mtDNA repletion during recovery from treatment with ethidium bromide, when mtDNA replication is stimulated *in vivo*. Preliminary analysis of mtDNA replication intermediates from cells overexpressing *Dm*mtSSB variants indicated that the defects in mtDNA replication are associated with the binding sites of the transcription termination factor DmTTF. Our findings suggest that mtSSB uses a repertoire of structural elements to interact functionally with pol γ and mtDNA helicase, to guarantee proper mtDNA replication in animal cells. Understanding the mechanisms of mtDNA replication via further biochemical, physiological and structural studies will provide valuable insights into the processes in which the mitochondrion is the key regulator in eukaryotic cells.

ACKNOWLEDGMENTS

I would like to thank first my thesis advisor, Dr. Laurie Kaguni, for the support and encouragement towards my training as a scientist. Although I still consider myself a geneticist, working with Laurie has helped me demystify the "world of biochemistry, enzymology and structural biology", and most importantly has established the basis for my aspiring future career in mitochondrial biology.

To the members of my committee, who have contributed with ideas and suggestions for the work presented in this thesis: Dr. David Arnosti, Dr. Bill Henry, Dr. Kyle Miller and Dr. Jim Geiger. I also would like to acknowledge Dr. Jon Kaguni for the discussions in our group meetings; Dr. Barb Sears and Jeannine Lee, director and secretary of the Genetics Program, respectively, for the endless administrative support; and Dr. Zach Burton for the help provided during my preparation for the comprehensive exams.

To all the former and current members of the Kaguni lab, who have been part of my academic and personal life for the last five years. I would like to thank Fernando Rosado-Ruiz, Roberto Negro, Carol Farr, Tawn Ziebarth, Yuichi Matsushima, Timo Kauppila, Johanna Lampinen, Magdalena Makowska-Grzyska, Magda Felczak, Minyoung So, Sundari Chodavarapu, Greg Farnum, and the numerous undergraduate students that have worked in the lab.

To the great people that I have had the pleasure to become friends with once I moved to Michigan (those that thankfully kept me distracted from my work): Irwin (my best man), Yvonne, Payam, Sabrina, Marcelo, Jacobo, Monica, Agustín, among many others.

To those that I had to leave painfully in order to face the Ph.D. challenge: in particular, my family – my mom Vilma, who has been my great supporter and friend, my brothers Paçoca and Teté, and my dad Zé Goiaba. I would like to give a special acknowledgment to my grandma Luzia and my uncle Cecílio, who passed away during my time away from home.

I would like to end by thanking immensely my new family, my wife Emily, and our girls Jambi and Orchid, for being by my side all this time. Thanks for taking care of me when I was tired, for feeding me when I was hungry, for being patient when I was cranky, for being my best friends, and for sharing your love with me every day of our lives. This path would have been much tougher to walk without all of you.

PREFACE

"Mitochondria are ubiquitous throughout the eukaryotic domain: with very few exceptions, eukaryotes cannot exist without them." (Burger *et al.* 2003)

The present thesis document comprises a compilation of scientific papers, both published and in-preparation, in which I have participated as the main experimentalist. The research conducted in Dr. Laurie Kaguni's lab involves the first steps (replication and transcription of mitochondrial DNA) of a complex and important cellular process called mitochondrial biogenesis. The mitochondrion is the organelle responsible for energy production in eukaryotic cells, and relies on the function of its five multi-subunit respiratory chain complexes to accomplish this with remarkable efficiency. In addition, the mitochondrion is involved in many other important cellular pathways that are related directly or indirectly to energy production, such as apoptosis, signaling, cellular differentiation, and the control of cell cycle and cell growth (McBride *et al.* 2006). Thus, it is understandable that mitochondrial (dys)function has been implicated in several human diseases, ranging from classical encephalomyopathies to complex and neurodegenerative disorders, such as diabetes, deafness and Parkinson's. Mutations in mtDNA-encoded genes, believed to cause increased production of reactive oxygen species by the mitochondrion, have also implicated this organelle in the aging process, and opened the path for a broad field of research.

Chapter 1 is a review of the literature in which Dr. Laurie Kaguni, Dr. Rafael Garesse (Universidad Autónoma de Madrid) and I explore the published research on mtDNA transactions (replication, repair, recombination and transcription) that makes use of animal models to provide a synthesis of the scientific advances in the field and to discuss the direction of future studies and

their relation to human diseases and ageing. Although mtDNA replication is the main focus of this thesis, this process is intimately associated with other mtDNA transactions. Chapter 1 thus serves as an extended introduction to my thesis work, and provides an essential background to some of the important questions in current mitochondrial biology. This work entitled "Animal models of mitochondrial DNA transactions in disease and ageing" was published in 2010 in Experimental Gerontology, volume 45, pages 485-502 (see Appendix 1 for complete list of publications).

Chapter 2 consists of a methods paper on the purification of recombinant mtDNA replication proteins. We focused on the long-standing protocols that have been used successfully in Dr. Laurie Kaguni's lab for purifying recombinant forms of DNA polymerase γ (pol γ) and the mitochondrial single-stranded DNA-binding protein (mtSSB) of *Drosophila melanogaster* and humans. As noted in Chapters 3-5, protein preparations of high yield and purity are essential for the biochemical characterization of mtSSB, pol γ and mtDNA helicase. This work entitled "Comparative purification strategies for *Drosophila* and human mitochondrial DNA replication proteins: DNA polymerase γ and mitochondrial single-stranded DNA-binding protein" was published in 2009 in the "Mitochondrial DNA Methods and Protocols" issue of Methods in Molecular Biology, volume 554, pages 37-58.

In Chapter 3, I present my first first-author research article while working in Dr. Laurie Kaguni's lab. The paper addresses biochemically the question of whether the termini of human mtSSB are involved in stimulating its partners at the mtDNA replication fork, pol γ and mtDNA helicase. The work shows for the first time the *in vitro* stimulation of the DNA polymerase activity of human pol γ by the human mtSSB, and suggests differences between the human and *Drosophila* systems. The conditions for the DNA polymerase stimulation assays reported here

were used in the research work published by Dr. Charles McHenry's group (University of Colorado), in which I am a co-author, as part of a screening program for specific inhibitors of DNA replicases from Gram-positive and Gram-negative bacteria ("Parallel multiplicative target screening against divergent bacterial replicases: identification of specific inhibitors with broad spectrum potential", Biochemistry 2010, volume 49, pages 2552-2562). Chapter 3 also sets the foundation for the biochemical experimentation reported in Chapter 4. "Functional roles of the N- and C-terminal regions of the human mitochondrial single-stranded DNA-binding protein" was published in 2010 in PLoS ONE, volume 5, article e15379.

In Chapter 4, a new set of mtSSB variants is examined biochemically and physiologically. We identified recombinant human variants with defects in stimulating pol γ and mtDNA helicase, and showed that the equivalent *Drosophila* proteins promote mtDNA depletion when expressed in S2 cells under various physiological conditions. We suggest new mechanisms of regulation of pol γ and mtDNA helicase by mtSSB in replicating mtDNA. This chapter, entitled "Reduced stimulation of recombinant pol γ and mtDNA helicase by mtSSB variants correlates with defects of mtDNA replication in animal cells", is part of a manuscript that will be submitted for publication in the near future.

The perspectives and future directions of the work presented in Chapters 3 and 4 are discussed in Chapter 5, in which I present three lines of experimentation: 1) a molecular model of physical interaction between pol γ and mtSSB that explains some of the biochemical and physiological defects observed with mtSSB variants, and that gives insights into the molecular mechanisms of a group of pol γ mutations associated with various human diseases; 2) biochemical data showing that the C-terminally truncated form of the human mtDNA helicase cannot interact functionally with mtSSB (in collaboration with Roberto Negro, who was a

visiting student from the Università di Bari); and 3) 2D-agarose gel electrophoresis studies of mtDNA replication intermediates from *Drosophila* cells with various defects in mtDNA replication. I hope these lines of experimentation can be pursued by a future member of the lab, to help enhance our understanding of the roles of mtSSB in mtDNA replication of healthy cells and under disease states.

TABLE OF CONTENTS

LIST OF TABLES

LIST OF FIGURES

LIST OF ABBREVIATIONS

3'-UTR – 3' untranslated region

ATP – adenosine tri-phosphate

BER – base excision repair

COX – cytochrome *c* oxidase

$CuSO_4$ – copper sulfate

CV – column volumes

*Dm*mtDNA helicase – *Drosophila melanogaster* mtDNA helicase

*Dm*mtSSB – *Drosophila melanogaster* mitochondrial single-stranded DNA-binding protein

*Dm*mtSSB$_{endo}$ – endogenous *Dm*mtSSB protein from S2 cells

*Dm*pol γ – *Drosophila melanogaster* DNA polymerase γ

DmTTF – mitochondrial transcription termination factor of *Drosophila melanogaster*

DNA – deoxyribonucleic acid

DSB – double-strand breaks

dsDNA – double-stranded DNA

dsRNA – double-stranded RNA

*Ec*SSB – *Escherichia coli* single-stranded DNA-binding protein

EtBr – ethidium bromide

GMSA – gel mobility shift assay

HR – homologous recombination

*Hs*mtDNA helicase – human mtDNA helicase

*Hs*mtSSB – human mitochondrial single-stranded DNA-binding protein

HSP1 – heavy mtDNA strand promoter 1

HSP2 – heavy mtDNA strand promoter 2

*Hs*pol γ – human DNA polymerase γ

IP subdomain – intrinsic processivity subdomain of DNA polymerase γ

KCl – potassium chloride

K_d – constant of dissociation

KPO_4 – potassium phosphate

LSP – light mtDNA strand promoter

mtDNA – mitochondrial DNA

MTERF1 – mitochondrial transcription termination factor 1

MTERF2 – mitochondrial transcription termination factor 2

MTERF3 – mitochondrial transcription termination factor 3

mtSSB – mitochondrial single-stranded DNA-binding protein

NaCl – sodium chloride

NCR – non-coding region

NHEJ – non-homologous end-joining.

NO – nitric oxide

nt – nucleotide

OB-fold – oligonucleotide/ oligosaccharide-binding domain

OGG1 – 8-oxoguanine glycosylase

O_H – origin of heavy (leading) mtDNA strand synthesis

O_L – origin of light (lagging) mtDNA strand synthesis

OXPHOS – oxidative phosphorylation system

PCR – polymerase chain reaction

PD – Parkinson's disease

PEO – progressive external ophthalmoplegia

pol γ – DNA polymerase γ

pol γ-α – catalytic subunit of DNA polymerase γ

pol γ-β – accessory subunit of DNA polymerase γ

qPCR – quantitative real-time polymerase chain reaction

RIs – replication intermediates

RITOLS – RNA incorporated throughout the lagging strand

RNA – ribonucleic acid

ROS – reactive oxygen species

RPA – replication protein A

S2 – *Drosophila melanogaster* Schneider cell line 2

SDS-PAGE – sodium dodecyl-sulfate – polyacrylamide gel electrophoresis

*Sf*9 – *Spodoptera frugiperda* cell line 9

SSB – single-stranded DNA-binding protein

ssDNA – single-stranded DNA

T4 gp32 – bacteriophage T4 gene 32 single-stranded DNA-binding protein

T7 gp2.5 – bacteriophage T7 gene 2.5 single-stranded DNA-binding protein

T7 gp4 – bacteriophage T7 gene 4 primase-helicase

TFAM – mitochondrial transcription factor A

Twinkle – mtDNA helicase

CHAPTER 1

ANIMAL MODELS OF MITOCHONDRIAL DNA TRANSACTIONS IN DISEASE AND AGEING

Summary

Mitochondrial DNA (mtDNA) transactions, processes that include mtDNA replication, repair, recombination and transcription constitute the initial stages of mitochondrial biogenesis, and are at the core of understanding mitochondrial biology and medicine. All of the protein players are encoded in nuclear genes: some are proteins with well-known functions in the nucleus, others are well-known mitochondrial proteins now ascribed new functions, and still others are newly discovered factors. In this article we review recent advances in the field of mtDNA transactions with a special focus on physiological studies. In particular, we consider the expression of variant proteins, or altered expression of factors involved in these processes in powerful model organisms, such as *Drosophila melanogaster* and the mouse, which have promoted recognition of the broad relevance of oxidative phosphorylation defects resulting from improper maintenance of mtDNA. Furthermore, the animal models recapitulate many phenotypes related to human ageing and a variety of different diseases, a feature that has enhanced our understanding of, and inspired theories about, the molecular mechanisms of such biological processes.

Introduction

In animals, the mitochondrial DNA (mtDNA) is a small, compact, circular molecule that encodes 13 essential polypeptides, all of which are subunits of the mitochondrial oxidative phosphorylation system (OXPHOS). Animal mtDNA also encodes the RNA components of the mitochondrial translational system, which include 22 transfer RNAs and 2 ribosomal RNAs (Figure 1). As with all genetic material, the information encoded in mtDNA must be read and interpreted correctly for proper function of the eukaryotic cell, and transmitted accurately as these cells and whole organisms reproduce. These processes, comprising the initial stages in mitochondrial biogenesis, involve mtDNA replication, repair, recombination and transcription, and are defined herein as mtDNA transactions. The factors required for these transactions (Table 1), along with ~1500 other polypeptides found in the mitochondrion, are encoded by the nuclear DNA (Wallace 2005) and when their genes are mutated, absent or overexpressed they may cause severe mitochondrial dysfunctions, leading to diseases and ageing. Despite rearrangements in the order of the genes encoded in the mtDNA that are commonly found in different animal taxa (Boore 1999), the overall structure and gene content of the genome and the proteins required for mtDNA transactions are largely conserved, offering scientists the opportunity to use animal models to understand mitochondrial biology and medicine.

Links between mitochondrial dysfunction and human disease-related states and with ageing have become increasingly evident in the last few years as research on cancer, diabetes, neurodegenerative disorders and premature ageing progresses (Wallace and Fan 2009). Interestingly, many mitochondrial disorders exhibit a delayed onset and progressive course, and result in many of the same clinical manifestations that are observed in age-related diseases (Druzhyna et al. 2008). This and other data lend support to the mitochondrial theory of ageing

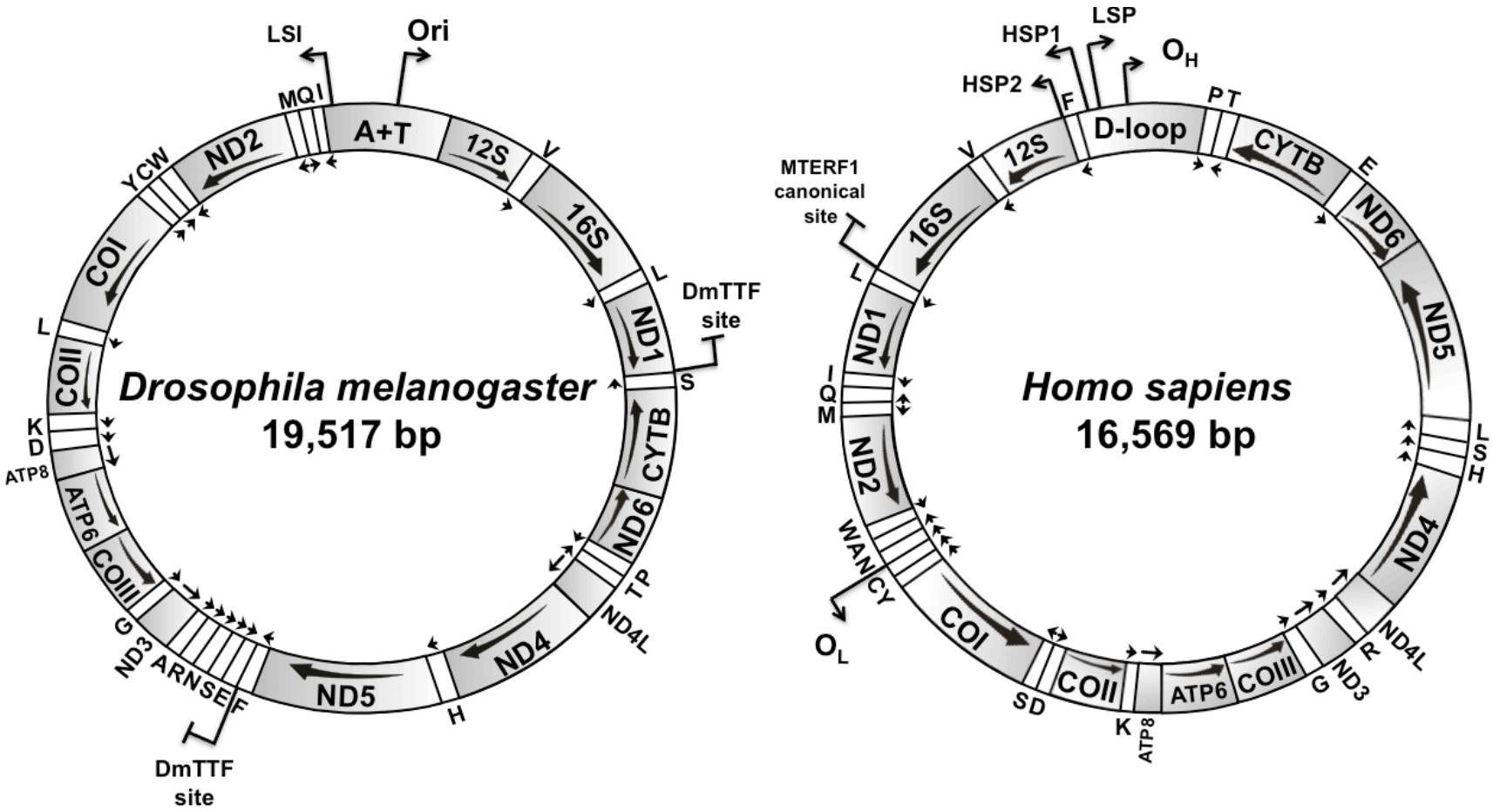

Figure 1. Schematic representation of *Drosophila* and human mtDNA. These genomes represent a typical gene organization found in insect and mammalian mtDNAs, respectively. The major non-coding regions of mtDNA, denoted as "A+T" for *Drosophila* and "D-loop" for human, are the regions where most sequence variation is found among animal species. The arrows below each gene indicate the direction of transcription. tRNA genes are indicated by one-letter symbols, and the 12S and 16S rRNA genes appear as 12S and

16S, respectively. In the fruitfly genome: Ori, origin of replication (initiation of leading strand synthesis); LSI, initiation of lagging strand synthesis, according to Goddard and Wolstenholme (1980). In the human genome: O_H, origin of heavy (leading) strand synthesis; O_L, origin of light (lagging) strand synthesis, according to the strand-displacement model of mtDNA replication; LSP, light strand promoter; HSP1 and 2, heavy strand promoters 1 and 2. Only the canonical binding site for MTERF1 is shown; for more details on other binding sites, see the text and Hyvärinen *et al.* (2007).

Table 1. Proteins involved in mtDNA transactions and their functions

Transaction	Protein	Function
Replication	TFAM*	Nucleoid organization; compaction and packing of mtDNA
	pol γ	DNA polymerase and exonuclease
	mtDNA helicase	dsDNA unwinding
	mtSSB	ssDNA-binding; stimulation of pol γ and mtDNA helicase activities
	RNase H1	primer formation and/ or processing
	Top1mt	vertebrate topoisomerase type IB
	Top2β	topoisomerase type II
	Top3α	topoisomerase type IA
Repair/ recombination	pol γ	exonuclease, lyase and gap-filling
	UDG	uracil DNA glycosylase
	OGG1	8-oxoguanine DNA glycosylase and lyase activities
	MUTYH	MutY glycosylase
	NTH	thymine glycol glycosylase
	APE1	apurinic/ apyrimidinic endonuclease
	DNA ligase III	nick sealing
	Fen1	flap endonuclease
	Dna2	flap endonuclease
	p53	exonuclease; interactions with pol γ, TFAM and mtSSB
	parkin	E3-ligase**
Transcription	mtRNAP	RNA polymerase
	mtTFB2	activation of mitochondrial transcription
	DmTTF	regulation of mitochondrial transcription termination in *Drosophila*
	mtDBP	regulation of mitochondrial transcription termination in sea urchin
	MTERF1	regulation of mitochondrial transcription termination/ replication pausing in humans
	MTERF2	activation of mitochondrial transcription
	MTERF3	negative regulation of mitochondrial transcription

* because TFAM functions in packaging and compaction of mtDNA in mitochondrial nucleoids, it is likely involved in all mtDNA transactions.

** the mechanism associating this activity with mtDNA repair is not clear (see text for more details).

(Harman 1972), which states that reactive oxygen species (ROS) generated by mitochondrial OXPHOS can cause damage to various macromolecules and primarily, mtDNA. Mutated mtDNA will encode defective OXPHOS polypeptides, subsequently leading to increased ROS levels and oxidative damage, and creating a vicious cycle that ultimately leads to lifespan limitation. Although this theory is not supported completely by some recent experiments (discussed in this Review), it is easy to understand the importance of the proteins involved in mtDNA transactions. Maintenance of the integrity of mtDNA and its expression is paramount in maintaining healthy mitochondria and ultimately, healthy organisms.

In this review, we will focus on the nuclear-encoded factors required for mtDNA replication, repair, recombination and transcription and on consequences to mtDNA, mitochondria and the whole organism when the expression of these proteins is altered or variant proteins are expressed instead. For this purpose, scientists have taken advantage of powerful animal and cell culture models, giving special attention to the mouse and the fruit fly, *Drosophila melanogaster*. These models have helped to demonstrate that OXPHOS defects have broad relevance to the genetics, biochemistry and physiology of human diseases, and to the ageing process (Wallace 2008). We acknowledge that all mtDNA transactions take place in the context of nucleoprotein complexes called mitochondrial nucleoids, but we will not discuss nucleoid organization and its dynamics in this review; rather, we refer the reader to recent papers by Bogenhagen (2010), Spelbrink (2010) and Wallace and Fan (2009).

mtDNA Replication

The field of mtDNA replication has experienced a recent expansion as a result of several key findings. First, mutations in the human genes encoding three of the four known constituents

of the mtDNA replication fork (Figure 2), the catalytic and accessory subunit of pol γ, pol γ-α and β, respectively (review in Copeland 2008), and the mtDNA helicase (Spelbrink *et al.* 2001), have been found in association with the human diseases progressive external ophthalmoplegia (PEO), Alper's syndrome, and ataxia-neuropathy. These are associated with mtDNA depletion and/ or accumulation of mtDNA point mutations and deletions, and manifest with neurological and/ or muscular problems due to mitochondrial dysfunction. Second, the development by Jacobs, Holt, and co-workers of the two-dimensional agarose gel electrophoresis (2DAGE) procedure, applied in association with various nucleic acid-modifying enzymes to analyze mtDNA replication intermediates (RIs), has prompted new models for vertebrate mtDNA replication that differ from the traditional strand-displacement model that has been studied by Clayton and co-workers for over 30 years. Though some controversy has been generated as a result (Bogenhagen and Clayton 2003a,b, Holt and Jacobs 2003), it seems reasonable that the numerous models for mtDNA replication that populate the current literature may be a reflection of the different modes that operate *in vivo*, and represent adaptive processes to ensure appropriate mtDNA copy number and mitochondrial gene expression, and hence ATP production via OXPHOS. Thus, a brief explanation of the current models may help the reader to understand the new findings obtained from whole animal and cell culture models.

The original model of mtDNA replication derives from electron microscopy and end mapping of mtDNA purified by equilibrium sedimentation in cesium chloride density gradients (Clayton 1982). In this model, the synthesis of the mtDNA leading strand (known as the heavy strand in vertebrate mtDNA because of its guanine-rich composition) initiates within the non-coding region at a site designated as O_H (see Figure 1), and proceeds continuously. When leading strand synthesis reaches about two thirds of the distance around the mtDNA genome, the

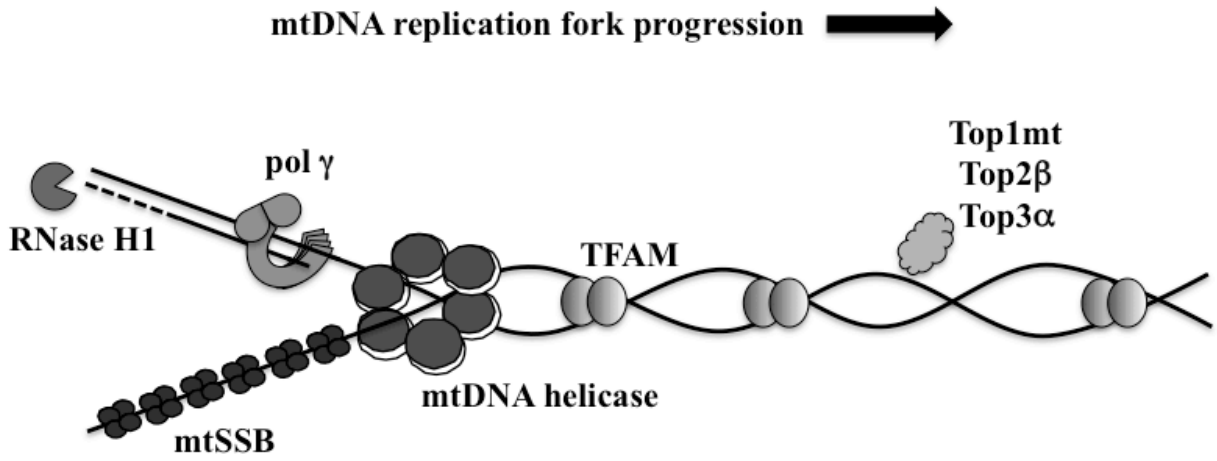

Figure 2. Factors involved in mtDNA replication in animals. Solid lines represent DNA, and the dashed line represents RNA. The diagram is not to scale, nor is it meant to depict protein or DNA structure, or specific protein-protein interactions. See Table 1 and the text for descriptions of the factors.

origin of the lagging strand (the light strand in vertebrate mtDNA) synthesis O_L is exposed and replication of the lagging strand is initiated and synthesis proceeds continuously. The overall process is thus unidirectional, continuous and asymmetric. In contrast, studies using 2DAGE (Holt *et al.* 2000, Reyes *et al.* 2005, Yang *et al.* 2002, Yasukawa *et al.* 2006, among others) have revealed evidence for bidirectional replication and fully DNA theta replication intermediates indicative of coupled leading and lagging DNA strand synthesis, as in nuclear and bacterial DNA replication. Furthermore, a new class of RIs was discovered: extensive segments of RNA were found incorporated on the lagging strand, giving rise to the RITOLS (RNA Incorporated Throughout Lagging Strand) model. This model also implies strand-coupled replication with the RNA RIs subsequently being maturated into DNA, though in this case, replication appears to proceed unidirectionally. Because no primase activity has been detected in the mtDNA helicase (Farge *et al.* 2008, Matsushima and Kaguni 2009), a homologue of the bifunctional bacteriophage T7 gp4 primase-helicase, it is believed that the RNA RIs of the RITOLS model, and likely the RNA primers in the theta and strand-displacement models, are generated by the transcriptional machinery of the mitochondrion (discussed below).

Perhaps the strongest contribution of the development of the 2DAGE technique to mtDNA has been its application to studying replication *in vivo* when the activities of pol γ, mtDNA helicase, or other proteins involved in mtDNA transactions are compromised. In a study by Wanrooij *et al.* (2007), human HEK293 Flp-In^{TM} T-REx^{TM} cell lines expressing catalytic mutants of pol γ-α (D890N and D1135A, required for 5'-3' polymerase activity) and mtDNA helicase (K421A, implicated in ATP binding and hydrolysis; G575D, implicated in DNA binding; and a deletion of residues 70–343 that shows similarity with the T7 gp4 primase domain) showed mtDNA depletion, altered nucleoid localization, and replication stalling

phenotypes. Notably, the stalling caused by pol γ and mtDNA helicase mutants differs. The RIs observed in the mtDNA helicase stalling mutants were most likely double-stranded DNA (dsDNA) with loss of RITOLS, which the authors explain as an increased rate of lagging strand initiation and/ or RNA-DNA maturation relative to the rate of fork movement, consistent with the role of the mtDNA helicase in unwinding dsDNA. On the other hand, expression of pol γ mutants induced replication stalling but maintained RITOLS and single-stranded RIs, primarily because of delayed lagging-strand DNA synthesis or its maturation. mtDNA replication stalling associated with impaired mtDNA helicase function has also recently been shown for human cell cultures expressing mtDNA helicase carrying autosomal dominant PEO (adPEO) mutations (Goffart *et al.* 2009). The RIs found in this study resemble those obtained with the expression of catalytic mutants of mtDNA helicase.

In mice, the introduction of adPEO mutants of the mtDNA helicase, T360A and duplication of residues 353-365, partially recapitulated features of human patients (Tyynismaa *et al.* 2005). The T360A mutant only showed a mild phenotype, whereas mice over one year of age carrying the 353-365 deletion presented negative COX staining and enlarged mitochondria with concentric cristae in muscle fibers. Multiple mtDNA deletions were detected in the brain and curiously, a predominant 3-Kb fragment of the mtDNA containing the 12S and 16S rRNA genes and the NCR was found in the muscles. mtDNA copy number did not appear to be affected in heart and muscles, but was clearly reduced in the brain to ~ 40% when compared to control animals. Analysis of the mtDNA RIs of young mutant mice (6-weeks-old) showed accumulation of RIs indicative of replication stalling in the heart, muscle, kidney and brain, but not in the liver (Goffart *et al.* 2009). This difference may result from variations in tissue-specific expression of the mutant mtDNA helicase (e.g., transcript levels were 16% in the liver, and varied in other

tissues from 13-59% as compared to endogenous levels of the wild-type enzyme), self-regenerating capacity, resistance to apoptosis, and/ or mode of replication.

Our group has studied the effects of active site and adPEO mutants of mtDNA helicase in *Drosophila* Schneider cells (Matsushima and Kaguni 2007, Matsushima and Kaguni 2009). The overexpression of the mtDNA helicase mutants K388A and D483A, analogous to Lys^{318} in the Walker A motif and Asp^{424} in the Walker B motif in the helicase domain of bacteriophage T7 gp4, respectively induced a severe dominant-negative phenotype resulting in lethality within 4-6 weeks. Furthermore, mtDNA copy number and transcription were reduced drastically to 4-10 and 20% of control cells, respectively. Likewise, overexpression of *Drosophila* mtDNA helicase variants I334T and A442P that are located in the linker region and helicase domain, respectively, and are analogous to mutant alleles of human mtDNA helicase in adPEO patients (I367T and A475P), induced phenotypes as severe as the active site mutations. mtDNA copy number was reduced 7-11 fold, indicating conservation of structure/ function between the fly and human enzymes (Matsushima and Kaguni 2007). Mutations in the N-terminal domain are also associated with adPEO. We found that *Drosophila* Schneider cells overexpressing mtDNA helicase carrying W282L, R301Q, and P302L amino acid substitutions that are analogous to the W315L, R334Q, and P335L alleles found in human adPEO patients also showed reduced mtDNA copy number. Because we have failed to demonstrate a DNA primase activity in this region of the mitochondrial enzyme (Matsushima and Kaguni 2009) as found in T7 gp4, our current data argue that the N-terminal region plays a role in the C-terminal helicase function of the enzyme.

We have also evaluated the importance of the C-terminal region of the mtDNA helicase using a combination of *in vitro* and *in vivo* approaches (Matsushima *et al.* 2008). Deletion and

alanine substitution mutations revealed that residues Lys^{574}, Arg^{576}, Tyr^{577}, Phe^{588} and Tyr^{595} of the fly protein are important for mtDNA maintenance and cell viability; overexpression of these mutants caused drastic mtDNA copy number reduction and lethality, again comparable to the Walker A and B active-site mutants. We produced recombinant forms of the human mtDNA helicase carrying the analogous mutations R609A, F621A, and F628A and found that these showed defects in DNA-dependent ATPase activity. Compared to the wild-type helicase, we observed 4- and 10- fold reduction in ATP hydrolysis for the F628A and F621A mutants, respectively. R609A showed no ATPase activity consistent with the role of this residue as the arginine finger in the human mtDNA helicase (Matsushima *et al.* 2008).

Disruption of pol γ activity has also been the target of many studies employing *Drosophila* and mouse as models of mitochondrial biogenesis. In *Drosophila melanogaster*, pol γ mutants with defects in the gene encoding the catalytic subunit, *tamas*, were isolated in a screen of pupal-lethal lines that showed a reduction in the larval response to light due to a primary deficit in locomotion (Iyengar *et al.* 1999). These mutants failed to undergo behavioral changes characteristic of the larval wandering stage: the foraging third instar larvae remained in the food substrate for a prolonged period and died at, or just before, pupariation. Mutant alleles resulted in truncated proteins via frame-shifting and an E814V amino acid substitution in the polymerase domain, and an E595A substitution in the linker region of the pol γ catalytic core, concomitant with severe disruption of the pattern of mitochondrial distribution in the larval central nervous system. Several years later, Iyengar *et al.* (2002) described the first pol γ accessory subunit mutants found in animals. A G31E amino acid substitution and a truncation caused by a 74 bp insertion in the N-terminal domain of pol γ-β led to loss of mtDNA, disruption of mitochondrial morphology and impairment of cell proliferation in the larval brain, and

consequent lethality at the early pupal stage. Recently, a mutation in the human pol γ-β gene has been found in adPEO patients (review in Copeland 2008).

Miller and colleagues have employed both the pol γ-α and β mutants described above to study mitochondrial biogenesis and mitochondrial axonal transport when mtDNA replication is disrupted (Baqri *et al.* 2009). Here they found that mitochondrial density in the larval proximal nerves and muscles is increased ~12% relative to control animals and surprisingly the flux of bidirectional mitochondrial transport along the axon was increased by nearly 2 fold. Mitochondrial biogenesis is believed to take place in the cell body, such that newly made healthy mitochondria are transported in the anterograde direction towards the axon terminal, whereas damaged, depolarized mitochondria show a retrograde transport towards the cell body for degradation or recycling (Miller and Sheetz 2004). The data on disruption of mtDNA replication in *Drosophila* suggests that mitochondrial biogenesis and degradation are both increased, and that the elevated transport observed may represent a futile attempt to supply the axon with functional mitochondria. This study is particularly relevant to understand the roles of mitochondria in neurodegenerative diseases. In this regard we have reported that overexpression of *Drosophila* pol γ-α in the nervous system reduces median life span of adult flies to 39-52% of control animals, with only a moderate reduction in pupal eclosion (Martínez-Azorín *et al.* 2008). At the same time, OXPHOS activity and resistance to the ROS-generating agent paraquat were reduced by 70 and 40-50%, respectively. Surprisingly, we found that mtDNA was depleted by ~ 2-fold, and *in organello* DNA synthesis indicated that mtDNA in these flies is synthesized at a much lower rate (~50%). Finally we observed that the level of apoptosis in the larval brain was increased by ~30%. In contrast with the phenotypes observed in adult flies in the nervous-system overexpression model, we showed in an earlier study that constitutive overexpression of pol γ-α

in the whole animal is lethal at the pupal stage (Lefai *et al.* 2000). We observed that pupal mtDNA copy number and mitochondrial transcript levels in the constitutive overexpression model were reduced to 30-40% of those in control animals, suggesting that the excess of pol γ-α might cause mtDNA replication stalling due to its 50-fold reduced catalytic activity in the absence of comparable levels of pol γ-β, or alternatively as a result of its interaction with and sequestration of other mtDNA replication proteins, such as mtSSB. Interestingly, muscle-specific overexpression of pol γ-α produces nearly complete pupal lethality and a 60% reduction in life span of survivor adult flies, recapitulating the phenotype of constitutive overall overexpression and highlighting the potentially very different effects of altered levels of pol γ-α in relation to tissue-specific physiology (Martínez-Azorín *et al.*, in preparation).

In a very recent study, Di Re *et al.* (2009) showed that knockdown of pol γ-β in human 143B osteosarcoma cells caused mtDNA depletion (45%), and increased the number of mitochondrial nucleoids after six days of treatment. In contrast, overexpression of the accessory subunit in HEK and U2OS cells did not affect mtDNA copy number, although the number of nucleoids was reduced and their size increased. These findings prompted the authors to suggest that pol γ-β has an additional role other than in mtDNA synthesis *per se*, in regulating nucleoid structure via binding to the mtDNA D-loop region.

A "mtDNA mutator" mouse strain was obtained by replacement of pol γ-α gene with a proofreading-deficient catalytic core, which has a D257A substitution in the exonuclease domain of the enzyme (Edgar *et al.* 2009, Kujoth *et al.* 2005, Trifunovic *et al.* 2004, Vermulst *et al.* 2007, 2008). mtDNA mutation rate is increased in these mice as predicted, and longevity is reduced: the median life span is ~48 weeks and maximum age is 61 weeks. Signs of premature ageing were detected at 24-25 weeks of age, characterized by a loss of weight, kyphosis,

alopecia, anemia, infertility, hearing loss and reduced hair density. Further analysis showed reduced subcutaneous fat content and whole-body bone mineral density and content. At an age of ~40 weeks, the mtDNA mutator mice showed an enlarged cardiac left ventricle cavity, COX deficiency and abnormal mitochondria. Both deletion and nucleotide substitution mutations were found in the mtDNA of these mice, although the nature of mutations that cause this complex phenotype remains a controversial topic. Vermulst *et al.* (2007, 2008) argue that deletions in mitochondrial protein-coding and/ or RNA genes are the driving force of such phenotypes, disagreeing with Edgar et al (2009) who claim that random nucleotide substitutions with major effects in protein-coding genes are causal. Linear mtDNA molecules of ~11 Kb containing the genomic region between O_H and O_L have also been found, and evidence presented suggests that such molecules are produced as a result of enhanced replication pausing/ fragile sites (Bailey *et al.* 2009). Concern has been registered regarding the extrapolation of the conclusions drawn from the mouse data to human ageing, because the levels of mtDNA mutations in this model typically are more than an order of magnitude higher than those found in aged humans. For further discussion of the subject, we recommend the articles by Khrapko *et al.* (2006) and Kraytsberg *et al.* (2009).

Notwithstanding the number and type of mtDNA mutations associated with the ageing phenotype in this mouse model, the resultant defects may be expected to cause increased ROS production. However, ROS levels and mitochondrial oxidative stress were unchanged in the liver, and in cardiac and skeletal muscles of the mtDNA mutator mouse, failing to support a role for oxidative stress in the mitochondrial theory of ageing. Interestingly, widespread induction of apoptosis was detected in various mitotic and postmitotic tissues (Kujoth *et al.* 2005), suggesting that deregulation of programmed cell death may contribute to the profound ageing phenotype.

Tissue dysfunction due to mtDNA mutations is likely to arise through apoptosis and subsequent loss of critical, irreplaceable cells. Remarkably, high levels of apoptosis were also observed in the fly model of polγ-α overexpression (as discussed above), the mouse model of RNase H1 knockout, the fly model of mtTFB2 knockdown, and various cell culture systems (as discussed below). Because mitochondrial dysfunction shows pronounced tissue-specific effects, it seems possible that although ROS are not increased in the organs that were analyzed (liver and striated muscles) in the mtDNA mutator mice, they may be increased in others that have not yet been examined. It remains possible that ROS are not involved in ageing whatsoever, but the pronounced phenotype of the mtDNA mutator mouse clearly shows the involvement of mtDNA mutations in this process. The roles of ROS and apoptosis in promoting ageing remain a fertile problem and in this regard, one concern in relating directly the findings observed in the mutator mouse with ageing is that the accumulation of mtDNA mutations in the mouse model takes place largely during embryogenesis. It will be important to generate animal models that express the mutator phenotype in postmitotic tissues, which represent the actual target of the ageing process.

In addition to pol γ and the mtDNA helicase, the mitochondrial single-stranded DNA-binding protein, mtSSB, also functions at the mtDNA replication fork. Our lab has demonstrated that *Drosophila* mtSSB can stimulate 15-20 fold both *in vitro* DNA synthesis and the 3'-5' exonuclease activity of *Drosophila* pol γ (Farr *et al.* 1999, Thömmes *et al.* 1995). The human mtSSB has been shown to stimulate specifically the unwinding activity of the human mtDNA helicase (Korhonen *et al.* 2003) and together with pol γ and mtDNA helicase, reconstitute a minimal mtDNA replisome *in vitro* (Korhonen *et al.* 2004). The biochemical data is consistent with an important role for mtSSB in initiation and elongation of DNA synthesis in mtDNA replication. This has been documented genetically by the observation that an insertion in the

third intron of the *Drosophila* gene (*lopo*) results in developmental lethality in third instar larvae prior to metamorphosis (Maier *et al.* 2001). Molecular, histochemical and physiological experiments showed reduced cell proliferation in the central nervous system, with loss of mtDNA and concomitant loss of respiratory capacity. Interestingly, the number and morphology of mitochondria were not altered in the larval brain. Consistent with these results, the knockdown of mtSSB in *Drosophila* Schneider cells depletes mtDNA to 20% of the control level and results in growth defects (Farr *et al.* 2004). At the same time, overexpression of mtSSB restores cell growth and mtDNA copy number. However, the overexpression of a W79T/ F85A double mutant, a protein deficient both in ssDNA-binding and in stimulating pol γ activity, neither rescues the cell growth defect nor the mtDNA depletion phenotype.

As discussed above, the extent of RNA molecules associated with mtDNA replication may vary according to the mode of replication operating. Notwithstanding this consideration, synthesis and processing of RNA primers represent essential steps in the replication process. Crouch and co-workers showed for the first time the link between RNase H1 and mtDNA maintenance when they knocked out the *Rnaseh1* gene in mouse. Despite the dual nuclear and mitochondrial localization of RNase H1, the main features of *Rnaseh1*$^{-/-}$ animals were embryonic lethality concomitant with loss of mtDNA and COX activity, increased apoptosis and the presence of enlarged mitochondria with abnormal cristae (Cerritelli *et al.* 2003). Developmental arrest at the transition between the last larval instar and pupariation was also observed in *Rnaseh1*$^{-/-}$ flies (Filippov *et al.* 2001); although mtDNA maintenance was not analyzed directly, this phenotype is reminiscent with those already described in the various genetic and molecular genetic fly models of mtDNA transactions. The lethality caused by *Rnaseh1* knockout is most likely due to the deficiency of RNase H1 either in generating RNA

primers for lagging DNA strand synthesis from the long stretches of RNA associated with mtDNA, or in promoting the maturation of the RNA-containing RIs into fully-duplex progeny DNA molecules.

mtDNA replication, and the other mtDNA transactions reviewed here, create topological constraints on mtDNA and in particular, as a result of progression of replication forks and the transcriptional machinery. In addition, catenated DNA molecules likely arise from replication of supercoiled mtDNA (review in Zhang *et al.* 2007). The animal mitochondrion has three potential topoisomerases to deal with these topological problems: one type IA (Top3α), one type IB (Top1mt) and one type II (Top2β). Top2β and Top3α are primarily nuclear proteins that are targeted to the mitochondria via posttranscriptional mechanisms. Despite the lack of mtDNA analysis, animal models of *Top3α* knockout in *Drosophila* and mouse were shown to cause developmental lethality due to nuclear DNA instability (Li and Wang 1998, Plank *et al.* 2005). Top1mt, a paralog of the nuclear Top1, is found exclusively in the mitochondria of vertebrates and binds and cleaves mtDNA at three sites clustered within a 150 bp region downstream from the D-loop (Zhang and Pommier 2008, Figure 1). In a series of experiments, Dalla Rosa *et al.* (2009) explored the physiological differences between the mitochondrial and nuclear isoforms by targeting Top1mt to the nucleus and Top1 to the mitochondria of human HT-1080 fibrosarcoma cells. In the first scenario, Top1mt failed to interact with metaphase chromosomes, yet no phenotypic alterations were observed. On the other hand, the targeting of Top1 to mitochondria promoted strong inhibition of mitochondrial transcription followed by a gradual decline in mtDNA content. The exact mechanism for this phenotype is not clear, but the data indicate clearly that in spite of the high sequence similarity between the two paralogs, they have adapted early in the evolution of vertebrates to the environment of their cellular compartments,

which necessitates interactions with DNA in different conformations, and with their distinct replication and transcriptional machineries.

Repair and Recombination

mtDNA is a prime target for oxidative damage for two key reasons. First, most cellular ROS are produced in mitochondria. Second, a variety of environmental toxins accumulate in mitochondria, and directly or indirectly modify the mtDNA (review in Bandy and Davidson 1990). Furthermore, antiviral therapeutic drugs, including HIV-1 reverse transcriptase inhibitors, affect mtDNA content and integrity via inhibition of the polymerase and exonuclease activities of pol γ (reviewed in Kaguni 2004). One of the consequences of these susceptibilities is manifested in the high mutation rates reported in animal mtDNA as compared to the nuclear genome (Brown *et al.* 1979), despite the high nucleotide selectivity and exonucleolytic proofreading functions of pol γ (reviewed in Kaguni 2004). Historically, it was thought that neither replicative nor post-replicative DNA repair mechanisms were present in mitochondria, and that excessively damaged mtDNA molecules would be degraded and replaced by newly synthesized molecules copied from undamaged mtDNAs (Druzhyna *et al.* 2008). It was not until the late 1980's that the 3'-5' exonuclease activity was identified in pol γ with our work in *Drosophila* (Kaguni and Olson 1989), and that of others in vertebrates (Insdorf and Bogenhagen 1989, Kunkel and Soni 1988). It is clear now that the integrity of the mitochondrial genome is also enforced by various post-replicational repair mechanisms, primarily base excision repair (BER) (Figure 3).

Mitochondrial single-nucleotide BER apparently proceeds by a mechanism similar to nuclear BER, in which a damaged or inappropriate base is recognized and removed by the action

of DNA glycosylase, such as uracil DNA glycosylase (UDG), 8-oxoG DNA glycosylase/AP lyase (OGG1), MUTYH glycosylase, and thymine glycol glycosylase (NTH). Upon hydrolysis of the *N*-glycosydic bond, the resulting 5'-deoxyribose phosphate is cleared by the lyase activity associated with these glycosylases or by that in pol γ (Longley *et al.* 1998). Apurinic/ apyrimidinic endonuclease 1 can then cleave the 5' phosphodiester bond, creating a gap that can be filled by the actions of pol γ and DNA ligase III (Figure 3, left). With the exception of pol γ, all of these enzymes have been found both in the nucleus and mitochondria of animal cells, either as a result of expression of both mitochondrial and nuclear isoforms, or by nucleus-to-mitochondria translocation (Englander *et al.* 2002, Lakshmipathy and Campbell 1999, Nishioka *et al.* 1999, Slupphaug *et al.* 1993, Tomkinson *et al.* 1988). When the expression of the human OGG1 protein was targeted to the mitochondria of HeLa cells in culture, their capacity to repair mtDNA oxidative damages that are induced by various agents was enhanced significantly, leading to an increase in cell survival under oxidative stress (Chatterjee *et al.* 2006). At the same time, when the R229Q mutant of the OGG1 protein that is found in human patients with leukemia was targeted to mitochondria, mtDNA integrity and survival of HeLa cells were reduced under oxidative stress, pointing to a link between defects in mtDNA repair and certain types of cancer.

Studies with cell lines derived from the central nervous system of mammals have indicated that the mtDNA repair system is regulated differently in neurons and glial cells. Mitochondria from astrocytes can repair oxidative damage in mtDNA more efficiently than mitochondria from oligodendrocytes and microglia, with a positive correlation in oxidative damage-induced apoptosis (Hollensworth *et al.* 2000, LeDoux *et al.* 1998). Targeting OGG1 to

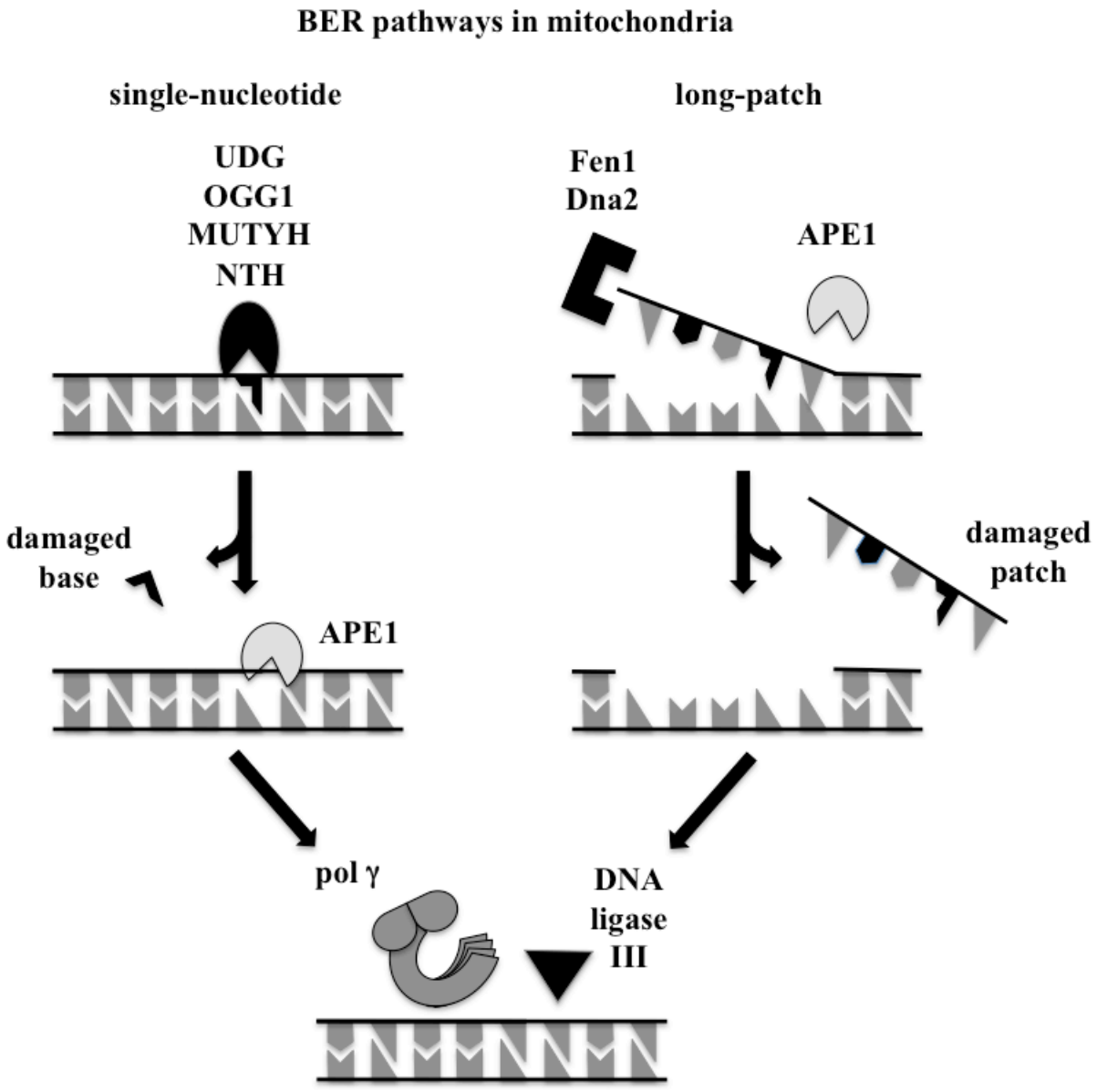

Figure 3. Possible pathways for post-replicative mtDNA repair. Both single-nucleotide (left) and long-patch (right) BER are believed to end with the concerted action of pol γ and DNA ligase III. The diagram is not to scale, nor is it meant to depict protein or DNA structure, or specific protein-protein interactions. See Table 1 and the text for descriptions of the factors.

the mitochondria of oligodendrocytes promoted an increase in mtDNA repair and a decrease in caspase 9-dependent apoptosis after exposure of the cells to menadione (Druzhyna *et al.* 2003). Similar results were obtained when oligodendrocytes containing OGG1-enriched mitochondria were exposed to inflammatory cytokines, a process that increases cellular nitric oxide (NO) by inducing expression of NO synthase. NO accumulates in brains of human patients with multiple sclerosis (Druzhyna *et al.* 2005); it can damage mtDNA directly or indirectly and inhibit the activity of DNA repair enzymes (Jaiswal *et al.* 2001). The increase in mtDNA integrity and cell viability under oxidative stress was also observed when the yeast apurinic/ apyrimidinic endonuclease Apn1 was targeted to the mitochondria of a neuronal cell line derived from rat substantia nigra (Ho *et al.* 2007). Surprisingly, when the *Drosophila* OGG1 and RpS3 (ribosomal protein S3) glycosylases were targeted to the mitochondria of Schneider cells, they became more susceptible to hydrogen peroxide or paraquat treatment and apoptosis was increased relative to the control cells, despite the decrease of 1.4 to 6.7 fold in damaged mtDNA (Radyuk *et al.* 2006). The expression of such proteins in *Drosophila* mitochondria may actually cause a perturbation in the BER pathway, so the authors speculate that despite enhancement of the glycosylase and lyase activities, the capacity of pol γ and DNA ligase III to complete the repair process is not increased, leading to the accumulation of nicked and/ or gapped mtDNA molecules and subsequent cell death. Interestingly however, *Drosophila* cells carrying OGG1- and RpS3-enriched mitochondria were more resistant to *S*-nitroso-*N*-acetylpenicillamine, an NO donor, probably due to alleviation of the glycosylase inhibition caused by NO (Jaiswal *et al.* 2001).

A second BER system that has been studied recently in mitochondria is the long-patch BER pathway. Fen1 and Dna2, familiar players in the processing of DNA intermediates during replication and repair in the nucleus, have been also identified in mitochondria. Fen1 is an

endonuclease that binds and cleaves specifically flap DNA structures (Liu *et al.* 2004). Liu *et al.* (2008) have shown that 2-deoxyribonolactone (dL), present in mtDNA as a product of oxidative damage, blocks both the polymerase and exonuclease activities of pol γ, and that such a lesion is processed by a long-patch BER pathway dependent on Fen1 activity found in mitochondrial extracts of human GM1310 lymphoblasts. The knockdown of Fen1 in HeLa cells, without detectably compromising cell proliferation (Fen1 is also required for Okazaki fragments maturation during nuclear DNA replication), led to more pronounced oxidative damage in mtDNA immediately after H_2O_2 treatment, and the recovery of repaired mtDNA was delayed. Dna2 is a member of the nuclease/ helicase family whose nuclease activity is also dependent on a flap DNA structure. Unlike Fen1, Dna2 removes a portion of DNA in the middle of the ssDNA flap (Bae and Seo 2000). Interestingly, the comparison of the well-studied yeast protein with the human Dna2 indicated that the human protein, as well as other vertebrate Dna2s, lacks the nuclear localization sequence and the replication protein A binding domain (Zheng *et al.* 2008). In HeLa, fibroblast and melanoma H294T cells, human Dna2 was predominantly localized to mitochondria, and *in vitro* experiments showed that it interacts physically and functionally with pol γ to promote DNA synthesis, and with Fen1 to perform efficient long-patch BER and RNA primer processing. *In vivo* Dna2 knockdown followed by H_2O_2 treatment revealed that mtDNA accumulates significantly more oxidative damage, and that the recovery from such stress is delayed. At the same time, nuclear genome does not suffer more damage in Dna2-depleted cells as compared to the control cells. In a similar study, Duxin *et al.* (2009) showed that in addition to the accumulation of mtDNA damage, the knockdown of Dna2 affects mtDNA replication quantitatively via a decrease in replication intermediates. Furthermore, the authors observed that Dna2 is important to maintain nuclear DNA stability, consistent with their localization of Dna2

in the nucleus of human BJ, HeLa, HEK293, U2OS, and 143B cells. Although function of Dna2 in the nucleus of mammalian cells warrants further investigation, it is clear that Dna2 plays an important role in mtDNA integrity. Thus it seems reasonable that Fen1 and Dna2, as well as the RNA/ DNA helicase Pif1, would function in maturation of the putative Okazaki fragments in semi-discontinuous mtDNA replication (reviewed in Holt 2009).

Large deletions in mtDNA are frequently associated with mitochondrial disorders and as such, constitute an important class of damaged DNA. Recently, in addition to models that suggest they are caused by errors in mtDNA replication, it was proposed that the generation of these deletions results from double-strand breaks (DSB) in mtDNA followed by DNA repair (Krishnan *et al.* 2008). Cellular repair mechanisms generally associated with DSB are homologous recombination (HR) or non-homologous end-joining (NHEJ). HR involves exchange of material between homologous segments (as short as 5 bp in similarity) of damaged and undamaged DNA, whereas NHEJ involves the protection of DNA ends against nucleases by the joining of two unrelated segments. To our knowledge, no candidate enzymes, such as recombinases or junctional resolvases, have been identified in the mitochondrial proteome or isolated from animal mitochondria, but evidence for both mitochondrial HR and NHEJ processes have been reported (Bacman *et al.* 2009, D'Aurelio *et al.* 2004, Fukui and Moraes 2009, Kajander *et al.* 2001, Morel *et al.* 2008, Pohjoismäki *et al.* 2009, Srivastava and Moraes 2005, Tang *et al.* 2000, Thyagarajan *et al.* 1996, Zsurka *et al.* 2005). In *Drosophila* Schneider cells, a mitochondrial DSB repair mechanism was shown to be activated upon induction of DSBs with bleomycin (Morel *et al.* 2008): in a time-course experiment the authors showed that 50% of mtDNA with DSB was repaired in 5 minutes after treatment with bleomycin; after 2 hours, nearly all molecules were repaired.

Moraes and coworkers have developed transgenic mice expressing mitochondrial-targeted bacterial endonucleases in order to study the effects of DSB in mtDNA. First, they expressed a mitochondrial-targeted *Pst*I nuclease in mouse skeletal muscles (Srivastava and Moraes 2005). They showed induction of DSB in mtDNA such that transgenic founders developed a mitochondrial myopathy associated with mtDNA depletion. A specific set of ~7 kb mtDNA deletions was identified, predominantly involving one of the *Pst*I sites and the 3′-end of the D-loop region (adjacent to the $tRNA^{Pro}$ and $tRNA^{Thr}$ genes, see Figure 1), with either no or small direct repeats at the breakpoint regions. Notably, the breakpoints correspond to those observed in the multiple mtDNA deletions found in human muscles due to mitochondrial disease or ageing. Fukui and Moraes (2009) targeted the same restriction enzyme to the neuronal mitochondria of the brain cortex, hippocampus, and striatum of the mouse. When expressed constitutively, the enzyme caused limb-clasping, a well recognized neurological phenotype. In contrast, when the enzyme was expressed only during embryological development and the first three weeks of age, no apparent neurological problem was detected, but life span was shortened significantly. The mtDNA deletions that were generated and accumulated in these mouse brains differed in size, perhaps as a result of different mechanism of recombination. Finally, Bacman *et al.* (2009) introduced DSB into mtDNA by targeting *Sca*I to the mitochondria of heteroplasmic mice and HP202B cells in culture, taking advantage of the haplotype differences to trace the origin of the recombined molecules. Because *Sca*I has multiple recognition sites in the mouse mtDNA, the authors were able to identify hotspots of recombination, which primarily involved a region adjacent to the D-loop. In addition, inter-molecular recombination was observed, albeit at a very low frequency.

The final step in DNA replication, repair, and recombination processes in mitochondria is

thought to require the action of DNA ligase III. Knockdown of DNA ligase III resulted in decreased mtDNA copy number and a 47-75% decrease in respiration in human fibrosarcoma-derived HT1080 cells (Lakshmipathy and Campbell 2001). Furthermore, the remaining mtDNA molecules contained numerous ssDNA breaks, suggesting that these cells are defective in sealing nicks generated during DNA replication and/ or repair. Exposure of DNA ligase III knockdown cells to γ-radiation showed that reduction in DNA ligase III diminished drastically the capacity of the cells to restore mtDNA copy number during a recovery period as compared to control cells, demonstrating the essential role of DNA ligase III in mtDNA maintenance.

There has been a recent increase in reports showing the participation of different types of proteins in the maintenance of mtDNA integrity through mechanisms that are not completely understood. Here, we will focus attention on two of these, p53 and parkin, because their association with mtDNA is relatively better understood. 30 years of study of the tumor suppressor p53 have shown that it functions as a global suppressor of inappropriate cell proliferation through induction of apoptosis, senescence or transient cell-cycle arrest, and that mutations in its gene are present in a high proportion of human cancers, irrespective of their histological type (reviewed in Hainaut and Wiman 2009, and Vousden and Ryan 2009). Novel functions of p53, beyond its traditional role as guardian of the nuclear genome, are related to mitochondrial function in diverse ways. These include: regulation of expression of nuclear genes involved in glucose metabolism and mitochondrial respiration and in particular, in genes required for cytochrome *c* oxidase assembly (Ma *et al.* 2007); the direct activation of Bax via translocation to mitochondria to mediate programmed cell death (Chipuk *et al.* 2004); physical association with mtDNA (Achanta *et al.* 2005, Heyne *et al.* 2004); and physical and functional interactions with pol γ, mitochondrial transcription factor A (TFAM) and mtSSB (Achanta *et al.*

2005, Wong *et al.* 2009a,b, Yoshida *et al.* 2003). Achanta *et al.* (2005) observed that different types of human $p53^{-/-}$ cells in culture were extremely vulnerable to mtDNA depletion and respiratory deficiency after treatment with ethidium bromide (EtBr), a DNA intercalating agent known to affect preferentially mtDNA at low concentrations. In $p53^{+/+}$ cells, treatment with EtBr and rotenone, an inhibitor of complex I of mitochondrial OXPHOS and therefore a ROS generator, showed an enrichment of p53 in the mitochondria and its co-localization with pol γ, which implied that mtDNA damage is the primary signal for p53 translocation to mitochondria. Mitochondrial nucleoid remodeling is triggered by the presence of either EtBr or another DNA intercalating agent, doxorubicin, which is used in cancer therapy (Ashley and Poulton 2009). Treatment with doxorubicin of human fibroblasts in which p53 was knocked down or chemically inhibited resulted in fewer nucleoids of larger sizes, reminiscent of the results obtained with cells derived from the mtDNA mutator mouse. In another recent study, Lebedeva *et al.* (2009) showed that steady-state mtDNA copy number, mitochondrial membrane potential and mitochondrial mass are reduced 50, 30, and 40%, respectively, in $p53^{-/-}$ mouse neonatal fibroblasts, and in p53 knockdown in primary human fibroblasts in culture. In addition, TFAM and p53R2, the p53-regulated subunit of ribonucleotide reductase (mutations in this gene have been associated with mtDNA depletion syndromes; Bourdon *et al.* 2007), protein levels were significantly reduced, and cellular ROS homeostasis was disrupted, as reduced superoxide and increased H_2O_2 levels were observed. Taken together, these results are relevant to cancer research, especially involving the effects of mtDNA mutations in cancer progression.

Initially identified as an E3-ligase protein, parkin, a protein in which mutations are associated with the most common cases of autosomal recessive Parkinson's disease (PD) in

humans (Park *et al.* 2009), has recently been found associated physically with mtDNA in the proliferating and differentiated human dopaminergic neuroblastoma cell line (SH-SY5Y), and in brain tissue of mouse and human origin (Rothfuss *et al.* 2009). Other genes causing PD, such as PINK1 and DJ-1 (Andres-Mateos *et al.* 2007, Pridgeon *et al.* 2007), are also linked to mitochondrial function, but have not yet been identified in association with mtDNA. Rothfuss *et al.* (2009) have shown that the overexpression of parkin in cell culture promotes increased mtDNA copy number and transcription, and protects mtDNA from oxidative stress-induced damage: a 50% reduction in mtDNA lesions were observed in these cells compared to the control cells. In addition, mtDNA repair was increased ~ 50% after H_2O_2 exposure followed by 2 hours of recovery. In human parkin-mutant fibroblasts, mtDNA copy number is reduced ~ 20%, and the genome is more susceptible to ROS-induced damage. Detailed experimentation on mouse (Goldberg *et al.* 2003, Palacino *et al.* 2004) and fly models (Greene *et al.* 2003; Pesah *et al.* 2004; Cha *et al.* 2005) has established a link between parkin and mitochondrial function. In particular, *Drosophila* has helped to establish the hypothesis that parkin is translocated inside the mitochondria via interactions with the mitochondrial-targeted serine/ threonine kinase PINK1. The parkin-PINK1 pathway is likely involved in mitochondrial fusion and fission processes (Park *et al.* 2009, and references therein), and the new findings that parkin is associated with mitochondrial nucleoids implies that it functions in proper nucleoid segregation during mitochondrial division (Rothfuss *et al.* 2009). However, how parkin protects mtDNA integrity is unclear and warrants further investigation.

mtDNA Transcription

The core machinery for animal mitochondrial transcription (Figure 4) consists of a

bacteriophage T-odd-related RNA polymerase (mtRNAP), the mitochondrial transcription factor A (TFAM) and two homologues of bacterial rRNA methyltransferases, the transcription factors B1 and B2 (mtTFB1 and mtTFB2, respectively). Among all mitochondrial nucleoid proteins, TFAM is the most abundant and well studied component (Garrido *et al.* 2003, Kanki *et al.* 2004, Kaufman *et al.* 2007, Larsson *et al.* 1998). Despite its involvement in *in vitro* reconstitution of the human mitochondrial transcription machinery (Falkenberg *et al.* 2002, Gaspari *et al.* 2004, McCulloch *et al.* 2002), the major role of TFAM is in mtDNA maintenance via packaging and compaction, similar to nuclear histones and the bacterial HU proteins (Alam *et al.* 2003, Kanki *et al.* 2004). We recommend the review by Wallace and Fan (2009) for a summary of mouse models of TFAM knockout.

Transcription in mammalian mtDNA originates from three regions located in the NCR: HSP1 and HSP2 are heavy strand promoters and LSP is the light strand promoter (Figure 1). Polycistronic transcripts comprising nearly the entire genome originate from HSP2 and LSP; they are then processed by the excision of tRNAs, which flank the majority of the protein-coding and rRNA genes, liberating the mRNAs and rRNAs. Transcription from HSP1 generates a transcript that comprises primarily the two rRNAs, permitting the mitochondria to produce more rRNA independent of mRNA production (reviewed in Bonawitz *et al.* 2006, Falkenberg *et al.* 2007).

In vivo studies with mtTFB1 and mtTFB2 were initiated in *Drosophila* Schneider cells and extended to human HeLa cell culture, transgenic flies and knockout mice (Adán *et al.* 2008, Cotney *et al.* 2007, Matsushima *et al.* 2004, Matsushima *et al.* 2005, Metodiev *et al.* 2009). We first knocked down mtTFB2 in *Drosophila* Schneider cells and evaluated the effects in mtDNA transcription and maintenance (Matsushima *et al.* 2004). mtTFB2 knockdown reduced cell

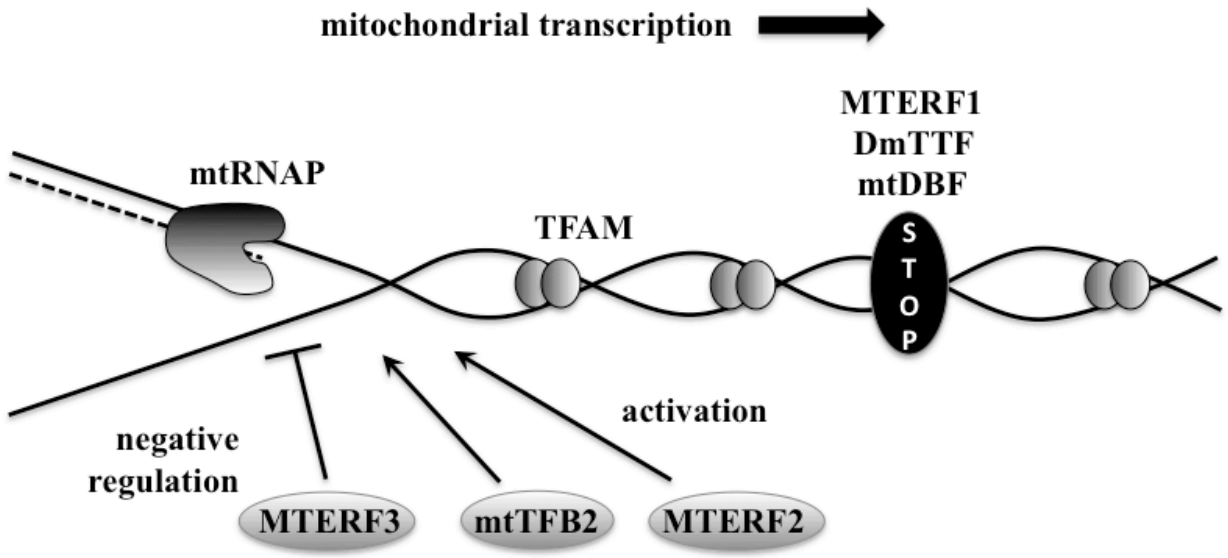

Figure 4. Overview of transcription in animal mitochondria and the proteins involved in the process. Solid lines represent DNA, and the dashed line represents RNA. The diagram is not to scale, nor is it meant to depict protein or DNA structure, or specific protein-protein interactions. See Table 1 and the text for descriptions of the factors.

growth, the abundance of 12S rRNA, ND4, and Cytb transcripts (57, 16, 13% of control cells, respectively), and mtDNA copy number (38% of control). On the other hand, overexpression of mtTFB2 had no effect on cell growth or viability, but it promoted an ~2 fold increase in the mitochondrial transcripts and mtDNA copy number. The knockdown of mtTFB2 was also examined in transgenic flies constitutively expressing an inverted repeat fragment containing a *Drosophila* mtTFB2 cDNA (Adán *et al.* 2008). The transgenic animals died at the third larval instar stage, although this stage was dramatically prolonged (3-fold longer than in control larvae), and the larvae exhibited a 50% decrease in mass. Further analysis showed that mtTFB2 knockdown had only a moderate effect on mtDNA copy number, but transcript levels were reduced by 50%, concomitant with a decrease in OXPHOS activity and cell proliferation in larval brain, and an increase in apoptosis in wing imaginal discs. Interestingly, the long-lived larvae partially restored ATP synthesis by promoting a metabolic shift to glycolysis, and showed increased levels of mtTFB1 mRNA and protein (1.5-1.75 fold), suggesting a retrograde compensatory signaling in its nuclear gene expression. These results indicate that mtTFB2 is essential for mitochondrial transcription and animal development, and that it cannot be compensated by mtTFB1, despite their exchangeability in *in vitro* transcription assays (Falkenberg *et al.* 2002, McCulloch *et al.* 2002). A second retrograde signal affecting mtTFB1 levels was observed by Shadel and collaborators when they overexpressed mtTFB2 in human HeLa cells (Cotney *et al.* 2007). The authors observed a ~2 fold increase in mtTFB1 levels, concomitant with a 2-fold increase in mitochondrial transcripts and mtDNA copy number that was consistent with results with mtTFB2 overexpression in *Drosophila* Schneider cells (Matsushima *et al.* 2004), and an increase in mitochondrial translation. In composite, the data in both models argue that mtTFB2 serves an important role *in vivo* in mitochondrial transcription

and in transcription-primed mtDNA replication (discussed in mtDNA replication session).

The first *in vivo* evidence that mtTFB1 and mtTFB2 have clearly distinct function in mitochondria, despite their homology and equivalent *in vitro* functions as transcription activators (Falkenberg *et al.* 2002, McCulloch *et al.* 2002) and rRNA methyltransferases (Cotney and Shadel 2006), came from our studies of mtTFB1 in Schneider cells (Matsushima *et al.* 2005). Here, the knockdown of mtTFB1 resulted in moderate cell growth retardation, with no change in the levels of mitochondrial transcripts or in mtDNA copy number. However, mtDNA-encoded proteins were reduced to 40% of those in control cells, suggesting a role for mtTFB1 in mitochondrial translation. Overexpression of mtTFB1 showed no significant effect on mtDNA copy number, mitochondrial transcription or translation. Again, similar findings were obtained upon overexpression of mtTFB1 in human HeLa cells (Cotney *et al.* 2007). Furthermore, the level of mtTFB2 was unchanged when mtTFB1 expression was altered in both *Drosophila* and human cells. Recently, Metodiev *et al.* (2009) showed that the knockout of mtTFB1 in mice result in embryonic lethality due to respiratory chain deficiency. Cardiac and skeletal muscle-specific *Tfb1m*$^{-/-}$ mice had a shorter life span, and all of them died before 24 weeks of age, with increased heart weight, increased mitochondrial mass (> 50%) and an increased number of mitochondria with abnormal cristae in cardiomyocytes, despite presenting a progressive deficiency in OXPHOS function. Consistent with the increase in mitochondrial mass, these knockout mice had elevated mtDNA copy number (~50%), elevated TFAM (3.5 fold) and mtTFB2 protein levels, and decreased MTERF3, a negative regulator of mammalian mtDNA transcription (discussed below). In combination, elevated TFAM and mtTFB2, and decreased MTERF3 likely promoted the 2.5 fold increase in *de novo* mitochondrial transcription. However, the steady-state levels of the 12S rRNA were dramatically reduced (~40% of control), along with

a more dramatic reduction in mtDNA-encoded proteins (~10% of control). These results suggested that mtTFB1 participates directly in the stability of the 125 rRNA via its rRNA methyltransferase activity, and this hypothesis was confirmed when the authors verified that the 12S rRNA of *Tfb1m*$^{-/-}$ mice lacked a dimethyl group in the conserved hairpin loop at the 3'-end of the molecule, which led to a specific loss of the small subunit of the mitochondrial ribosome. Altogether, the work in the *Drosophila*, human cell, and mouse models has demonstrated distinct and non-redundant roles of mtTFB1 and mtTFB2 in animal mitochondrial biogenesis: mtTFB1 has conserved its ancestral role *in vivo* as an rRNA methyltransferase and thus in protein translation, and mtTFB2 has evolved a role in promoting transcription of mitochondrial genes.

As important as are activation and initiation of transcription in mitochondria, is the regulation of these transactions via termination and/ or repression. Human mTERF, *Drosophila* DmTTF and the sea urchin mtDBP have all been shown to bind specific sequences in their respective genomes and promote transcription termination (reviewed in Roberti *et al.* 2009). In sea urchin, mtDBP is a strong transcriptional terminator, but it also controls the expansion of the small mtDNA D-loop via its counter-helicase activity, possibly coordinating the events of transcription and replication (Polosa *et al.* 2005, Roberti *et al.* 2009). In *Drosophila*, DmTTF binds two specific regions located at the end of blocks of mtDNA genes that are transcribed in opposite directions, and promotes transcription termination *in vitro* (Roberti *et al.* 2005). *In vivo*, DmTTF knockdown in *Drosophila* D.Mel-2 cells showed that the levels of transcripts from the mitochondrial genes located downstream from DmTTF binding sites (assuming that transcriptional initiation occurs in the mtDNA NCR in flies, also known as the A+T-rich region, Figure 1) was higher than in the control cells, and that the transcript levels of the genes located between the A+T-rich region and DmTTF binding sites were reduced (Roberti *et al.* 2009),

suggesting a possible role in transcriptional activation similar to the human MTERF1 (discussed below). Although mtDNA copy number, and TFAM, mtTFB1 and mtTFB2 mRNA levels were not affected, changes in *de novo* mitochondrial protein synthesis correlated with changes in the mitochondrial mRNA levels. Overexpression of DmTTF decreased the transcript levels of genes mapping downstream of the DmTTF binding sites on both strands but surprisingly, *de novo* protein synthesis experiment showed either a reduction or no change in any of the mtDNA-encoded proteins. Thus, it is clear that the roles of DmTTF in regulating mitochondrial transcription and protein synthesis are complex, prompting future research.

The human mTERF protein, also known as MTERF1 (discussed below), is arguably the most important factor regulating the production of the transcript originating from the HSP1 promoter. It binds to a region at the 3'-end of the $tRNA^{Leu(UUR)}$ gene and at the HSP1 region (Figure 1), which creates a loop between HSP1 and the end of the 16S rRNA gene, possibly facilitating reinitiation of transcription and enhancing production of the mitochondrial rRNAs, and therefore also functioning as a transcriptional activator (Fernandez-Silva *et al.* 1997, Martin *et al.* 2005). The binding of MTERF1 to HSP1 may also terminate transcription originated from the LSP promoter. Recently, a new role for MTERF1 in pausing of mtDNA replication has been proposed based on *in vivo* studies with human HEK293T, 143B osteosarcoma, Jurkat and HeLa cells, and in organ samples (Hyvärinen *et al.* 2007). First, the authors identified new MTERF1 binding sites throughout the mtDNA in addition to the canonical site in the $tRNA^{Leu(UUR)}$ gene, by overexpressing the protein in cell culture and performing electrophoretic mobility shift assays and mtDNA immunoprecipitation. Interestingly, they observed that these new binding sites coincided relatively well with sites of mtDNA replication pausing, as analyzed by 2DAGE. However, replication pausing was not observed at all sites concomitantly; there was a great

variability that depended on the cell type or organ tissue analyzed. Overexpression of MTERF1 in general enhanced the RIs representing replication pausing, and it appeared that the level of 7S DNA, which is part of the triple-stranded D-loop region, was increased. The knockdown of the protein had an opposite effect: pause sites were substantially decreased, especially in the region containing its canonical binding site. Like the sea urchin mtDBP, human MTERF1 may coordinate the passage of the mitochondrial replication and transcription machineries, safeguarding the integrity of the mtDNA and facilitating efficient gene expression.

Recent bioinformatic and phylogenetic analyses have identified three additional paralogs of the human MTERF1 in the nuclear genome, named MTERF2 to MTERF4 (Linder *et al.* 2005). The biochemical and physiological roles of these proteins have just very recently been addressed in animals. MTERF3 was the first shown to have mitochondrial localization and an important mitochondrial function (Park *et al.* 2007, Roberti *et al.* 2006, Roberti *et al.* 2009). In *Drosophila* D.Mel-2 cells, the overexpression of MTERF3 promoted a decrease of 0.2-0.6 fold in the steady-state levels of the 12S rRNA, COI, and ND2 transcripts (Roberti *et al.* 2009). mtDNA copy number and the levels of TFAM, mtTFB1 and mtTFB2 mRNA were not affected, indicating a role of MTERF3 as a negative regulator of mitochondrial transcription. In contrast, MTERF3 knockdown had no effect on the levels of mitochondrial transcripts, but *de novo* synthesis of mtDNA-encoded proteins decreased overall (Roberti *et al.* 2006). Furthermore, analysis of TFAM, mtTFB1 and mtTFB2 mRNA levels showed that TFAM and mtTFB1 were depleted in MTERF3 knockdown cells (Roberti *et al.* 2009). The authors explained the unaltered levels of mitochondrial transcripts as a counterbalanced effect of depleting the negative regulator MTERF3 and the activator TFAM at the same time. The reduction of mtDNA-encoded proteins was likely due to mtTFB1 depletion. In the mouse, Park *et al.* (2007) showed that the knockout

of MTERF3 resulted in embryonic lethality due to respiratory chain deficiency, similar to the results in *Tfb1m*$^{-/-}$ mice. Specific disruption of MTERF3 in the heart and skeletal muscle shortened life span to a maximum of 18 weeks, due to a progressive deterioration of the activity and assembly of OXPHOS complexes I, III-V. The mice exhibited increased heart weight, increased mitochondrial mass (143-192%) and an increased number of abnormal mitochondria in cardiomyocytes. mtDNA copy number was unchanged as compared to the control mice, but mitochondrial transcripts were generally elevated, especially the HSP transcripts. mtDNA immunoprecipitation revealed that MTERF3 binds to a region containing the HSP promoters, indicating that it regulates transcription at the level of initiation.

To our knowledge, no physiological studies have been reported to date on MTERF4. On the other hand, Wenz *et al.* (2009) have reported on MTERF2 function and its possible interactions with MTERF1 and MTERF3 in regulating mtDNA transcription. Unlike MTERF3, the constitutive knockout of MTERF2 in the mouse was not lethal; the knockout animals had no alterations in life span, basal metabolism or heat production, despite a slight decrease in body weight. However, *Mterf2*$^{-/-}$ mice showed defects in OXPHOS function due to decreased steady-state levels of the individual OXPHOS complexes primarily in skeletal muscle, leading to mitochondrial myopathy. When the knockout mice were metabolically challenged with a ketogenic-rich diet that forces the animals to produce ATP via fatty acid oxidation and mitochondrial OXPHOS, the myopathy phenotype was enhanced, memory deficits observed, and OXPHOS defects were found in different tissues. As frequently observed for deficiencies in OXPHOS, knockout of MTERF2 triggered compensatory responses to promote mitochondrial biogenesis, including increased mtDNA copy number, but these mitochondria were enlarged with abnormal morphology. Interestingly, none of these effects were observed in the mouse

heart, indicating tissue-specific regulation of MTERF2. Finally, the authors showed that the decrease in OXPHOS proteins were due to a decrease in the steady-state levels of mitochondrial mRNAs and imbalanced tRNA levels, suggesting that MTERF2 is a positive regulator of transcription, opposite to MTERF3. Electrophoretic mobility shift analysis, mtDNA immunoprecipitation and protein coimmunoprecipitation showed that MTERF1, MTERF2, and MTERF3 bind specifically to the HSP promoter region, and may coordinate initiation of mitochondrial transcription, possibly influencing the assembly of the transcriptional machinery. Thus, although a complete understanding of the regulation of mitochondrial transcription remains elusive, these new findings advance the field and document its clearly complexity.

Concluding Remarks and Perspectives

Mitochondrial research has advanced at a fascinating pace, such that this Review, covering the current status of mtDNA transactions as an important part of the mitochondrial biogenesis process, will likely be out-of-date in a matter of few years. We expect here to have given an extended summary of the scientific progress that the field has observed, especially for the last decade, by discussing the contributions from the work of ours and others in different animal models. It is clear to that the processes involved in mtDNA transactions play a central role in the biology and medicine of mitochondria and therefore, in the life of eukaryotic organisms. Human ageing and diseases including adPEO, PD and numerous others can be modeled by deregulating many of the mtDNA transaction processes. At the same time, the increase in ROS as a result of this deregulation is not completely clear. The DNA repair mechanisms in mitochondria, now shown to be diverse and relatively efficient, clearly protect mtDNA from ROS-induced damage. p53 knockout/ knockdown, for example, produces ROS

imbalance and decreases mtDNA integrity and copy number. However, ROS levels are apparently not changed in the cells of the mtDNA mutator mouse, despite the constant increase in mtDNA mutations throughout the life span. For a detailed discussion of ROS production and mitochondrial function, we suggest the articles by Druzhyna *et al.* (2008), Jang and Van Remmen (2009), Thompson (2006), and Wallace and Fan (2009).

As we reviewed here, mutations in and/ or deregulation of expression of the well-known proteins involved in mtDNA organization, replication and transcription (pol γ, mtDNA helicase, mtSSB, mtTFB2 and MTERF1) promote mitochondrial dysfunction with different outcomes: null mutations of pol γ-α, pol γ-β and mtSSB in *Drosophila* result in lethality; overexpression/ knockdown of MTERF1 in cell culture demonstrate that regulation of mtDNA replication and transcription are tightly linked; overexpression of pol γ and mtDNA helicase mutants in cell culture promotes distinct aberrations in mtDNA replication; expression of an adPEO mutant of mtDNA helicase in mouse causes an adPEO-like phenotype; expression of a proofreading-deficient mutation of pol γ-α created the mtDNA mutator mouse and caused premature ageing with reduced life span; constitutive and neuron-specific overexpression of pol γ-α in *Drosophila* causes lethality and reduced life span, respectively; and knockdown of mtTFB2 caused lethality in *Drosophila*. In many of these cases, increased compensatory mitochondrial biogenesis is stimulated in the cells, despite the lack of success to restore ATP production via OXPHOS. Notably, where apoptotic markers were examined, higher levels of mitochondrial dysfunction-induced apoptosis were observed, indicating a conserved mechanism of elimination of cells containing damaged mitochondria and a possible role for this process in ageing, and suggesting a rich area for future research.

Regarding mitochondrial transcription, former issues have been resolved and new

regulators identified. *In vivo* studies have shown that mtTFB1 and mtTFB2 are not redundant proteins: mtTFB1 methylates 12S rRNA and, is required for translation of mtDNA-encoded proteins, whereas mtTFB2 regulates mitochondrial transcription and transcription-mediated mtDNA replication, and is necessary for animal development. MTERF3 has been shown to be required for mouse development due to its ability to down-regulate mitochondrial transcription. MTERF2, on the other hand, appears to up-regulate transcription, but it is not absolutely required for development. Further investigations of the regulation of mitochondrial transcription through the interactions of transcription factors, terminators and mtDNA are warranted to expand our understanding of this apparently complex system.

With regard to current models of mtDNA replication, substantial future experimentation is needed to identify new protein players such as a primase, helicase loader and/ or an initiator, for full reconstitution of the mtDNA replisome *in vitro*, and to examine comprehensively multiple animal models through the application of approaches such as 2DAGE and electron microscopy. This will allow us to address the potentially multifarious responses of a particular cell type to ensure appropriate mtDNA copy number and mitochondrial gene expression. We might envision that different cell types would be able to switch among various mtDNA replication modes, and/ or that specific replication modes may be related to specific types of mtDNA organization comprising dynamic mtDNA: protein complexes. This latter possibility has recently been evidenced in human heart and brain, and mouse heart mtDNA (Pohjoismäki *et al.* 2009), and represents a new avenue for understanding tissue variability in mitochondrial diseases.

CHAPTER 2

COMPARATIVE PURIFICATION STRATEGIES FOR *Drosophila* AND HUMAN MITOCHONDRIAL DNA REPLICATION PROTEINS: DNA POLYMERASE γ AND MITOCHONDRIAL SINGLE-STRANDED DNA-BINDING PROTEIN

Summary

The mitochondrion is the eukaryotic organelle that carries out oxidative phosphorylation, fulfilling cellular requirements for ATP production. Disruption of mitochondrial energy metabolism can occur by genetic and biochemical mechanisms involving nuclear-encoded proteins required at the mitochondrial DNA replication fork, which often leads to human disorders and to animal lethality during development. DNA polymerase γ (pol γ), the mitochondrial replicase, and the mitochondrial single-stranded DNA-binding protein (mtSSB) have been the focus of study in our lab for a number of years. Here we describe the purification strategies our lab has developed for obtaining the recombinant forms of pol γ and mtSSB from both *Drosophila melanogaster* and humans. Despite the fact that similar approaches can be used for purifying the homologous proteins, we have observed that there are differences in the behavior of the proteins in some specific steps that may reflect differences in their structural and biochemical properties. Their purification in homogeneous, active form represents the first step towards our long-term goal to understand their biochemistry, biology, and functions at the mitochondrial DNA replication fork.

Introduction

Animal mitochondrial DNA (mtDNA) is a circular, compact, double-stranded molecule of about 16 kb, whose gene content is a remnant of the genome of the α-proteobacterium that was incorporated by a nucleated cell early in the evolution of the eukaryotes, according to the endosymbiont theory of mitochondrial origin (Gray *et al.* 1999). Because mitochondria retain a genome with genes essential for energy production in eukaryotic cells, they require enzyme systems for mtDNA replication and expression. So far, only three nuclear-encoded proteins have been identified at the mtDNA replication fork in animal cells: DNA polymerase γ, the mitochondrial single-stranded DNA-binding protein, and the Twinkle DNA helicase. Together these proteins function to synthesize and proofread new DNA strands, destabilize the DNA helix and protect single-stranded DNA regions, and unwind the duplex DNA, respectively (Kaguni 2004, Korhonen *et al.* 2004).

After the first identification in animal cells and through the development of purification strategies for the enzyme, the biochemical and structural properties of pol γ have been studied in a number of organisms, with an emphasis on *Drosophila melanogaster* and humans (Kaguni 2004, Fan *et al.* 2006, Fan and Kaguni 2001, Yakubovskaya *et al.* 2006). The *Drosophila* pol γ holoenzyme consists of a heterodimer of a catalytic subunit, pol γ-α, and an accessory subunit, pol γ-β (Kaguni 2004). On the other hand, the human homologue comprises a catalytic core in a heterotrimeric complex with a dimer of the accessory subunit (Yakubovskaya *et al.* 2006, Lee *et al.* 2009). In both cases, pol γ-α retains 5'- 3' DNA polymerase and 3'-5' exonuclease activities, whereas pol γ-β is responsible for stimulating pol γ-α activity and enhancing holoenzyme processivity and DNA binding properties (Fan *et al.* 2006). Recently, some studies have stressed the importance of pol γ in human diseases and animal development: functional defects due to

mutations in human pol γ-α lead to mitochondrial disorders (Longley *et al.* 2005, Luoma *et al.* 2005); a mutation in *Drosophila* pol γ-α causes mitochondrial and nervous system dysfunction and developmental lethality in the larval third instar (Iyengar *et al.* 1999); site-directed mutagenesis of *Drosophila* pol γ-α and human pol γ-β alter enzyme activity, processivity, and DNA binding affinity (Fan *et al.* 2006, Luo and Kaguni 2005); and null mutations of *Drosophila* pol γ-β cause lethality during early pupation, concomitant with loss of mtDNA and mitochondrial mass, and reduced cell proliferation in the central nervous system (Iyengar *et al.* 2002).

mtSSBs share similar physical and biochemical properties with *Escherichia coli* SSB (Curth *et al.* 1994, Thommes *et al.* 1995), with which they exhibit a high degree of amino acid sequence conservation. Like *E. coli* SSB, mtSSBs are homotetramers of 13 to 16 kDa polypeptides. It has been demonstrated that *Drosophila* mtSSB can stimulate 15-20 fold *in vitro* DNA synthesis and the 3'-5' exonuclease activity of pol γ, in an assay that mimics lagging DNA strand synthesis in mitochondrial replication (Thommes *et al.* 1995, Farr *et al.* 1999). Furthermore, human mtSSB is able to stimulate specifically the unwinding activity of Twinkle helicase (Korhonen *et al.* 2003) and, along with pol γ and Twinkle helicase, reconstitute a minimal mtDNA replisome *in vitro* (Korhonen *et al.* 2004). The biochemical data are consistent with an important role for mtSSB in initiation and elongation of DNA strands in mtDNA replication, which has been documented genetically by the fact that an insertion in the third intron of the *Drosophila* gene (*lopo*, "*low power*") results in developmental lethality, concomitant with the loss of mtDNA and respiratory capacity (Maier *et al.* 2001). It is important to note the striking conservation of some biological processes from flies to humans. When a *Drosophila* homologue of an essential but poorly understood mammalian gene is identified, as

happens with a large number of mitochondrial genes, powerful genetic and molecular techniques available in *Drosophila* can be applied to its characterization (Fernández-Moreno *et al.* 2006).

In this chapter, we review the strategies our lab has developed over the years for purifying the recombinant forms of *Drosophila* pol γ and mtSSB (Farr *et al.* 1999, Wernette and Kaguni 1986, Wang and Kaguni 1999, Farr and Kaguni 2002a,b), and we include comparative schemes for purification of the human homologues (Fan *et al.* 2006, Luoma *et al.* 2005). Ziebarth and Kaguni (2009) address the approaches we have taken to study the human Twinkle helicase, the other major component of the mtDNA replication fork. With regard to the purification protocols presented, we have found that the chromatographic methods we employ are generally efficacious for proteins involved in nucleic acid metabolism. In addition, hydroxylapatite, double- and single-stranded DNA cellulose, ATP agarose and protein affinity chromatography resins, as used for the purification of the native forms of *Drosophila* pol γ and mtSSB (Farr and Kaguni 2002a,b), are also generally useful. However, the production of a C-terminally histidine-tagged pol γ-α and consequently, the use of nickel-nitrilotriacetic acid (Ni-NTA) agarose chromatography have facilitated the purification of the recombinant protein by reducing the number of chromatographic steps required to achieve homogeneity. The order of use can be varied to good purpose but as a rule of thumb, phosphocellulose as a first step is effective to eliminate ~90% of bulk mitochondrial protein while retaining nucleic acid binding proteins, and velocity sedimentation is useful as a final step to remove adventitious nuclease activities that are invariably of low molecular mass, and to remove any small ligands introduced in affinity chromatography steps. Furthermore, different from its *Drosophila* homologue because the human pol γ-β dimer does not require co-overexpression with pol γ-α to obtain a soluble form, we have benefited by use of *Escherichia coli* as the overexpression system, as we have

done for overexpression of both fly and human mtSSBs. In principle, after preparation of a soluble fraction, a single chromatographic step combined with a final step of velocity sedimentation is sufficient to obtain highly pure proteins. Velocity sedimentation is of course also useful to link activity and polypeptide profiles, and to obtain an *S* value of the protein of interest to help in the determination of subunit structure. Again, these approaches can be used as general guidelines for proteins involved in mitochondrial nucleic acid metabolism. The authors are please to address any queries by electronic mail and wish all success in the development of new purification strategies.

Materials

Recombinant Drosophila melanogaster *DNA polymerase γ purification*

The ionic strength of all buffers is determined using a Radiometer conductivity meter.

1. Construction of recombinant transfer vectors and baculoviruses encoding the two subunits of *Drosophila melanogaster* pol γ is described in Wang and Kaguni (1999). Briefly, the complete coding sequences were cloned into the baculovirus transfer vector pVL1392/1393 (PharMingen) and viruses were constructed using linearized wild-type baculovirus AcMNPV DNA (BaculoGold) (PharMingen). The recombinant baculoviruses used here, $\alpha_{C\text{-}HIS}$ (α with a C-terminal hexahistidine tag inserted between Ser1145 and the stop codon) and β may be obtained from the authors.
2. *Sf9* (*Spodoptera frugiperda*) cells (PharMingen).
3. TC-100 insect cell culture medium and fetal bovine serum (GIBCO-BRL).
4. Insect cell transfection buffer and Grace's medium (PharMingen).

5. Phosphate-buffered saline (PBS): 135 mM NaCl, 10 mM Na_2HPO_4, 2mM KCl, 2 mM KH_2PO_4.

6. Phosphocellulose P-11 (Whatman), prepared according to the manufacturer's directions.

7. Ni-NTA agarose (QIAGEN).

8. 3 M Ammonium sulfate [$(NH_4)_2SO_4$], ultrapure.

9. 1 M Sucrose, ultrapure.

10. 1 M HEPES-OH, pH 8.0, stored at 4^oC.

11. 1 M Tris-HCl, pH 7.5.

12. 0.5 M Ethylenediaminetetraacetic acid (EDTA), pH 8.0.

13. 1 M Dithiothreitol (DTT). Store aliquots at -20^oC.

14. 2-Mercaptoethanol.

15. 1 M Imidazole.

16. 10% Triton X-100.

17. 2 M Potassium chloride (KCl).

18. 1 M Potassium phosphate (K_2HPO_4/KH_2PO_4), pH 7.6.

19. 5 M Sodium chloride (NaCl).

20. Phenylmethylsulfonyl fluoride (PMSF) (Sigma) prepared as a 0.2 M stock solution in isopropyl alcohol and stored at -20^oC.

21. Sodium metabisulfite is prepared as a 1.0 M stock solution at pH 7.5 and stored at -20^oC.

22. Leupeptin is prepared as a 1 mg/ml stock solution in 50 mM Tris-HCl, pH 7.5, and 2mM EDTA, and stored at -20^oC.

23. 7 mL Dounce homogenizer.

24. Collodion membranes (Schleicher & Schuell).

25. Polyallomer centrifuge tubes (14 x 89 mm, Beckman).

26. All potassium phosphate buffers are at pH 7.6.

27. All buffers used throughout the purification contain 5 mM 2-mercaptoethanol, 1 mM phenylmethylsulfonyl fluoride (PMSF), 10 mM sodium metabisulfite, and leupeptin at 2 μg/ml. Where indicated, buffers also contain 0.015% Triton X 100.

28. Homogenization buffer (50 mM Tris-HCl, pH 7.5, 100 mM KCl, 280 mM ultrapure sucrose, 5 mM EDTA).

29. 10 mM potassium phosphate buffer (10 mM potassium phosphate, pH 7.6, 20% glycerol).

30. 80 mM potassium phosphate buffer – phospho-cellulose equilibration buffer (80 mM potassium phosphate, pH 7.6, 20% glycerol).

31. 100 mM potassium phosphate buffer – phospho-cellulose wash buffer (100 mM potassium phosphate, pH 7.6, 20% glycerol).

32. 150 mM potassium phosphate buffer – phospho-cellulose elution buffer (150 mM potassium phosphate, pH 7.6, 20% glycerol).

33. 350 mM potassium phosphate buffer – phospho-cellulose elution buffer (350 mM potassium phosphate, pH 7.6, 20% glycerol).

34. 600 mM potassium phosphate buffer – phospho-cellulose elution buffer (600 mM potassium phosphate, pH 7.6, 20% glycerol).

35. Ni-NTA agarose equilibration buffer (20 mM Tris-HCl, pH 7.5, 500 mM KCl, 8% glycerol, and 5 mM imidazole).

36. Ni-NTA agarose elution buffer 1 (20 mM Tris-HCl, pH 7.5, 500 mM KCl, 8% glycerol, and 25 mM imidazole).
37. Ni-NTA agarose elution buffer 2 (20 mM Tris-HCl, pH 7.5, 500 mM KCl, 8% glycerol, and 250 mM imidazole).
38. Ni-NTA agarose elution buffer 3 (20 mM Tris-HCl, pH 7.5, 500 mM KCl, 8% glycerol, and 500 mM imidazole).
39. Glycerol gradient buffer (50 mM potassium phosphate, pH 7.6, 200 mM $(NH_4)_2SO_4$, 0.015% Triton X-100).
40. Stabilization buffer (25 mM HEPES, pH 8.0, 2 mM EDTA, 80% glycerol, 0.015% Triton X-100).

Recombinant human DNA polymerase γ-α purification

1. Human $\alpha_{C\text{-}HIS}$ recombinant baculovirus encoding the catalytic subunit of human pol γ was obtained from Dr. William C. Copeland, Laboratory of Molecular Genetics, National Institutes of Environmental Health Sciences, Research Triangle Park, NC.
2. All potassium phosphate buffers are at pH 7.6.
3. All buffers used throughout the purification contain 5 mM 2-mercaptoethanol, 1 mM phenylmethylsulfonyl fluoride (PMSF), 10 mM sodium metabisulfite, and leupeptin at 2 μg/ml. Where indicated, buffers also contain 0.015% Triton X 100.
4. Homogenization buffer (50 mM Tris-HCl, pH 7.5, 100 mM KCl, 5 mM EDTA).
5. 10 mM potassium phosphate buffer (10 mM potassium phosphate, pH 7.6, 20% glycerol).
6. 80 mM potassium phosphate buffer – phospho-cellulose equilibration buffer (80 mM potassium phosphate, pH 7.6, 20% glycerol).

7. 100 mM potassium phosphate buffer – phospho-cellulose wash buffer (100 mM potassium phosphate, pH 7.6, 20% glycerol).
8. 150 mM potassium phosphate buffer – phospho-cellulose elution buffer (150 mM potassium phosphate, pH 7.6, 20% glycerol).
9. 350 mM potassium phosphate buffer – phospho-cellulose elution buffer (350 mM potassium phosphate, pH 7.6, 20% glycerol).
10. 600 mM potassium phosphate buffer – phospho-cellulose elution buffer (600 mM potassium phosphate, pH 7.6, 20% glycerol).
11. Ni-NTA agarose equilibration buffer (20 mM Tris-HCl, pH 7.5, 500 mM KCl, 8% glycerol, 0.1% Tx-100, and 5 mM imidazole).
12. Ni-NTA agarose elution buffer 1 (20 mM Tris-HCl, pH 7.5, 500 mM KCl, 8% glycerol, and 25 mM imidazole).
13. Ni-NTA agarose elution buffer 2 (20 mM Tris-HCl, pH 7.5, 500 mM KCl, 8% glycerol, and 250 mM imidazole).
14. Ni-NTA agarose elution buffer 3 (20 mM Tris-HCl, pH 7.5, 500 mM KCl, 8% glycerol, and 500 mM imidazole).
15. Glycerol gradient buffer (30 mM Tris-HCl, pH 7.5, 100 mM KCl, 2 mM EDTA).
16. Stabilization buffer (25 mM HEPES, pH 8.0, 2 mM EDTA, 80% glycerol, 0.015% Triton X-100).
17. Other materials are as in the previous sub-session.

DNA polymerase assay

1. Pol γ, approx 0.1 unit/mL.

2. DNase-I activated calf thymus DNA, 2 mg/ml stock, prepared as described (Fansler and Loeb 1974).

3. 5X Polymerase buffer (250 mM Tris-HCl, pH 8.5, 20 mM $MgCl_2$, 2 mg/ml BSA).

4. 1 M DTT (Sigma).

5. 2 M KCl.

6. Stock mix of deoxynucleoside triphosphates containing 1mM each of dGTP, dATP, dCTP and dTTP (Amersham Pharmacia Biotech).

7. [^{3}H]-dTTP (ICN Biochemicals).

8. 100% Trichloroacetic acid (TCA).

9. 0.1 M Sodium pyrophosphate (NaPPi).

10. Acidic wash solution (1 M HCl, 0.1 M NaPPi).

11. 95% Ethanol.

12. Glass fiber filter paper (Schleicher and Schuell).

13. 10 X 75 mm disposable culture tubes (Fisher).

Recombinant human DNA polymerase γ-β purification

1. pQESL encoding the human pol γ-β without the mitochondrial presequence was obtained from Dr. William C. Copeland, Laboratory of Molecular Genetics, National Institutes of Environmental Health Sciences, Research Triangle Park, NC.

2. *Escherichia coli* (*E. coli*) XL-1 Blue.

3. Bacterial media (L broth): 1% tryptone (Difco), 0.5% yeast extract (Difco), 0.5% NaCl, pH 7.5.

4. 100 mg/mL Ampicillin. Filter-sterilize with a 0.2-µm syringe filter, aliquot, and store at -20^{o}C.

5. 10 mg/mL Tetracycline in 70% Ethanol. Filter-sterilize with a 0.2-µm syringe filter, aliquot, and store at -20^{o}C.

6. 100 mM Isopropyl-ß-D-thiogalactopyranoside (IPTG). Aliquot and store at -20^{o}C.

7. Ultrasonic Processor model W-225 (Heat Systems, Ultrasonics, Inc.).

8. 1 M Tris-HCl, pH 7.5.

9. 0.5 M EDTA, pH 8.0.

10. 5 M NaCl.

11. 3 M KCl.

12. 1 M Potassium phosphate (K_2HPO_4/KH_2PO_4), pH 7.6.

13. 100% Glycerol, anhydrous (J. T. Baker).

14. 80% Sucrose, ultrapure.

15. 0.2 M Phenylmethylsulfonyl fluoride (PMSF) in isopropanol. Store aliquots at -20^{o}C.

16. 1 M sodium metabisulfite, prepared as a 1.0 M stock solution at pH 7.5 and stored at -20^{o}C.

17. Leupeptin is prepared as a 1 mg/mL stock solution in 50 mM Tris-HCl, pH 7.5, 2 mM EDTA, and stored at -20^{o}C.

18. 1 M Imidazole.

19. 10% Sodium dodecyl sulfate (SDS).

20. 5X SDS loading buffer (50% glycerol, 2 M Tris base, 0.25 M DTT, 5% SDS, 0.1% bromophenol blue). Aliquots are stored at -20^{o}C.

21. 10% SDS-polyacrylamide resolving gels (8 cm X 10 cm X 1 mm) with 4% stacking gels.

22. Polyallomer centrifuge tubes (14 x 89 mm, Beckman).

23. Ni-NTA Agarose (QIAGEN).

24. All buffers used throughout the purification contain 5 mM 2-mercaptoethanol, 1 mM phenylmethylsulfonyl fluoride (PMSF), 10 mM sodium metabisulfite, and leupeptin at 2 μg/ml.

25. Tris-sucrose buffer (50 mM Tris-HCl, pH 7.5, 10% sucrose).

26. Resuspension buffer (35 mM Tris-HCl, pH 7.5, 150 mM NaCl, 25 mM imidazole, 0.1% (v/v) Triton X-100).

27. Ni-NTA agarose equilibration buffer (35 mM Tris-HCl, pH 7.5, 500 mM KCl, 25 mM imidazole).

28. Ni-NTA agarose elution buffer 1 (35 mM Tris-HCl, pH 7.5, 500 mM KCl, 25 mM imidazole).

29. Ni-NTA agarose elution buffer 2 (35 mM Tris-HCl, pH 7.5, 500 mM KCl, 250 mM imidazole).

30. Ni-NTA agarose elution buffer 3 (35 mM Tris-HCl, pH 7.5, 500 mM KCl, 500 mM imidazole).

31. Glycerol gradient buffer (35 mM Tris-HCl, pH 7.5, 100 mM NaCl, 1 mM EDTA).

Recombinant Drosophila *mtSSB purification*

1. pET-11a encoding *Drosophila* mtSSB without the mitochondrial presequence, available from this lab.

2. *E. coli* BL21 (lDE3) pLysS (Stratagene).

3. Bacterial media (L broth): 1% tryptone (Difco), 0.5% yeast extract (Difco), 0.5% NaCl, pH 7.5.

4. 100 mg/mL Ampicillin. Filter-sterilize with a 0.2-µm syringe filter, aliquot, and store at -20^{o}C.

5. 100 mM IPTG. Aliquot and store at -20^{o}C.

6. 1 M Tris-HCl, pH 7.5.

7. 0.5 M EDTA, pH 8.0.

8. 5 M NaCl.

9. 3 M Sodium thiocyanate (NaSCN).

10. 1 M Potassium phosphate (K_2HPO_4/KH_2PO_4), pH 7.6.

11. 80% Sucrose, ultrapure.

12. 100% Glycerol, anhydrous (J. T. Baker).

13. 0.2 M Phenylmethylsulfonyl fluoride (PMSF) in isopropanol. Store aliquots at -20^{o}C.

14. 1 M sodium metabisulfite, prepared as a 1.0 M stock solution at pH 7.5 and stored at -20^{o}C.

15. Leupeptin is prepared as a 1 mg/mL stock solution in 50 mM Tris-HCl, pH 7.5, 2 mM EDTA, and stored at -20^{o}C.

16. 1 M DTT. Store aliquots at -20^{o}C.

17. 1 M Spermidine trihydrochloride ($SpCl_3$, Sigma). Store at -20^{o}C.

18. 3 M Ammonium sulfate [$(NH_4)_2SO_4$], ultrapure.

19. 100% TCA. Store at 0-4^{o}C.

20. 10% SDS.

21. 5X SDS loading buffer (50% glycerol, 2 M Tris base, 0.25 M DTT, 5% SDS, 0.1% bromophenol blue). Aliquots are stored at -20^{o}C.

22. 17% SDS-polyacrylamide resolving gels (8 cm X 10 cm X 1 mm) with 4% stacking gels.

23. 5% Tween 20.

24. Centricon-30 spin concentrators (Amicon/Millipore).

25. Polyallomer centrifuge tubes (14 x 89 mm, Beckman).

26. Blue Sepharose CL-6B (Amersham Pharmacia Biotech).

27. All buffers used throughout the purification contain 1 mM phenylmethylsulfonyl fluoride (PMSF), 10 mM sodium metabisulfite, leupeptin at 2 μg/ml, and 2 mM DTT.

28. Tris-sucrose buffer (50 mM Tris-HCl, pH 7.5, 10% sucrose).

29. 5X Lysis buffer (1.25 M NaCl, 25 mM DTT, 100 mM $SpCl_3$, 10 mM EDTA, 1.5 mg/mL lysozyme).

30. Dilution buffer (30 mM Tris-HCl, pH 7.5, 10% glycerol, 2 mM EDTA)

31. Blue Sepharose equilibration buffer (30 mM Tris-HCl, pH 7.5, 10% glycerol, 100 mM NaCl, 2 mM EDTA).

32. Blue Sepharose wash buffer (30 mM Tris-HCl, pH 7.5, 10% glycerol, 800 mM NaCl, 2 mM EDTA).

33. Blue Sepharose elution buffer 1 (30 mM Tris-HCl, pH 7.5, 10% glycerol, 0.5 M NaSCN, 2 mM EDTA).

34. Blue Sepharose elution buffer 2 (30 mM Tris-HCl, pH 7.5, 10% glycerol, 1 M NaSCN, 2 mM EDTA).

35. Blue Sepharose elution buffer 3 (30 mM Tris-HCl, pH 7.5, 10% glycerol, 1.5 M NaSCN, 2 mM EDTA).

36. Glycerol gradient buffer (50 mM Tris-HCl, pH 7.5, 200 mM $(NH_4)_2SO_4$, 2 mM EDTA).

Recombinant human mtSSB purification

1. pET-11a encoding the human mtSSB without the mitochondrial presequence (beginning with the amino acid sequence: ESETTTSLV), available from this lab.
2. All buffers used throughout the purification contain 1 mM phenylmethylsulfonyl fluoride (PMSF), 10 mM sodium metabisulfite, leupeptin at 2 μg/ml, and 2 mM DTT.
3. Tris-sucrose buffer (50 mM Tris-HCl, pH 7.5, 10% sucrose).
4. 5X Lysis buffer (1.25 M NaCl, 25 mM DTT, 100 mM $SpCl_3$, 10 mM EDTA, 1.5 mg/mL lysozyme).
5. Dilution buffer (30 mM Tris-HCl, pH 7.5, 10% glycerol, 2 mM EDTA)
6. Blue Sepharose equilibration buffer (30 mM Tris-HCl, pH 7.5, 10% glycerol, 100 mM NaCl, 2 mM EDTA).
7. Blue Sepharose wash buffer (30 mM Tris-HCl, pH 7.5, 10% glycerol, 250 mM NaCl, 2 mM EDTA).
8. Blue Sepharose elution buffer 1 (30 mM Tris-HCl, pH 7.5, 10% glycerol, 400 mM NaCl, 2 mM EDTA).
9. Blue Sepharose elution buffer 2 (30 mM Tris-HCl, pH 7.5, 10% glycerol, 700 mM NaCl, 2 mM EDTA).
10. Blue Sepharose elution buffer 3 (30 mM Tris-HCl, pH 7.5, 10% glycerol, 1.5 M NaCl, 2 mM EDTA).

11. Glycerol gradient buffer (35 mM Tris-HCl, pH 7.5, 150 mM NaCl, 2 mM EDTA).

12. Other materials are as in previous sub-session.

Methods

Purification of recombinant Drosophila *DNA polymerase γ*

Sf*9 cell growth and soluble cytoplasmic fraction preparation*

1. Grow *Sf9* cells (500 ml) in TC-100 insect cell culture medium containing 10% fetal bovine serum at 27^{o}C to a cell density of 2 x 10^{6}, dilute to a cell density of 1 x 10^{6} with TC-100 containing 10% fetal bovine serum, and then infect with recombinant *Drosophila* pol γ-$\alpha_{C\text{-}HIS}$ and -β baculoviruses at a multiplicity of infection of 5. Harvest 48 h postinfection.
2. Pellet the cells at 400 x*g* for 5 min, wash with an equal volume of cold PBS, repeat the centrifugation and discard the supernatant.
3. Resuspend the cell pellet (approx 1 x 10^{9} cells) using 0.01 culture volume of homogenization buffer.
4. Lyse cells by 20 strokes in a Dounce homogenizer.
5. Centrifuge the homogenate at 1000 x*g* for 7 min.
6. Resuspend the resulting pellet using 0.005 culture volume of homogenization buffer and rehomogenize and centrifuge as in steps 4 and 5 (see Note 1).
7. Centrifuge the combined supernatant fractions at 8,000 x*g* for 15 min to pellet the mitochondria.
8. Remove the supernatant and centrifuge at 100,000 x*g* for 30 min to obtain the cytoplasmic soluble fraction (fraction I).

Phosphocellulose Chromatography and Ammonium Sulfate Fractionation

1. Adjust fraction I (70-90 mg protein) to an ionic equivalent of 80 mM potassium phosphate and load onto a phosphocellulose column equilibrated with 80 mM potassium phosphate buffer at a packing ratio of 6 mg protein per packed mL of resin, at a flow rate of 0.8 column volume (CV)/h (see Note 2).
2. Wash the column with 3 CV of 100 mM potassium phosphate buffer at a flow rate of 2 CV/h.
3. Elute proteins with a 3-CV linear gradient from 150 to 350 mM potassium phosphate buffer at a flow rate of 2 CV/h.
4. Follow the gradient with a 2-CV high-salt wash of 600 mM potassium phosphate buffer at the same flow rate.
5. Assay as described in DNA polymerase assay session, and pool active fractions (fraction II, see Note 3). Adjust to a final concentration of 10% sucrose.
6. Add solid ammonium sulfate (0.351 g/mL of fraction II) and incubate overnight on ice (see Note 4).
7. Collect the precipitate by centrifugation at 100,000 x*g* for 30 min at 4^{o}C.
8. Resuspend the pellet in 0.05-0.1 volume of fraction II with 10 mM potassium phosphate buffer containing 45% glycerol, and store at -20^{o}C (fraction IIb).

Ni-NTA agarose affinity purification

1. Dialyze fraction IIb (3-5 mg protein) against 10 mM potassium phosphate buffer in a collodion bag (M_r cutoff 25,000 kDa) until an ionic equivalent of 100 mM KCl is reached.

2. Mix dialyzed fraction IIb with 500 mL of precharged Ni-NTA agarose (QIAGEN) equilibrated in Ni-NTA agarose equilibration buffer.
3. Incubate the suspension for 10 h on ice with gentle shaking.
4. Allow the beads to settle and then wash twice with 1 mL of equilibration buffer for 30 min with gentle shaking.
5. Pack washed beads into a column (0.5 ml), and elute protein retained on the beads successively at 5 CV/h with elution buffer containing 25 mM imidazole (2 CV), 250 mM imidazole (2 CV) and 500 mM imidazole (2 CV). Collect 1/4-CV fractions.
6. Assay and pool active fractions (fraction III, approx 0.9 mL).

Glycerol gradient sedimentation

1. Layer fraction III onto two preformed 12-30% glycerol gradients prepared in polyallomer tubes for use in a Beckman SW 41 rotor.
2. Centrifuge at 140,000 x*g* for 60 h at 4^{o}C, and then fractionate by collecting five drop (200-300 ml) fractions.
3. Assay and pool active fractions, then add an equal volume of stabilization buffer and store the enzyme (fraction IV) at -20^{o}C, -80^{o}C, or under liquid nitrogen.

Purification of recombinant human DNA polymerase γ-α

Sf9 cell growth and soluble cytoplasmic fraction preparation

1. Grow and dilute *Sf9* cells (500 ml) as described in step 1 of previous sub-session, and then infect with recombinant human pol γ-$\alpha_{C\text{-}HIS}$ at a multiplicity of infection of 5. Harvest 48 h postinfection.
2. Pellet the cells at 400 x*g* for 5 min and wash with an equal volume of cold PBS, repeat the centrifugation and discard the supernatant.
3. Resuspend the cell pellet (approx 1 x 10^9 cells) using 0.03 culture volume of homogenization buffer.
4. Lyse cells by 20 strokes in a Dounce homogenizer.
5. Centrifuge the homogenate at 1,000 x*g* for 7 min.
6. Resuspend the resulting pellet using 0.01 culture volume of homogenization buffer, rehomogenize and centrifuge as in steps 4 and 5 (see Note 1).
7. Follow steps 7 and 8 of previous sub-session to obtain the cytoplasmic soluble fraction (fraction I).

Phosphocellulose chromatography and ammonium sulfate fractionation

1. Adjust fraction I (140-240 mg protein) to an ionic equivalent of 80 mM potassium phosphate and load onto a phosphocellulose column equilibrated with 80 mM potassium phosphate buffer at a packing ratio of 6 mg protein per packed mL of resin, at a flow rate of 0.8 CV/h (see Note 2).
2. Wash the column and elute proteins as described in steps 2-4 of previous sub-session.
3. Assay and pool active fractions (fraction II, see Note 3) and adjust to a final concentration of 10% sucrose.
4. Precipitate and pellet proteins as described in steps 6 and 7 of previous sub-session.

5. Resuspend the pellet in 0.05-0.1 volume of fraction II in 10 mM potassium phosphate buffer containing 45% glycerol, and store at -20^{o}C (fraction IIb).

Ni-NTA affinity chromatography

1. Dialyze fraction IIb (10-20 mg protein) against 10 mM potassium phosphate buffer in a collodion bag (M_r cutoff 10,000 kDa) until an ionic equivalent of approx 300-400 mM KCl is reached.
2. Load dialyzed fraction IIb onto an equilibrated Ni-NTA resin at a ratio of approx 7.5 mg protein per mL of packed resin, at a flow rate of 1-2 CV/h.
3. Wash the column with 2 CV of equilibration buffer and elute successively with elution buffers containing 25 mM imidazole (2 CV), 250 mM imidazole (2 CV) and 500 mM imidazole (2 CV), at a flow rate of 5 CV/h. Collect 1/4-CV fractions.
4. Assay and pool active fractions (fraction III, approx 1.6-2.3 mL).

Glycerol gradient sedimentation

1. Layer fraction III onto two preformed 12-30% glycerol gradients prepared in polyallomer tubes for use in a Beckman SW 41 rotor.
2. Centrifuge at 140,000 x*g* for 60 h at 4^{o}C, then fractionate by collecting five drop (200-300 ml) fractions.
3. Assay and pool active fractions, then add an equal volume of glycerol gradient buffer containing 80% glycerol or stabilization buffer, and store the enzyme (fraction IV) at -20^{o}C, -80^{o}C, or under liquid nitrogen.

DNA Polymerase Assay

This section describes an assay of DNA synthesis that utilizes a multiply-primed double-stranded DNA substrate and pol γ fractions. DNA polymerase activity can be measured at different salt concentrations to discriminate nuclear (low-salt stimulated) and mitochondrial (high-salt stimulated) DNA polymerase activities. The assay measures the incorporation of [^{3}H]-labeled dTMP into the DNA substrate, such that 1 unit of activity is that amount that catalyzes the incorporation of 1 nmol of deoxyribonucleoside triphosphate into acid insoluble material in 60 min at 30^{o}C.

1. Adjust the water bath to 30^{o}C.
2. Dry down the radioactive substrate by lyophilizing to less than half the original volume.
3. Prepare a master reaction mix using the stock solutions in Materials session in a microcentrifuge tube on ice such that each reaction (0.05 ml) contains 1X polymerase buffer, 10 mM DTT, 200 mM KCl (see Note 5), 30 μM each of dGTP, dATP, dCTP, and [^{3}H]dTTP (1000 cpm/pmol), and 250 mg/ml DNase I-activated calf thymus DNA. Vortex and spin briefly in the microcentrifuge.
4. Dispense the mix, 49 μL, to prechilled and numbered 10 X 75-mm tubes on ice.
5. Add the enzyme, approx 0.1 unit, to each tube avoiding bubbles and mix gently by flicking the tube three times.
6. Incubate the tubes for 30 min at 30^{o}C, then transfer to ice.
7. Stop the reactions with 1 ml of 10% TCA, 0.1 M NaPPi, mix, and leave on ice ≥ 5 minutes.

8. Filter samples through glass fiber filters. Wash the tube twice with acidic wash solution, then wash the filtration funnel three times with acidic wash solution and once with 95% ethanol.
9. Dry the filters under a heat lamp for approx 5 min, then count in scintillation fluid in a liquid scintillation counter.
10. Spot 1-2 µL of mix directly onto filters, dry, and count in scintillation fluid without filtration, to calculate the specific radioactivity of the mix.

Purification of recombinant human DNA polymerase γ-β

Bacterial cell growth and protein overproduction

1. Inoculate 2 L of L broth containing 15 µg/mL tetracycline and 100 µg/mL ampicillin with *E. coli* XL-1 Blue containing pQESL (complete human pol γ-β cDNA without the mitochondrial presequence) at A_{595} = 0.06 and grow with aeration at 37^{o}C (see Note 6).

2. At A_{595} = 0.6:

   a) Remove a 1.0-mL aliquot of uninduced cells to a microcentrifuge tube, pellet cells, aspirate supernatant, and resuspend cells in 200 µL of 1X SDS loading buffer. Use a 10-µL aliquot as control for SDS-PAGE.

   b) Induce target protein expression by adding IPTG to 0.3 mM final concentration and continue incubation at 37^{o}C with aeration for 2 hr.

3. Harvest cells:

   a) Save a 1.0-mL aliquot of induced cells as in step 2a. Use a 5-µL aliquot in SDS-PAGE.

   b) Harvest remaining cells in Sorvall GSA bottles by centrifugation at 3,600 x*g* for 5 min at 4^{o}C. Decant supernatant.

4. Resuspend cells in 1/10 volume of original culture in Tris-sucrose buffer. First resuspend pellets in one-half of the total resuspension volume, transferring to a chilled plastic beaker. Wash GSA bottles with remaining one-half of volume and combine.
5. Centrifuge washed cells in a Sorvall SS-34 at 3,000*g* for 5 min at 4^{o}C. Aspirate supernatant and freeze cell pellet in liquid nitrogen. Store at -80^{o}C.

Cell lysis and soluble fraction preparation

The following protocol uses a 2-L induced cell pellet (A_{595} = 1-1.2) as the starting material with an overall expression of approx 200 μg pol γ-β/mL of induced cells. The ionic strength of buffers is determined using a Radiometer conductivity meter (see Note 1).

1. Thaw cell pellet (2 L) on ice at least 30 min.
2. Resuspend cell pellet completely in 1/30 volume of original cell culture in resuspension buffer. Use one-half of the total volume to resuspend the cells and the remaining one-half divided to wash the tubes, combining all samples.
3. Lyse cells by sonication with an Ultrasonic Processor model W-225 for 20 pulses using microtip at maximum output and 50% usage. Cool the samples at least 1 min on ice. Repeat sonication and cooling (see Note 7).
4. Centrifuge in a Sorvall SS-34 rotor at 20,000 x*g* for 15 min at 4^{o}C.
5. Collect supernatant by pipetting into a fresh tube. Resuspend resulting pellet in 1/80 volume of original cell culture in resuspension buffer, sonicate and centrifuge as described in steps 3 and 4.
6. Collect supernatant and combine with the previous one (fraction I).

Ni-NTA chromatography and glycerol gradient sedimentation

The following protocol uses a soluble bacterial fraction from 2 L of induced cells loaded onto an equilibrated Ni-NTA column.

1. Load fraction I onto an equilibrated Ni-NTA resin at a ratio of approx 7.5 mg protein per mL of packed resin, at a flow rate of 2 CV/h.
2. Elute protein by successive washes with elution buffers containing 25 mM imidazole (3 CV), 250 mM imidazole (2 CV) and 500 mM imidazole (2 CV), at a flow rate of 2 CV/h. Collect 1/2-CV fractions for the first elution, 1/6-CV fractions for the second elution, and then 1/3-CV fractions for the last elution.
4. Analyze column fractions, 5 µl, by SDS-PAGE in 10% gels followed by silver nitrate staining.
5. Pool fractions containing pol γ-β (fraction II, approx 1.6-2.3 mL).
6. Prepare two (10-mL) 12-30% glycerol gradients and chill on ice at least 1 hour.
7. Layer 1-1.2 ml of Ni-NTA pool of pol γ-β onto each gradient and spin in a SW41 rotor at 170,000 x*g* for 60 hr at 4^{o}C.
8. Fractionate gradients by collecting 200-300-µl aliquots. Analyze 5 µL per fraction by SDS-PAGE in 10% gels followed by staining with silver nitrate.
9. Pool peak fractions of pol γ-β (fraction III). Pol γ-β typically sediments in fractions 10-16.
10. Aliquot pol γ-β, freeze in liquid nitrogen, and store at -80^{o}C (see Note 8).

Purification of recombinant Drosophila *mtSSB*

Bacterial cell growth and protein overproduction

1. Inoculate 1 L of L broth containing 100 μg/mL ampicillin with *E. coli* BL21 (lDE3) pLysS containing pET11a-*Drosophila* mtSSB (complete cDNA without the mitochondrial presequence) at A_{595} = 0.06 and grow with aeration at 37°C (see Note 6).

2. At A_{595} = 0.6:

   a) Remove a 1.0-mL aliquot of uninduced cells to a microcentrifuge tube, pellet cells, aspirate supernatant, and resuspend cells in 200 μL of 1X SDS loading buffer. Use a 10-μL aliquot as control for SDS-PAGE.

   b) Induce target protein expression by adding IPTG to 0.3 mM final concentration and continue incubation at 37°C with aeration for 2 hr.

3. Harvest cells:

   a) Save a 1.0-mL aliquot of induced cells as in step 2a. Use a 5-μL aliquot in SDS-PAGE.

   b) Harvest remaining cells in Sorvall GSA bottles by centrifugation at 3,600 x*g* for 5 min at 4°C. Decant supernatant.

4. Resuspend cells in 1/10 volume of original culture in Tris-sucrose buffer. First resuspend pellets in one-half of the total resuspension volume, transferring to a chilled plastic beaker. Wash GSA bottles with remaining one-half of volume and combine.

5. Aliquot washed cells into Sorvall SS-34 tubes, 200 mL cell equivalent per tube, and centrifuge cells at 3,000 x*g* for 5 min at 4°C. Aspirate supernatant and freeze cell pellets in liquid nitrogen. Store at -80°C.

Cell lysis and soluble fraction preparation

The following protocol uses 400-mL induced cell pellets (A_{595} = 1-1.2) as the starting material with an overall expression of 15 μg mtSSB/mL of induced cells. The ionic strength of buffers is determined using a Radiometer conductivity meter (see Note 2).

1. Thaw cell pellets (2 x 200 mL) on ice at least 30 min.
2. Resuspend cell pellets completely in 1/25 volume of Tris-sucrose buffer. Use one-half of the total volume to resuspend the cells and the remaining one-half divided to wash the tubes, combining all samples.
3. Add 5X lysis buffer to 1X final concentration. Incubate 30 min on ice, mixing every 5 min by inversion.
4. Freeze cell lysis suspension in liquid nitrogen. Thaw partially in ice water, then transfer to ice until thawed completely. Centrifuge in Sorvall SS-34 rotor at 17,500 x*g* for 30 min at 4^{o}C.
5. Collect soluble fraction (supernatant) by pipetting into a fresh tube. Adjust the sample to 100 mM NaCl by addition of dilution buffer.

Blue Sepharose chromatography and glycerol gradient sedimentation

The following protocol uses a soluble bacterial fraction from 400 mL of induced cells loaded onto 10 mL of equilibrated Blue Sepharose resin.

1. Load salt-adjusted soluble fraction (approx 15-20 mg protein) at a flow rate of 1 CV/hr onto a 10-mL column of Blue Sepharose equilibrated with 10 CV equilibration buffer.
2. Wash column with 4 CV of wash buffer at a flow rate of 2 CV/hr, collecting 1 CV fractions.
3. Elute column with three steps of increasing NaSCN stringency at 2 CV/hr:
   a) 4 CV of elution buffer containing 0.5 M NaSCN, collecting 1/2 CV fractions.
   b) 4 CV of elution buffer containing 1 M NaSCN, collecting 1/3 CV fractions.

c) 4 CV of elution buffer containing 1.5 M NaSCN, collecting 1/4 CV fractions.

Drosophila mtSSB elutes in the 1.5 M NaSCN step.

4. Analyze column fractions, 5 µl, by SDS-PAGE in 17% gels.
5. Pool fractions containing mtSSB and spin-concentrate sample in a Centricon-30 concentrator (pretreated with 5% Tween 20, see Note 9) to desalt. Exchange elution buffer for 50 mM potassium phosphate, pH 7.6, 8% glycerol, 200 mM $(NH_4)_2SO_4$, 2 mM EDTA.
6. Prepare three (10-mL) 12-30% glycerol gradients and chill on ice at least 1 hour.
7. Layer 1-1.2 ml of concentrated mtSSB pool onto each gradient and spin in SW41 rotor at 170,000 x*g* for 60 hr at 4^{o}C.
8. Fractionate gradients by collecting 200-300-µl aliquots. Analyze 30 µL per fraction by TCA precipitation followed by SDS-PAGE in 17% gels followed by staining with silver nitrate.
9. Pool peak fractions of tetrameric mtSSB, which typically sediments in fractions 25-31 (see Note 10). Concentrate gradient pool using a Centricon-30 spin concentrator (pre-treated with 5% Tween 20, see Note 9).
10. Aliquot concentrated mtSSB, freeze in liquid nitrogen, and store at -80^{o}C (see Note 8).

Purification of recombinant human mtSSB

Bacterial cell growth and protein overproduction

1. Inoculate 2 L of L broth containing 100 µg/mL ampicillin with *E. coli* BL21 (lDE3) pLysS containing pET11a-human mtSSB (complete cDNA without the mitochondrial presequence) at A_{595} = 0.06 and grow with aeration at 37^{o}C (see Note 6).
2. At A_{595} = 0.6:

a) Remove a 1.0-mL aliquot of uninduced cells to a microcentrifuge tube, pellet cells, aspirate supernatant, and resuspend cells in 200 µL of 1X SDS loading buffer. Use a 10-µL aliquot as control for SDS-PAGE.

b) Induce target protein expression by adding IPTG to 0.2 mM final concentration and continue incubation at 37^{o}C with aeration for 3 hr.

3. Harvest cells:

a) Save a 1.0-mL aliquot of induced cells as in step 2a. Use a 5-µL aliquot in SDS-PAGE. Stain the gel with Coomassie blue (see Note 11).

b) Harvest remaining cells in Sorvall GSA bottles by centrifugation at 3600 x*g* for 5 min at 4^{o}C. Decant supernatant.

4. Resuspend cells in Tris-sucrose buffer as described in step 4 of previous sub-session.

5. Centrifuge washed cells into a Sorvall SS-34 tube at 3000 x*g* for 5 min at 4^{o}C. Aspirate supernatant and freeze cell pellet in liquid nitrogen. Store at -80^{o}C.

Cell lysis and soluble fraction preparation

The following protocol uses 2-L induced cell pellet (A_{595} = 1-1.3) as the starting material with an overall expression of approx 250 µg mtSSB/mL of induced cells. The ionic strength of buffers is determined using a Radiometer conductivity meter (see Note 2).

1. Thaw cell pellet (2 L) on ice at least 30 min.

2. Resuspend cell pellet in Tris-sucrose buffer as described in step 2 of previous sub-session.

3. Follow steps 3-5 of previous sub-session to obtain soluble fraction (see Note 12). Adjust the sample to 100 mM NaCl by addition of dilution buffer.

Blue Sepharose chromatography and glycerol gradient sedimentation

The following protocol uses a soluble bacterial fraction from 2 L of induced cells loaded onto 10 mL of equilibrated Blue Sepharose resin.

1. Load salt-adjusted soluble fraction (approx 75 mg protein) at a flow rate of 1 CV/hr onto a 10-mL column of Blue Sepharose equilibrated with 10 CV equilibration buffer.
2. Wash column with 4 CV of wash buffer at a flow rate of 2 CV/hr, collecting 1 CV fractions.
3. Elute column with three steps of increasing NaCl stringency at 2 CV/hr:

   a) 4 CV of elution buffer containing 400 mM NaCl, collecting 1/2 CV fractions.

   b) 4 CV of elution buffer containing 700 mM NaCl, collecting 1/4 CV fractions.

   c) 4 CV of elution buffer containing 1.5 M NaCl, collecting 1/4 CV fractions.

   Human mtSSB elutes between the 700 mM and 1.5 M NaCl steps.
4. Analyze column fractions, 10 µl, by SDS-PAGE in 17% gels followed by Coomassie blue staining.
5. Pool fractions containing mtSSB and spin-concentrate sample in a Centricon-30 concentrator (pretreated with 5% Tween 20, see Note 9) to desalt. Use the dilution buffer to adjust the salt concentration of the sample to 100 mM NaCl.
6. Prepare two (10-mL) 12-30% glycerol gradients and chill on ice at least 1 hour.
7. Layer concentrated mtSSB pool onto each gradient, spin, and collect fractions as described in steps 7 and 8 of previous sub-session. Analyze 10 µL per fraction by SDS-PAGE in 17% gels followed by staining with Coomassie blue.
8. Pool peak fractions of tetrameric mtSSB, which typically sediments in fractions 20-31 (see Note 10).

9. Aliquot pooled mtSSB, freeze in liquid nitrogen, and store at -80^{o}C (see Note 8 and 13).

Notes

1. An aliquot of the homogenized cells can be analyzed under the microscope to check for cell lysis. If more than 10% of the cells are not lysed, the pellet may be resuspended, rehomogenized and centrifuged again as in steps 4-6.
2. All chromatographic and velocity sedimentation operations are performed at 0-4^{o}C.
3. In addition to the DNA polymerase assay, the fractions can be analyzed by immunoblotting and Bradford determination of protein concentration. These procedures may help to determine the fractions to be pooled.
4. Add 1/10 of the final amount of $(NH_4)_2SO_4$ and wait until the salt goes into solution. Repeat until the total amount has been added. The sample must be stirring during incubation.
5. For the purification of the human pol γ-α, prepare the master mix such that each reaction contains 60 mM KCl.
6. The volume of *E. coli* cell culture may vary from 1 to 2 L. The materials used for cell harvest and lysis may be adjusted proportionally.
7. Each time it is noticed that the samples are getting warm during sonication, stop pulses and cool them for 1 min on ice.
8. Alternatively, samples may be stabilized by the addition of an equal volume of stabilization buffer (20 mM KPO_4, pH 7.6, 80% glycerol, 2 mM EDTA) and stored at -20^{o}C.
9. Pretreatment consists of filling up the Centricon-30 tubes with 5% Tween 20 and allowing them to sit overnight at room temperature.

10. Avoid fractions that sediment slowly, trailing toward the top of the gradient. These fractions are likely to contain dimers and monomers of mtSSB.
11. It is important to stain the SDS-polyacrylamide gels used for human mtSSB analysis throughout the purification with Coomassie blue. We have observed that, especially for the gel analysis of the bacterial cell extract after induction with IPTG, a silver stained gel is not suitable for detection of human mtSSB.
12. To obtain the soluble fraction of mtSSB-expressing *E. coli* cells, we use 1.5 mg/mL lysozyme in the 5X lysis solution (final concentration in cell suspension: 0.3 mg/mL). In the Blue Sepharose chromatography step of the human mtSSB purification, we have observed that the lysozyme has the same elution profile of human mtSSB, constituting the major contaminant of the Blue Sepharose pool. Despite the fact that human mtSSB and lysozyme have similar sizes (approx 15 and 14 kDa, respectively), we are able to separate them in the glycerol gradient sedimentation step, because human mtSSB is a tetramer in solution and sediments as a 60 kDa protein. As an alternative cell lysis procedure, we have verified that a 5X buffer containing 1.25 M NaCl, 10 mM EDTA, and 10% sodium cholate [prepared as a 20% stock, pH 7.4, and stored at -20^{o}C (Cholic acid (Sigma) is dissolved in hot ethanol, filtered through Norit A (J.T. Baker Chemical Co.), and recrystallized twice before titration to pH 7.4 with sodium hydroxide)] is also very efficient (use final concentration of 1X buffer in the cell pellet suspension). Follow up the other steps as described in Purification of recombinant *Drosophila* mtSSB session. Interestingly, because human and *Drosophila* mtSSBs elute differently from the Blue Sepharose column, most of the lysozyme used in the purification of *Drosophila* mtSSB elutes during the wash of the column and does not constitute a major contaminant of the blue sepharose pool.

13. The purification procedure presented is suitable for most physical and biochemical experiments involving the human mtSSB, including analysis of quaternary structure, single-stranded DNA binding, pol γ stimulation, etc. However, we note that on occasion a double-stranded DNA-unwinding contaminant is present in the preparation, which is detected in mtDNA helicase stimulation assays (data not shown). This contaminant can be eliminated by the addition of a phosphocellulose chromatographic step prior to the glycerol gradient sedimentation, which is performed similarly to that described in Purification of recombinant *Drosophila* DNA polymerase γ session, with the following changes: the Blue Sepharose fraction is adjusted to an ionic equivalent of 60 mM potassium phosphate and loaded onto a phosphocellulose column equilibrated with 60 mM KPO_4, 10% glycerol, 2 mM EDTA, at a packing ratio of 0.5 mg protein/ packed mL; the column is washed with the same buffer and the protein is eluted with a gradient from 60 to 150 mM KPO_4, 10% glycerol, 2 mM EDTA, followed by a final elution step of 350 mM KPO_4, 10% glycerol, 2 mM EDTA.

CHAPTER 3

FUNCTIONAL ROLES OF THE N- AND C-TERMINAL REGIONS OF THE HUMAN MITOCHONDRIAL SINGLE-STRANDED DNA-BINDING PROTEIN

Summary

Biochemical studies of the mitochondrial DNA (mtDNA) replisome demonstrate that the mtDNA polymerase and the mtDNA helicase are stimulated by the mitochondrial single-stranded DNA-binding protein (mtSSB). Unlike *Escherichia coli* SSB, bacteriophage T7 gp2.5 and bacteriophage T4 gp32, mtSSBs lack a long, negatively charged C-terminal tail. Furthermore, additional residues at the N-terminus (notwithstanding the mitochondrial presequence) are present in the sequence of species across the animal kingdom. We sought to analyze the functional importance of the N- and C-terminal regions of the human mtSSB in the context of mtDNA replication. We produced the mature wild-type human mtSSB and three terminal deletion variants, and examined their physical and biochemical properties. We demonstrate that the recombinant proteins adopt a tetrameric form, and bind single-stranded DNA with similar affinities. They also stimulate similarly the DNA unwinding activity of the human mtDNA helicase (up to 8-fold). Notably, we find that unlike the high level of stimulation that we observed previously in the *Drosophila* system, stimulation of DNA synthesis catalyzed by human mtDNA polymerase is only moderate, and occurs over a narrow range of salt concentrations. Interestingly, each of the deletion variants of human mtSSB stimulates DNA synthesis at a higher level than the wild-type protein, indicating that the termini modulate negatively functional interactions with the mitochondrial replicase. We discuss our findings in the context of species-specific components of the mtDNA replisome, and in comparison with various prokaryotic DNA replication machineries.

Introduction

Single-stranded DNA-binding proteins (SSBs) are essential components in DNA metabolic processes, including replication, repair and recombination. In addition to their protective single-stranded DNA-coating properties, it has been demonstrated that SSBs from distantly-related species have far more complex roles that include the organization and/ or mobilization of all aspects of DNA metabolism (reviewed in Shereda *et al.* 2008). In eukaryotic cells, there are two compartmentalized SSBs: replication protein A (RPA) is found in the nucleus, whereas mtSSB is found in the mitochondrion. Despite sharing a similar single-stranded DNA-binding domain (oligonucleotide/oligosaccharide binding domain or OB-fold) together with bacterial and viral SSBs (Shamoo *et al.* 1995, Yang *et al.* 1997, Raghunathan *et al.* 1997, Bockharev *et al.* 1997, Hollis *et al.* 2001), and performing analogous functions in their respective cellular compartments, mtSSB and RPA are not related evolutionarily. mtSSBs are homologues of eubacterial SSBs, whose prototype is the well studied *Escherichia coli* SSB (*Ec*SSB) (Figure 5), a fact that is in agreement with the endosymbiont theory of mitochondrial origin (Gray *et al.* 1999).

At the mitochondrial DNA (mtDNA) replication fork, mtSSB interacts functionally with DNA polymerase γ (pol γ) and mtDNA helicase (also known as Twinkle) to promote mtDNA replication. *In vitro*, the *Drosophila melanogaster* mtSSB (*Dm*mtSSB) stimulates 15- to 20-fold the DNA polymerase and 3′-5′ exonuclease activities of *Drosophila* pol γ (*Dm*pol γ) on a singly-primed single-stranded DNA (ssDNA) template (Farr *et al.* 1999). The human mtSSB (*Hs*mtSSB) stimulates the DNA unwinding activity of the human mtDNA helicase (*Hs*mtDNA helicase) (Korhonen *et al.* 2003), and is required for strand-displacement DNA synthesis in the presence of human pol γ (*Hs*pol γ) and *Hs*mtDNA helicase (Korhonen *et al.* 2004). *In vivo*,

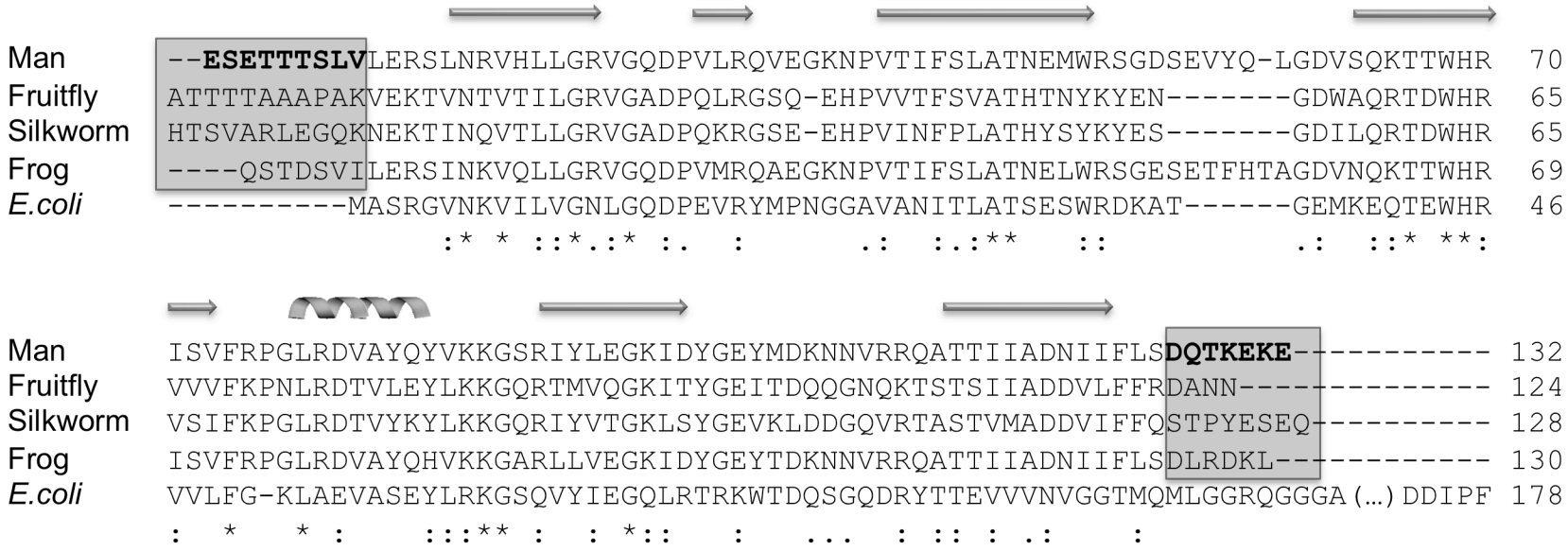

Figure 5. Sequence alignment of animal mtSSBs with *E. coli* SSB, and mutagenesis of *Hs*mtSSB. Thirteen mtSSB sequences (notwithstanding the mitochondrial presequence) from various species across the animal kingdom were aligned with the *E. coli* SSB sequence using Clustal X (Thompson *et al.* 1997). Only the representative mtSSB sequences from humans (GenBank accession: NP_003134), fruitfly (*Drosophila melanogaster*; GenBank accession: AAF16936), silkworm (*Bombyx mori*; GenBank accession: ABF51293), and frog (*Xenopus laevis*; GenBank accession: NP_001095241) are shown. The gray boxes denote the N- and C-terminal regions of animal mtSSB that are not conserved in *E. coli* SSB. The amino acid residues indicated in bold in the *Hs*mtSSB sequence were targeted for deletion mutagenesis. Amino acid residues 13-123 in the *Hs*mtSSB sequence comprise the OB-fold domain (see the text for details).

deleterious mutations in the mtSSB gene cause loss of mtDNA that results in developmental arrest in *Drosophila* (Maier *et al.* 2001), and growth limitation due to mitochondrial dysfunction in *Saccharomyces cerevisiae* (Van Dyck *et al.* 1992). Our group has shown that the knockdown of the endogenous *Dm*mtSSB in *Drosophila* Schneider cells results in mtDNA copy number reduction and growth retardation (Farr *et al.* 2004). The overexpression of the wild-type protein rescues the phenotype, whereas a ssDNA-binding mutant of *Dm*mtSSB is unable to do so. Very recently, the knockdown of *Hs*mtSSB in human HeLa cells was shown to promote a gradual decline in mtDNA copy number and a severe reduction in 7S DNA synthesis (Ruhanen *et al.* 2010).

In this Report, we examine the biochemical and physical properties of four *Hs*mtSSB proteins: the mature full-length protein (notwithstanding the mitochondrial presequence, *Hs*mtSSBwt), a deletion variant lacking the first 9 residues in the N-terminus (*Hs*mtSSBΔN), a deletion variant lacking the last 7 residues in the C-terminus (*Hs*mtSSBΔC), and a variant that lacks both termini (*Hs*mtSSBΔNΔC). The target regions are of particular interest for several reasons: 1) they represent two of the few regions of significant amino acid sequence variability between mtSSBs and bacterial SSBs – the N-terminal extension is absent in bacterial SSBs, whereas the C-terminus is short and uncharged in mtSSBs (Figure 5); 2) they appear disordered in the crystal structure of *Hs*mtSSB (Yang *et al.* 1997), suggesting flexibility and/or dynamism of these regions without apparent interactions with the ssDNA-binding domain; and 3) in *Ec*SSB, bacteriophage T7 gp2.5 and T4 gp32 SSBs, the C-terminal region interacts with other components of DNA metabolic processes, and regulates ssDNA binding negatively. We evaluate our findings in the context of functions at the mitochondrial replication fork, and discuss them in comparison with other DNA replication systems.

Results

Purification of amino- and carboxyl-terminal deletion variants of Hs*mtSSB, and determination of oligomeric state*

In order to study the possible roles of the N- and C-terminal regions of *Hs*mtSSB at the mtDNA replication fork, we produced three deletion variants together with *Hs*mtSSBwt: *Hs*mtSSBΔN, *Hs*mtSSBΔC, and *Hs*mtSSBΔNΔC. The overexpression of untagged recombinant proteins in *E. coli* using the pET-11a system resulted in high levels of soluble proteins, except for *Hs*mtSSBΔC; the extraction and solubility of *Hs*mtSSBΔC was dependent on inclusion of a dodecyl-maltoside detergent. From this point on, the purification of the proteins was identical. We modified earlier protocols for purification of *Dm*mtSSB (Farr *et al.* 1999) and *Hs*mtSSB (Oliveira and Kaguni 2009) in order to obtain highly pure proteins (Figure 6). In particular, substitution of velocity sedimentation, used previously as a final step, by phosphocellulose chromatography followed by assay of ATP-dependent dsDNA unwinding activity in each fraction, was a critical improvement towards the elimination of a highly active bacterial contaminant (see Materials and Methods session for details).

With near-homogeneous *Hs*mtSSBwt and the terminal deletion variants in hand, we evaluated the possible consequences of the lack of the termini on its physical and biochemical properties. SDS-PAGE of *Hs*mtSSBwt, ΔN, ΔC, and ΔNΔC reveals polypeptides of ~ 15, 14, 14, and 13 kDa, respectively (Figure 6). To investigate their oligomeric state in solution, we employed hydrodynamic methods to estimate native molecular mass. We observed single peaks for each recombinant protein both in velocity sedimentation and in Superdex 75 gel filtration (Figure 7). The sedimentation coefficient was 4.2 *S* for all of the proteins, and the Stokes' radii were 3.4, 3.2, 3.2, and 3.0 nm respectively for wild type, ΔN, ΔC, and ΔNΔC. Together, these

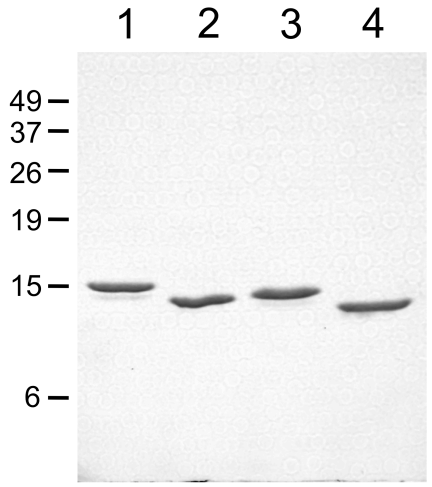

Figure 6. SDS-PAGE of terminal deletion variants of *Hs*mtSSB. Near-homogeneous fractions (~2 μg) of recombinant *Hs*mtSSBwt (*lane 1*), ΔN (*lane 2*), ΔC (*lane 3*), and ΔNΔC (*lane 4*) were subjected to SDS-PAGE in a 17% gel, followed by Coomassie blue staining as described under Materials and Methods. The sizes of molecular mass markers (BenchMark™ Pre-Stained Protein Ladder, Invitrogen™) are indicated in kDa at *left*.

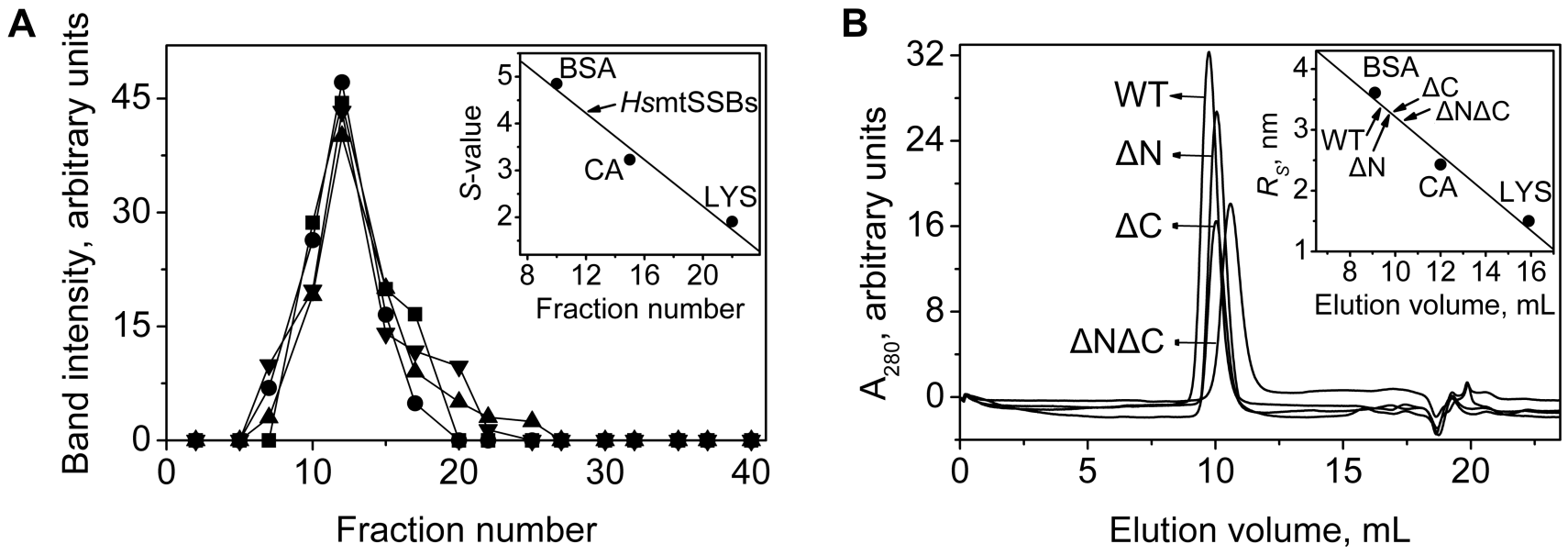

Figure 7. Terminal deletion variants of *Hs*mtSSB form tetramers in solution. Hydrodynamic analysis of *Hs*mtSSBwt and deletion variants. **A**, *Hs*mtSSBwt (●), ΔN (■), ΔC (▲), and ΔNΔC (▼) were sedimented in 12-30% glycerol gradients for 63 hr at 264,000 x *g*, and the gradient fractions were analyzed by 17% SDS-PAGE. **B**, the *Hs*mtSSB proteins were chromatographed on a Superdex 75 gel filtration column, and fractions were analyzed by absorption at 280 nm. Standard protein markers used were: bovine serum albumin (BSA: 4.85 *S*, R_S 3.61 nm), carbonic anhydrase (CA: 3.23 *S*, R_S 2.43 nm), and lysozyme (LYS: 1.91 *S*, R_S 1.5 nm).

indexes indicate native molecular masses of ~ 56, 53, 53, and 51 kDa, respectively, consistent with the size of homotetrameric forms.

Terminal deletion variants of Hs*mtSSB bind to ssDNA with similar affinities*

We proceeded to evaluate the *Hs*mtSSB deletion variants by examining their biochemical activities as compared to the wild-type protein. Using a gel mobility shift assay (GMSA), we examined the apparent DNA-binding affinities of *Hs*mtSSBwt and the terminal deletion variants using a 48-mer ssDNA oligonucleotide (Figure 8), whose size is close to the binding-site size determined previously for *Hs*mtSSB (Curth *et al.* 1994). A titration of the proteins at 50 mM NaCl revealed no significant differences in ssDNA-binding affinities between *Hs*mtSSBwt and the deletion variants, with apparent K_ds of ~5 nM. Interestingly, the lack of the C-terminal region does not appear to interfere with the ssDNA-binding efficacy of *Hs*mtSSB, in contrast to *Ec*SSB and T7 gp2.5. A recent report by Kozlov *et al.* (2010) shows that an increased ssDNA binding of *Ec*SSB lacking the C-terminus is observed only at 100 and 200 mM NaCl, and not at low salt concentration (20 mM NaCl). We also performed the GMSA assays with the *Hs*mtSSB proteins at 20 and 100 mM NaCl, but failed to observe any differences in binding affinities (data not shown). At the 20-100 mM range, salt does not seem to affect the ssDNA-binding affinity of either the wild-type or variant forms of *Hs*mtSSB.

Salt-dependent stimulation of Hs*pol γ by* Hs*mtSSB terminal deletion variants*

To evaluate the capacity of the *Hs*mtSSB variants to stimulate the DNA polymerase activity of *Hs*pol γ *in vitro*, we first examined the effects of KCl concentration on DNA synthesis by reconstituted *Hs*pol γ holoenzyme on singly-primed M13 DNA in the presence and absence of

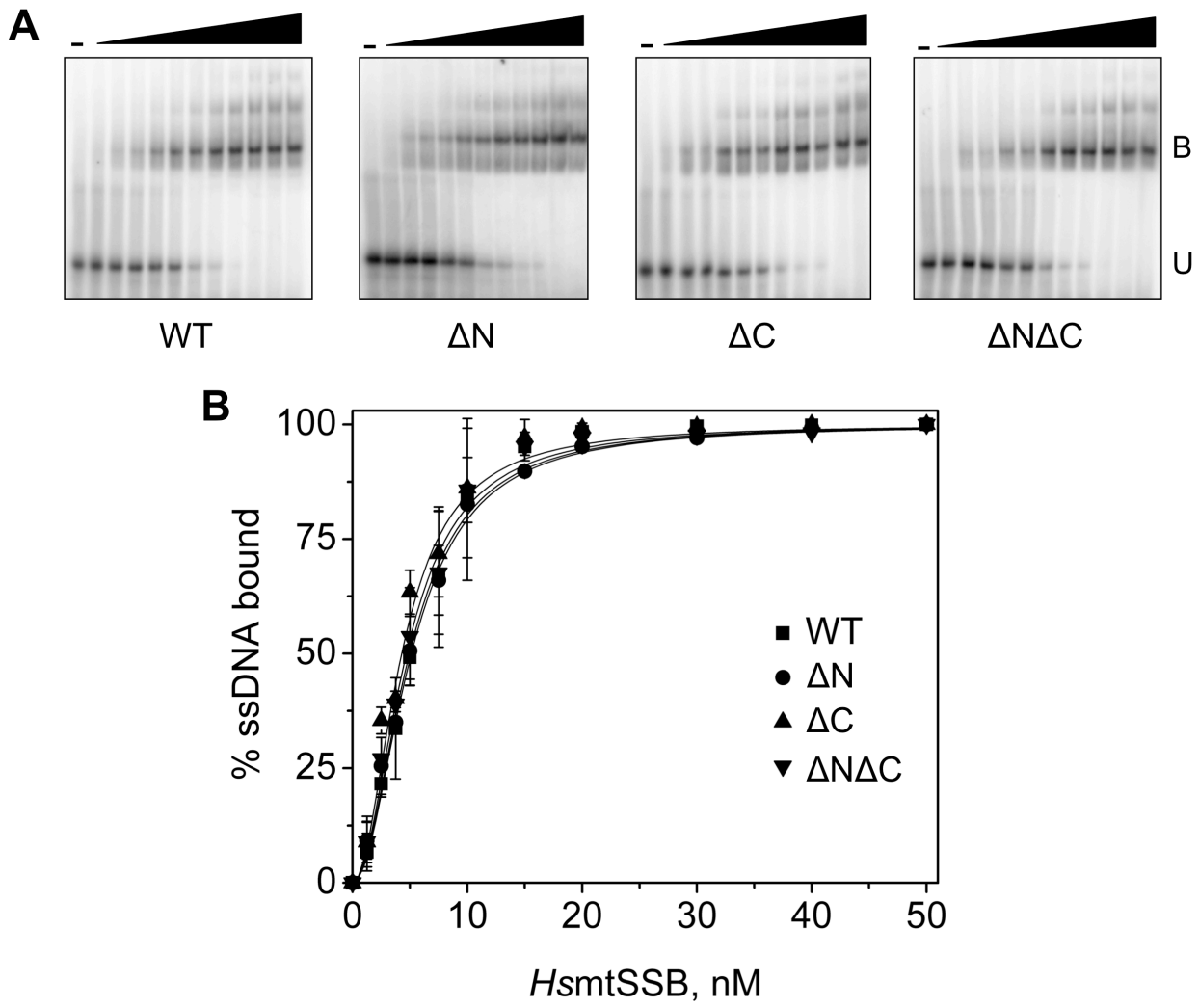

Figure 8. Terminal deletion variants of *Hs*mtSSB bind to ssDNA with similar affinities. A, ssDNA-binding affinity was evaluated by GMSA. *Hs*mtSSBwt and its deletion variants were pre-incubated with a radiolabeled 48-mer oligonucleotide at 50 mM NaCl in the presence of increasing mtSSB concentrations: 1.25, 2.5, 3.75, 5, 7.5, 10, 15, 20, 30, 40 and 50 nM (as tetramer), as described under Materials and Methods. "–" denotes no added protein. The fractions of unbound (U) and bound (B) oligomer were quantitated, and the data were plotted in **B** as the percent of substrate utilized. The data represent the average of three experiments.

*Hs*mtSSBwt (Figure 9). In the absence of *Hs*mtSSBwt, *Hs*pol γ activity is stimulated ~2 fold as the concentration of KCl in the reaction increases from 20 to 100 mM, in agreement with previously published data (Lim *et al.* 1999). Unlike *Dm*pol γ stimulation by *Dm*mtSSB that occurs over a broad range of KCl concentrations (0-130 mM) (Farr *et al.* 1999), the stimulation of *Hs*pol γ by *Hs*mtSSBwt is only observed at 20 mM KCl, and reaches its maximum at a concentration of *Hs*mtSSBwt sufficient to cover the entire singly-primed M13 DNA substrate (according to our GMSA data). At 50 mM KCl, the presence of *Hs*mtSSBwt at low levels promotes a slight stimulation of DNA synthesis by *Hs*pol γ, but it becomes somewhat inhibitory at higher levels. At 100 mM KCl, where the activity of *Hs*pol γ alone is highest, the presence of *Hs*mtSSBwt is completely inhibitory. The maximal stimulation of DNA synthesis by *Hs*pol γ in the presence of *Hs*mtSSBwt at 20 mM KCl is only moderate, albeit ~3-fold higher than the activity of *Hs*pol γ alone at 100 mM KCl. Judging by the fact that the ssDNA-binding affinity of *Hs*mtSSBwt does not change over the range of 20-100 mM KCl, the data suggest that increasing ionic strength inhibits the ability of *Hs*pol γ to displace *Hs*mtSSB from ssDNA template during the course of *in vitro* DNA synthesis.

Next, we evaluated the ability of the terminal deletion variants of *Hs*mtSSB to stimulate DNA synthesis by *Hs*pol γ (Figure 10). Overall, the effect of KCl concentration is similar among the variants: at 20 mM, DNA synthesis is stimulated; at 50 mM, we observe no stimulation and/ or slight inhibition; at 100 mM, *Hs*pol γ is inhibited completely. Notably, under low salt conditions, *Hs*mtSSBΔN, ΔC, and ΔNΔC show 1.4- to 2-fold higher stimulation of *Hs*pol γ as compared to *Hs*mtSSBwt. This increased stimulation is not apparent at low concentrations of the *Hs*mtSSBs, but it is clearly evident and reproducible at saturating levels. The data argue that the N- and C-terminal regions of *Hs*mtSSB have functionally inhibitory roles on its

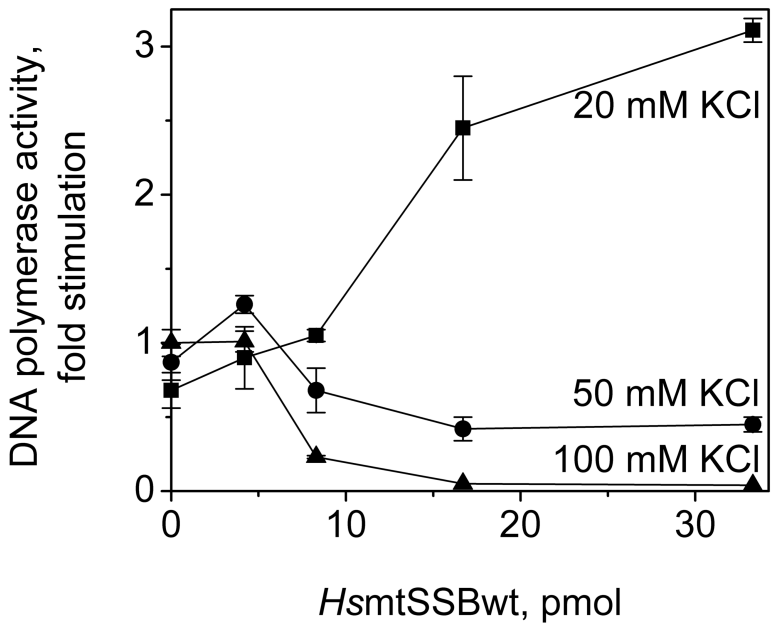

Figure 9. *Hs*mtSSBwt stimulates the DNA polymerase activity of *Hs*pol γ in a salt-dependent manner. DNA synthesis by reconstituted *Hs*pol γ holoenzyme was measured on singly-primed M13 DNA, as described under Materials and Methods, in the presence of the indicated KCl and *Hs*mtSSBwt concentrations. The data were normalized to the amount of nucleotide incorporated by *Hs*pol γ at 100 mM KCl in absence of *Hs*mtSSBwt (that was arbitrarily set as 1).

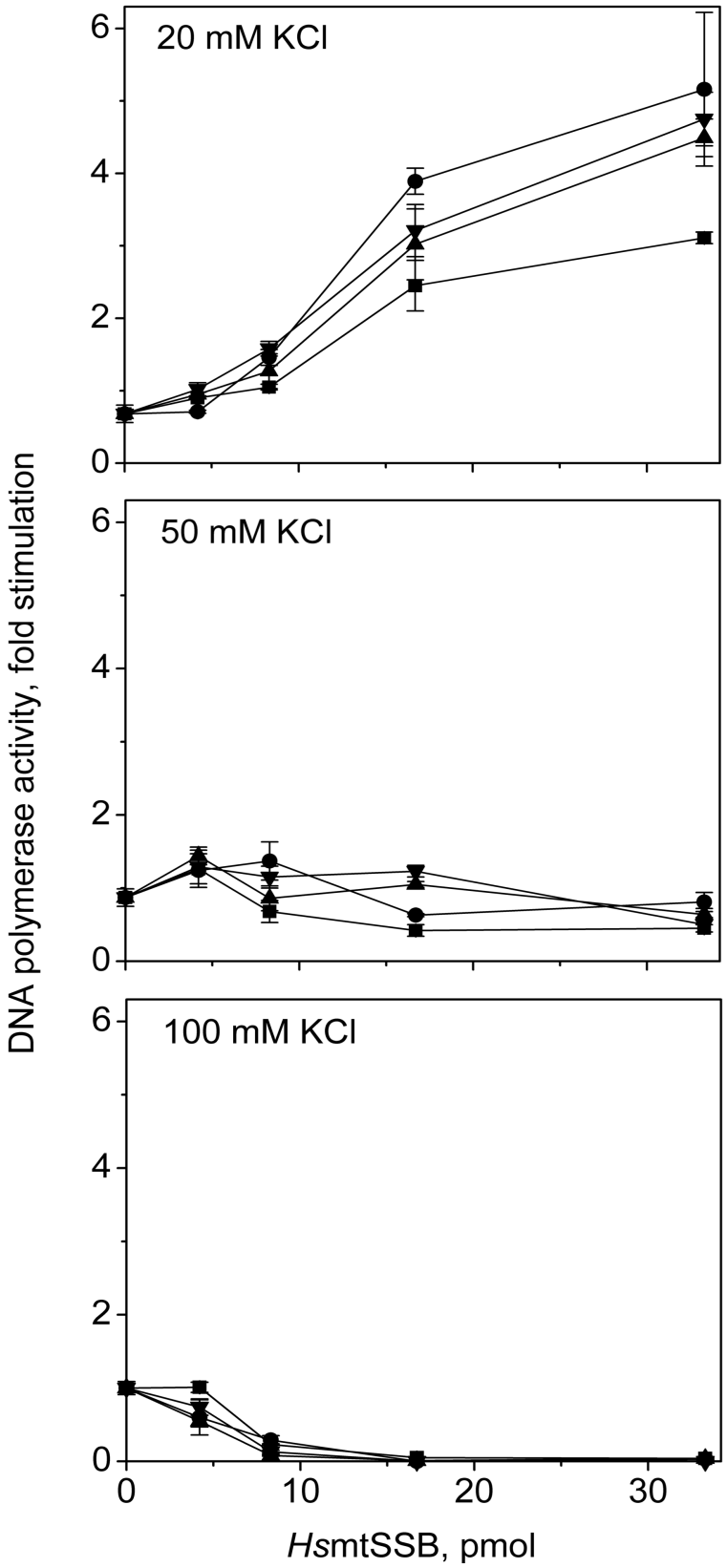

Figure 10. Stimulation of *Hs*pol γ by terminal deletion variants of *Hs*mtSSB. DNA synthesis

by reconstituted *Hs*pol γ holoenzyme was measured on singly-primed M13 DNA, as described under Materials and Methods, in the presence of the indicated concentrations of *Hs*mtSSBwt (■), ΔN (●), ΔC (▲), and ΔNΔC (▼), at 20 mM (upper), 50 mM (middle), and 100 mM (lower panel) KCl. The data were normalized to the amount of nucleotide incorporated by *Hs*pol γ at 100 mM KCl in absence of *Hs*mtSSBwt (that was arbitrarily set as 1).

ability to stimulate the DNA polymerase activity of *Hs*pol γ, suggesting a modulatory role *in vivo*.

Stimulation of DNA unwinding activity of Hs*mtDNA helicase by terminal deletion variants of* Hs*mtSSB*

As shown previously, *Hs*mtSSBwt stimulates the DNA unwinding activity of *Hs*mtDNA helicase *in vitro* (Korhonen *et al.* 2003). We examined the effects of the terminal deletion variants in stimulating the DNA unwinding activity of *Hs*mtDNA helicase using as substrate pBSKS+ ssDNA (2,958 nt), to which was annealed a 60-mer ssDNA oligonucleotide that creates a 40-nt 5′-single-stranded tail for helicase loading followed by 20 nt of paired sequence. First, we asked if varying KCl concentrations produced the same pattern of stimulation of *Hs*mtDNA helicase by *Hs*mtSSBwt as compared to its stimulation of *Hs*pol γ (Figure 11). We found that *Hs*mtDNA helicase shows a slightly better DNA unwinding activity at 100 mM KCl as compared to that at 20 and 50 mM KCl. We then evaluated various potassium salts, including phosphate, acetate and glutamate, and found that KCl provided the best stimulation (data not shown). In contrast to the results with *Hs*pol γ, stimulation of *Hs*mtDNA helicase in the presence of saturating amounts of *Hs*mtSSBwt is similar at the three KCl concentrations tested, suggesting that the results we show in Figures 3.5 and 3.6 are related specifically to functional interactions between *Hs*mtSSB and *Hs*pol γ.

We extended our analysis by titrating *Hs*mtSSBwt, ΔN, ΔC, and ΔNΔC in DNA unwinding assays conducted at 50 mM KCl (Figure 12). None of the concentrations of the *Hs*mtSSBs used were sufficient to cause any dsDNA destabilization in the absence of helicase (Figure 12A). *Hs*mtDNA helicase shows maximal DNA unwinding activity in the presence of

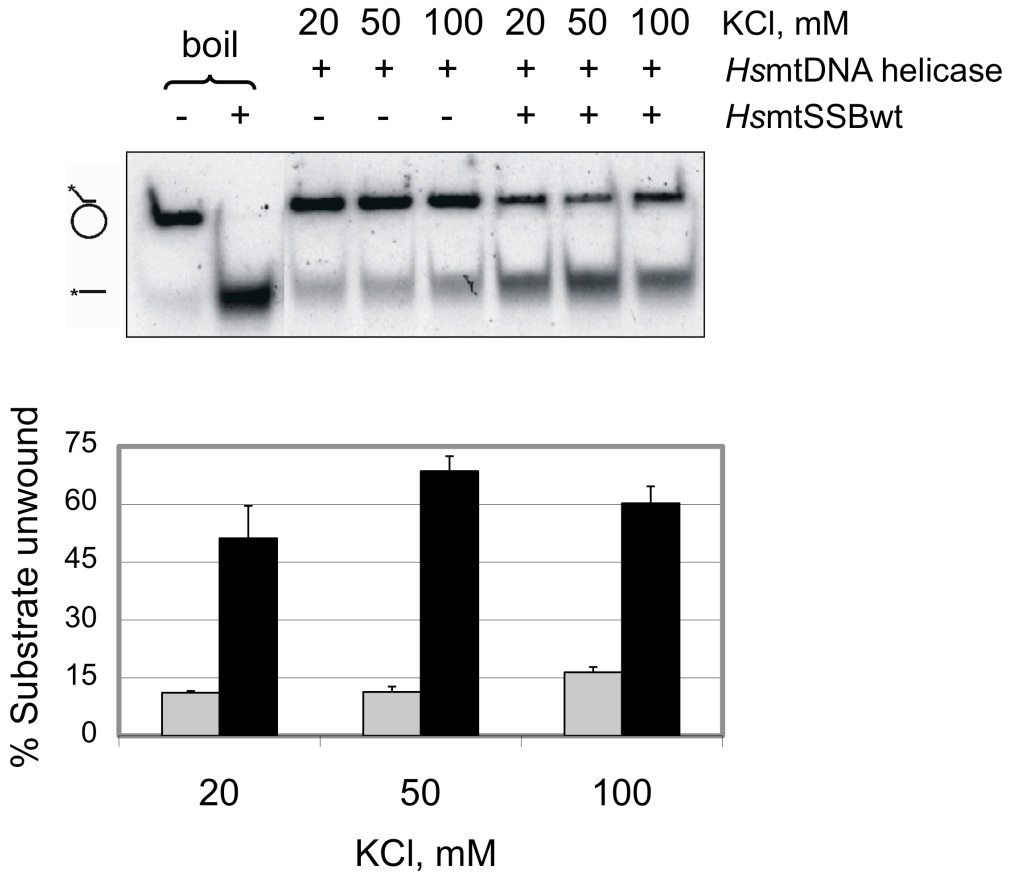

Figure 11. Stimulation of DNA unwinding activity of *Hs*mtDNA helicase by *Hs*mtSSBwt is independent of KCl concentration. DNA unwinding assays were performed as described under Materials and Methods. Upper panel, 3.5 nM of *Hs*mtDNA helicase (as hexamer) and 200 nM of *Hs*mtSSBwt (as tetramer) were used where indicated by "+". The concentration of KCl used is indicated above each lane. "–" and "+ boil" lanes represent the intact and denatured substrate (heated to 100^{o}C for 2 min prior to loading), respectively. Lower panel, analysis of the data shown in the upper panel together with the data from two other independent experiments. The gray and black bars represent the average of unwound substrate as percent in the absence and presence of *Hs*mtSSBwt, respectively.

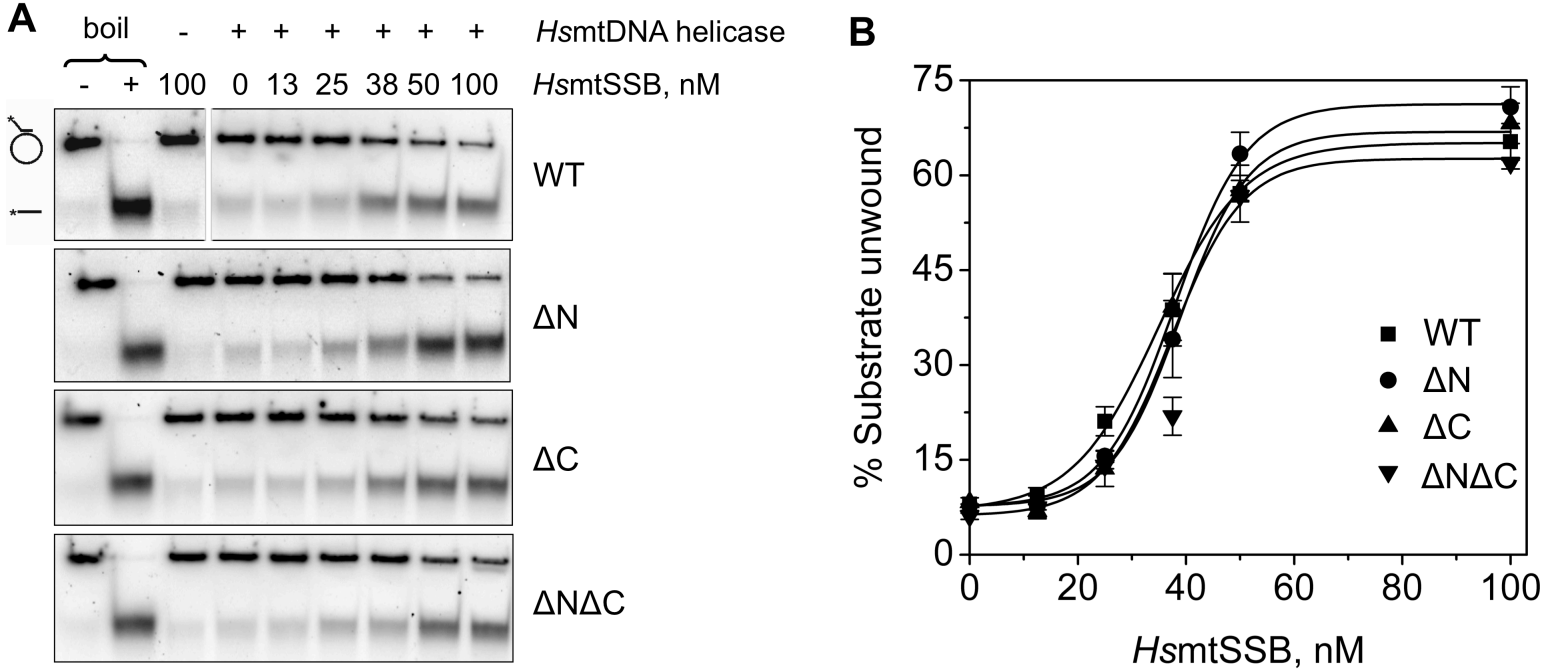

Figure 12. Stimulation of *Hs*mtDNA helicase by terminal deletion variants of *Hs*mtSSB. DNA unwinding assays were performed as described under Materials and Methods. **A**, a constant concentration of *Hs*mtDNA helicase (3.5 nM as hexamer) and KCl (50 mM) were used in each assay. The concentration of *Hs*mtSSBs (as tetramer) that was used is indicated above each lane. "–" and "+ boil" lanes represent the intact and denatured substrate (heated to 100^{o}C for 2 min prior to loading), respectively. **B**, analysis of the data shown in **A** together with the data from two other independent experiments. The data represent the average of unwound substrate as percent.

100 nM *Hs*mtSSB, a concentration corresponding to coating of ~80% of the ssDNA substrate (according to our GMSA data). No significant differences in stimulation were observed between *Hs*mtSSBwt and deletion variants; stimulation of the *Hs*mtDNA helicase was ~8 fold at the highest *Hs*mtSSB concentrations.

Discussion

Biochemical studies of the mtDNA replisome demonstrate that pol γ and the mtDNA helicase are stimulated by mtSSB. We have shown previously that *Dm*mtSSB can stimulate ~20-fold *in vitro* DNA synthesis by *Dm*pol γ over a broad range of KCl concentrations, primarily by enhancing primer recognition and binding (Farr *et al.* 1999, Thommes *et al.* 1995). Similarly, *Dm*mtSSB stimulates ~15-fold the 3′-5′ exonuclease activity of *Dm*pol γ over the same KCl range (Farr *et al.* 1999). Furthermore, *Hs*mtSSB has been shown to stimulate the DNA unwinding activity of the *Hs*mtDNA helicase (Korhonen *et al.* 2003) and together with *Hs*pol γ and *Hs*mtDNA helicase, reconstitutes a minimal mtDNA replisome *in vitro* (Korhonen *et al.* 2004). These data indicate that mtSSBs serve an important role in initiation and elongation of DNA synthesis in mtDNA replication, consistent with the observation that the disruption of the *Drosophila* (*lopo*) and yeast (*rim1*) mtSSB genes results in loss of mtDNA and respiratory capacity, and consequently, developmental lethality or impaired growth, respectively (Maier *et al.* 2001, Van Dyck *et al.* 1992).

mtSSBs are homologues of *Ec*SSB, with which they exhibit a high degree of amino acid sequence conservation in the OB-fold domain (Figure 5), and share similar physical, biochemical, and structural properties (Yang *et al.* 1997, Curth *et al.* 1994, Thommes *et al.* 1995, Tomaska *et al.* 2001). Animal mtSSBs, however, evolved at least two different sequences from

their eubacterial counterpart: their N- and C-termini. After import into mitochondria, the mitochondrial presequence is cleaved, producing the mature mtSSB protein. The mature polypeptide in humans contains 9 amino acids at the N-terminus that are absent in *Ec*SSB, and only 7 residues at the C-terminus, in contrast with the long acidic C-terminal tail of its eubacterial homologue; these potentially protrude from the ssDNA-binding core without any detectable secondary structure (Yang *et al.* 1997). Here, we sought to analyze the functional importance of the N- and C-terminal regions of *Hs*mtSSB in the context of mtDNA replication. We purified *Hs*mtSSBwt, *Hs*mtSSBΔN, *Hs*mtSSBΔC, and *Hs*mtSSBΔNΔC to near-homogeneity and showed that all of the proteins form tetramers in solution, indicating that the termini are not critical for the folding or stability of *Hs*mtSSB, as predicted by the crystallographic data (Yang *et al.* 1997).

Next, we analyzed the ssDNA-binding properties of the terminal deletion variants using a GMSA approach. The lack of either or both termini did not alter the ssDNA-binding affinity of *Hs*mtSSB, which is relatively high as observed for SSBs from various sources (Kornberg and Baker 1992). This is particularly relevant because we have shown previously that ssDNA-binding variants of *Dm*mtSSB fail to stimulate *Dm*pol γ efficiently *in vitro,* and promote mtDNA depletion and cell growth defects in *Drosophila* Schneider cells (Farr *et al.* 2004). Our findings distinguish biochemically the role of the C-terminal region of mtSSBs as compared to prokaryotic forms. The crystal structures of viral, eubacterial, eukaryotic nuclear and mitochondrial SSBs show that these proteins share a common structural domain for binding to ssDNA, the OB-fold (Shamoo *et al.* 1995, Yang *et al.* 1997, Raghunathan *et al.* 1997, Bockharev *et al.* 1997, Hollis *et al.* 2001), although they share no sequence homology. In addition, eubacterial and bacteriophage SSBs do share another structural feature: a long acidic C-terminal

tail, which is essential for DNA replication and viability of the organisms (Burke *et al.* 1980, Kim *et al.* 1994, Curth *et al.* 1996). The removal of the C-termini of *Ec*SSB, T7 gp2.5 and T4 gp32 increases their ssDNA-binding affinities significantly (Burke *et al.* 1980, Kim *et al.* 1992, Curth *et al.* 1996) but at the same time, abolishes interactions with other components of their cognate replication machinery (Shereda *et al.* 2008, Krassa *et al.* 1991, Hyland *et al.* 2003, He *et al.* 2003). Recently, Shereda *et al.* (2009) showed that proteins that interact with the C-terminus of *E. coli* SSB share a similar structural surface where the interaction occurs, demonstrating the presence of a signature contact structure. Interaction with the C-terminus of *E. coli* SSB via this signature structure appears to be highly regulated, because progressive truncations from its C-terminal end cause a progressive loss of both physical and functional interactions. Marintcheva *et al.* (2008) showed that the acidic C-terminus of T7 gp2.5 and ssDNA actually compete for binding to the ssDNA-binding cleft of the protein, which is located in the N-terminal OB-fold domain. A functional model proposes that in absence of DNA, the C-terminal region binds to the ssDNA-binding cleft, and is then displaced upon ssDNA binding, rendering it available for protein-protein interactions. Such an interaction between the C-terminus and the ssDNA-binding cleft is suggested to create an electrostatic shield that protects the binding cleft from random charged surfaces inside the cell. Our data shows clearly that the C-terminal region of *Hs*mtSSB does not influence the ssDNA-binding affinity of the protein, suggesting that this region of the eubacterial-like mtSSBs serves a role that differs from those of *Ec*SSB, T7 gp2.5 and T4 gp32. Indeed, in this sense, *Hs*mtSSB resembles the nuclear replication protein A (reviewed in Wold 1997); binding of random charged molecules to the ssDNA-binding cleft of eukaryotic SSBs is thus most likely prevented by a distinct mechanism.

To investigate further the functional properties of the N- and C-terminal regions of *Hs*mtSSB, we performed stimulation assays of *Hs*pol γ and *Hs*mtDNA helicase under varying conditions. We found that the stimulation of the DNA polymerase activity of *Hs*pol γ by *Hs*mtSSBwt is moderate (~3 fold) and observed only at low KCl concentrations (20 mM). Increasing KCl concentrations resulted in concentration-dependent inhibition, suggesting that electrostatic forces govern the functional interactions between *Hs*pol γ and *Hs*mtSSB. Interestingly, *in vitro* stimulation (up to 20 fold) of the DNA polymerase activity of *Dm*pol γ by *Dm*mtSSB is observed over a broad range of KCl concentrations (0 to 130 mM) (Farr *et al.* 1999). We speculate that this difference in the human and *Drosophila* systems likely reflects the different subunit composition of the mammalian and insect pol γs. *Hs*pol γ is a heterotrimeric enzyme comprising one catalytic and two accessory subunits ($\alpha\beta_2$) (Yakubovskaya *et al.* 2006, Lee *et al.* 2009); the α and dimeric β subunits can be expressed in heterologous systems and purified independently (Oliveira and Kaguni 2009, Lim *et al.* 1999), and the holoenzyme is subsequently reconstituted *in vitro*. In contrast, *Dm*pol γ has a heterodimeric composition, with one catalytic and one accessory subunit (αβ) (Wernette and Kaguni 1986); both folding and stability are interdependent, as evidenced by the fact that in a heterologous system, the two subunits must be co-expressed to reconstitute the *Dm*pol γ holoenzyme (Wang and Kaguni 1999). Furthermore, subunit interactions in the insect enzyme occur at multiple sites along the polypeptides (Fan and Kaguni 2001). That the differences in pol γ stimulation by the fly and human mtSSBs result from differences in pol γ structure is supported by the fact that both *Dm*mtSSB and *Ec*SSB stimulate similarly *Dm*pol γ (Williams and Kaguni 1995). Additional support for this hypothesis is also provided by a recent report, which shows that each protomer of the dimeric human accessory subunit serves distinct roles in DNA synthesis by *Hs*pol γ (Lee

et al. 2010). Thus, we speculate that the function of the *Hs*pol γ-β dimer in the human mtDNA replisome is at least in part performed by *Dm*mtSSB in the *Drosophila* system. Further investigation of the mechanism of pol γ stimulation by mtSSB is clearly warranted to promote understanding of the species-specific roles of these proteins at the mtDNA replication fork.

Our analysis of stimulation of *Hs*pol γ by the deletion variants of *Hs*mtSSB revealed an interesting and surprising feature: the lack of the N- and/or C-terminus of *Hs*mtSSB increases its capacity to stimulate *Hs*pol γ under low ionic strength conditions. This suggests that both termini may actually modulate the DNA polymerase activity of *Hs*pol γ by inhibiting its stimulation by *Hs*mtSSBwt. Whether this modulation is mediated through physical or functional interactions only remains to be determined, but it is clear that the relevant interactions do not involve a positive regulation, as is the case for *Ec*SSB, T7 gp2.5 and T4 gp32, and their respective DNA polymerase partners at the replication fork. In considering the electrostatic forces that may govern functional interactions, we examined the predicted isoelectric points (pIs) for various structural elements in *Hs*pol γ-α and wild-type *Hs*mtSSB. We were especially interested in a fragment of the spacer region domain of *Hs*pol γ-α assigned as the intrinsic processivity (IP) sub-domain in the recent crystal structure (Lee *et al.* 2009), because earlier studies from our lab suggested that residues in this sub-domain are important for the functional interaction between *Drosophila* pol γ and its cognate mtSSB (Luo and Kaguni 2005). Consistent with the hypothesis that the functional interactions between *Hs*pol γ and *Hs*mtSSB are electrostatic, we found a pI of 8.2 for wild-type *Hs*mtSSB, and 5.7 for the IP sub-domain of *Hs*pol γ-α, suggesting that increasing salt in the pol assays disrupts the electrostatic forces that allow *Hs*pol γ to displace *Hs*mtSSB from ssDNA. The only other domain of *Hs*pol γ-α that carries an overall negative charge is the accessory-interacting domain (pI 4.7), which interacts tightly with the proximal

protomer of the pol γ-β dimer. In examining the terminal deletion variants of *Hs*mtSSB we found pIs of 9.0 (ΔC), 9.2 (ΔN) and 9.5 (ΔNΔC), suggesting that lack of either or both termini causes a significant increase in the overall positive charges of the protein that may strengthen its interactions with *Hs*pol γ, stimulating DNA synthesis and allowing *Hs*pol γ to displace it from the ssDNA. At the same time, the ssDNA-binding affinities of the variant *Hs*mtSSBs are unaffected over the range of 20-100 mM KCl (Figure 8 and data not shown). As the *Hs*mtSSB becomes more positively charged without its termini, the electrostatic forces between *Hs*pol γ and *Hs*mtSSB likely increase at 20 mM KCl, increasing the stimulation and the ability of *Hs*pol γ to displace the *Hs*mtSSB variants more easily. However, whereas ssDNA binding by *Hs*mtSSB is stable at 50 mM KCl, this salt concentration is apparently sufficient to disturb interactions between *Hs*pol γ and both the wild-type and variant forms of *Hs*mtSSB, giving rise to its inhibitory effects. Although the effects we observe are modest, it seems possible that given the fluctuating ionic conditions that occur in the mitochondrion (Hackenbrock 1968, Srere 1980), they may play a role in regulating the interactions between *Hs*pol γ and *Hs*mtSSB *in vivo*.

In contrast with *Hs*pol γ, the stimulation of *Hs*mtDNA helicase by *Hs*mtSSB proteins is not salt-dependent, and the deletion variants of *Hs*mtSSB do not show a higher stimulatory effect than *Hs*mtSSBwt on the DNA unwinding activity of *Hs*mtDNA helicase. Taking into consideration that *Ec*SSB may not stimulate *Hs*mtDNA helicase as well as its cognate SSB (Korhonen *et al.* 2003), this result argues that the N- and C-terminal regions of *Hs*mtSSB are not involved directly in the 8-fold stimulation of *Hs*mtDNA helicase. However, it has been shown that *Ec*SSB can replace T7 gp2.5 *in vitro* to stimulate the T7 DNA polymerase holoenzyme activity on a singly-primed ssDNA template and in strand-displacement assays (the latter also involves the function of T7 gp4 primase-helicase), but it fails to promote either coupled leading

and lagging strand synthesis *in vitro*, or the growth of bacteriophage T7 mutants lacking the gp 2.5 gene, both of which require the coordinated function of the T7 replisome (Nakai and Richardson 1988, Kim and Richardson 1993). Therefore, our assays may be limited in assessing biochemically the possible defects of *Hs*mtSSB variants. In any case, one might argue that the mtDNA replication fork most likely comprises other unidentified components in addition to pol γ, mtDNA helicase and mtSSB, especially given the complexity of the myriad processes that occur in the mitochondrion (Wallace and Fan 2010), and the various modes of mtDNA replication that operate *in vivo* (Clayton 1982, Holt *et al.* 2000, Yang *et al.* 2002), which ensure appropriate mtDNA copy number and mitochondrial gene expression. Thus, physiological analysis of these and other mtSSB mutants, in addition to development of new *in vitro* assays that reconstitute fully the mtDNA replisome, will be informative in understanding the mechanism of mtDNA replication.

Materials and Methods

Nucleotides and nucleic acids

Unlabeled deoxy- and ribonucleotides were purchased from Amersham Bioscience. [α-^{32}P]dATP and [γ-^{32}P]ATP were purchased from MP Biomedicals. Recombinant M13 (10,650 nt) and pBSKS+ (2,958 nt) DNAs were prepared by standard laboratory methods. Oligodeoxynucleotides complementary to these DNAs were synthesized in an Applied Biosystems oligonucleotide synthesizer. The singly-primed M13 DNA used in DNA polymerase assays was prepared as described previously (Farr *et al.* 2004). For the DNA unwinding assays, a 60-mer oligodeoxyribonucleotide (5′T$_{(40)}$AGGTCGTTCGCTCCAAGCT3′) was radiolabeled at its 5′-end. The kinase reaction (50 μL) contained 50 mM Tris-HCl, pH 8.3, 10 mM $MgCl_2$, 0.1

mM EDTA, 5 mM dithiothreitol (DTT), 0.1 mM spermidine, [γ-^{32}P]ATP (0.66 μM, 4500 Ci/mmol), 700 pmol (as nt) of oligonucleotide, and 20 units of T4 polynucleotide kinase (New England BioLabs). Incubation was for 30 min at 37° C, and the 5′-end-labeled 60-mer oligonucleotide was purified using a Micro Bio-Spin P-30 Tris chromatography column (Bio-Rad), and annealed to pBSKS+ single-stranded plasmid DNA at 65^{O}C for 60 min, followed by incubation at 37^{O}C for 30 min, to generate a 20 bp double-stranded region with a 40-nt 5′-tail (the DNA unwinding substrate). The 48-mer oligodeoxynucleotide (5′GGACTATTTATTAAATATATTTAAGAACTAATTCCAGCTGAGCGCCGG3′) used in gel mobility shift assays was radiolabeled at its 5′-end as described above.

Mutagenesis and purification of Hs*mtSSB proteins*

The *Hs*mtSSB deletion variants were constructed by cloning of PCR fragments containing the coding region for *Hs*mtSSBΔN, ΔC and ΔNΔC into the *Nde*I site of the pET11a vector. PCRs were performed using the coding region of the mature *Hs*mtSSBwt cloned in pET11a vector as template, *Pfu* DNA polymerase (Stratagene) and standard laboratory methods. The oligonucleotides used for PCR mutagenesis were: 5′CCCGGGCATatgCTTGAAAGATCCCTGAATCG3′ and 5′CCCGGGCATATGCTACTCCTTCTCTTTCGTCTGG3′ for *Hs*mtSSBΔN; 5′CCCGGGCATATGGAGTCCGAAACAACTACCAG3′ and 5′CCCGGGCATATGctaACTCAGAAATATAATATTATCAG3′ for *Hs*mtSSBΔC; and 5′CCCGGGCATatgCTTGAAAGATCCCTGAATCG3′ and 5′CCCGGGCATATGctaACTCAGAAATATAATATTATCAG3′ for *Hs*mtSSBΔNΔC. The

underlined sequences correspond to *Nde*I restriction sites, and the lower case letters indicate the sites where mutations were introduced into the *Hs*mtSSB cDNA to create new start and stop codons. BL21(DE3) cells containing pET-11a plasmid expressing *Hs*mtSSBwt and deletion variants were grown at 37^{O}C with aeration in L-broth containing 0.1 mg/mL of ampicillin. When the bacterial cell culture reached an optical density of 0.6 at 595 nm, isopropyl β-D-1-thiogalactopyranoside was added to 0.2 mM, and the culture was incubated further for 3 hr. Cells were harvested by centrifugation, washed in 50 mM Tris-HCl, pH 7.5, 10% sucrose (Tris-sucrose), frozen in liquid nitrogen, and stored at -80^{O}C. All further steps were performed at 0-4^{O}C, and all buffers contained 5 mM DTT, 1 mM phenylmethylsulfonyl fluoride, 10 mM sodium metabisulfite, and 2 μg/mL leupeptin. The cell pellet was thawed on ice, and cells were resuspended in 1/25 volume of original cell culture in Tris-sucrose and lysed by addition of 5 X lysis buffer (1 M NaCl, 10 mM EDTA, and 10% sodium cholate – for *Hs*mtSSBΔC purification, 7.5% n-dodecyl-β-D-maltoside instead of 10% sodium cholate) to a final 1 X concentration, followed by incubation for 30 min on ice and freezing in liquid nitrogen. After thawing on ice, the suspension was centrifuged at 17500 x *g* for 30 min. The supernatant (soluble Fr I) was loaded onto a Blue Sepharose column equilibrated with 10 column volumes (CV) of 35 mM Tris-HCl, pH 7.5, 10% glycerol, 2 mM EDTA, 0.2 M NaCl at a packing ratio of 5-7 mg of total protein per mL of resin. The column was washed with 1 CV of equilibration buffer and 3 CV of 35 mM Tris-HCl, pH 7.5, 10% glycerol, 2 mM EDTA, 0.25 M NaSCN. The bound protein was eluted with 8 CV of a 0.4-1.2 M NaSCN linear gradient, followed by a final elution step of 1.5 M NaSCN buffer (2 CV). Fractions containing *Hs*mtSSB were pooled (Fr II) and dialysed against buffer containing 60 mM KPO_4, pH 7.6, 10% glycerol, 2 mM EDTA (Fr IIb) (for *Hs*mtSSBΔC,

dialysis buffer contained 40 mM KPO_4, pH 7.6). Fr IIb was then loaded onto a phosphocellulose column equilibrated with dialysis buffer at a packing ratio of 0.5 mg of total protein per mL of resin. The column was washed with 2.5 CV of the same buffer and the proteins were eluted with 5 CV of a 60-150 mM KPO_4 linear gradient, followed by a final step of 350 mM KPO_4 buffer (2 CV). The *Hs*mtSSB proteins typically elute at ~ 80 mM KPO_4. Pooled fractions (Fr III) were concentrated to ~ 1 mg/mL of protein in a Centricon-30 spin concentrator (Amicon) treated with 5% Tween 20 (Fr IIIb). Fr IIIb was frozen in liquid nitrogen and stored at -80^{o}C.

Purification of Hs*pol γ and* Hs*mtDNA helicase*

Recombinant human pol γ-α exo^{-} and pol γ-β were prepared from *Sf*9 and bacterial cells, respectively, as described by Oliveira and Kaguni (2009). Recombinant human mtDNA helicase was prepared from *Sf*9 cells, as described by Ziebarth *et al.* (2007).

Glycerol gradient sedimentation and gel filtration

*Hs*mtSSBwt and variants (100 μg) were layered onto preformed 12-30% glycerol gradients (10 mL) containing 35 mM Tris-HCl, pH 7.5, 100 mM NaCl, 2 mM EDTA, 5 mM DTT, 1 mM phenylmethylsulfonyl fluoride, 10 mM sodium metabisulfite, and 2 ug/mL leupeptin. Centrifugation was at 264,000 x *g* for 63 hrs at 4^{o}C in a Beckman SW41 rotor. Fractions were analyzed by SDS-PAGE and Coomassie blue staining. For Superdex 75 gel filtration, 200 μg *Hs*mtSSBwt and variants were chromatographed on a column equilibrated with the buffer described above containing 8% glycerol at a flow rate of 0.25 mL/min at 4^{o}C.

Fractions were analyzed by SDS-PAGE and Coomassie blue staining to confirm UV trace recordings. Standard protein markers used in both procedures were: bovine serum albumine (BSA, 4.85 *S*, R_S = 3.61 nm), carbonic anhydrase (CA, 3.23 *S*, R_S = 2.43 nm) and lysozyme (LYS, 1.91 *S*, R_S = 1.5 nm). The data were plotted as *S* value *versus* fraction number to obtain a sedimentation coefficient, and as R_S value *versus* the peak of protein elution in mL to obtain the Stokes radii for the *Hs*mtSSB proteins. The native molecular mass of the proteins were calculated using the formula: MW = 3.909 x *S* value x R_S.

ssDNA binding and gel mobility shift assay

Reaction mixtures (20 μL) contained 20 mM Tris-HCl, pH 7.5, 1 mM DTT, 4 mM $MgCl_2$, 50 mM NaCl, 36 fmol 5′-end-labeled 48-mer, and the indicated amounts of the *Hs*mtSSB proteins. Incubation was at 20^{O}C for 10 min. Samples were processed and electrophoresed in 6% native polyacrylamide gels. The amounts of shifted and free oligonucleotide were quantitated as follows: % ssDNA bound = (V_S / (V_S + V_F)) x 100, where V_S represents the volume of the shifted and V_F the volume of unshifted oligonucleotide in the sample lane of interest.

DNA polymerase γ stimulation assays

Reaction mixtures (50 μL) contained 50 mM Tris-HCl, pH 8.5, 4 mM $MgCl_2$, 400 μg/ml bovine serum albumin, 10 mM DTT, 20-100 mM KCl, 20 μM each dGTP, dATP, dCTP and

dTTP, [α-^{32}P]dATP (2 μCi), 10 μM (as nt) singly-primed recombinant M13 DNA, 10 ng *Hs*pol γ-α exo$^-$ Fr IV, 48 ng *Hs*pol γ-β Fr III, and the indicated amounts of *Hs*mtSSB proteins. Incubation was at 37^{o}C for 30 min. Samples were processed and nucleotide incorporation was quantitated in a liquid scintillation counter.

DNA unwinding assays

Reaction mixtures (50 μL) contained 20 mM Tris-HCl, pH 7.5, 10% glycerol, 500 μg/mL bovine serum albumin, 10 mM DTT, 4 mM $MgCl_2$, 3 mM ATP, 50 mM KCl (unless stated otherwise), 0.4 nM of DNA unwinding substrate, 3.5 nM of mtDNA helicase (as hexamer), and the indicated concentrations of *Hs*mtSSB proteins. The reactions were pre-incubated at 37^{o}C for 10 min prior to the addition of the helicase. Once the helicase was added, the reactions were incubated further at 37^{o}C for 30 min and then stopped by the addition of 5 μL of 10 X stop solution (6% SDS, 100 mM EDTA, pH 8.0), followed by 5 μL of 10 X loading buffer (50% glycerol, 0.25% bromophenol blue). DNA products were fractionated from substrate by electrophoresis in a 22% polyacrylamide gel (59:1 acrylamide/bisacrylamide) using 1 X TBE (90 mM Tris-HCl-borate, 2 mM EDTA) at 600 V for ~ 30 min. After electrophoresis, the gel was dried under vacuum with heat, and exposed to a Phosphor Screen (Amersham Biosciences). The data were analyzed by scanning the Phosphor Screen using a Storm 820 Scanner (Amersham Biosciences), and the volume of each band were determined, and background subtracted, by computer integration analysis using ImageQuant version 5.2 software (Amersham Biosciences). For all reactions, DNA unwinding is defined as the fraction of radiolabeled DNA species that is

single-stranded (product), as follows: % unwinding = (V_P / (V_S + V_P)) x 100, where V_P represents the volume of the product and V_S the volume of unreacted substrate in the sample lane of interest.

CHAPTER 4

REDUCED STIMULATION OF RECOMBINANT POL γ AND mtDNA HELICASE BY mtSSB VARIANTS CORRELATES WITH DEFECTS OF mtDNA REPLICATION IN ANIMAL CELLS

Summary

The mitochondrial single-stranded DNA-binding protein (mtSSB) is believed to coordinate the functions of the DNA polymerase γ (pol γ) and the mitochondrial DNA (mtDNA) helicase at the mtDNA replication fork. We generated five variants of the human mtSSB bearing mutations in amino acid residues specific to metazoans that map on the protein surface, removed from the single-stranded DNA (ssDNA) binding groove. Although the mtSSB variants bound ssDNA with only slightly different affinities, they exhibited very distinct capacities to stimulate the DNA polymerase activity of human pol γ and the DNA unwinding activity of human mtDNA helicase *in vitro*. Interestingly, we observed that the variants with defects in stimulating pol γ had unaltered capacities to stimulate the mtDNA helicase; at the same time, variants showing reduced stimulation of the mtDNA helicase activity promoted DNA synthesis by pol γ similarly to the wild-type mtSSB. The overexpression of the equivalent variants of *Drosophila melanogaster* mtSSB in S2 cells in culture caused mtDNA depletion under conditions of mitochondrial homeostasis. Furthermore, we observed more severe reduction of mtDNA copy number upon expression of these proteins during recovery from treatment with ethidium bromide, when mtDNA replication is stimulated *in vivo*. Our findings suggest that mtSSB uses distinct structural elements to interact functionally with its mtDNA replisome partners and to promote proper mtDNA replication in animal cells.

Introduction

Replication of animal mitochondrial DNA (mtDNA) is mediated by three protein players that function directly at the replication fork: DNA polymerase γ (pol γ), which catalyzes DNA synthesis *per se*; mtDNA helicase (also known as Twinkle), which unwinds double-stranded DNA to provide a single-stranded DNA (ssDNA) substrate for pol γ; and mitochondrial single-stranded DNA-binding protein (mtSSB), which binds ssDNA to protect it against damage and to coordinate the functions of pol γ and mtDNA helicase (Kaguni 2004, Korhonen *et al.* 2004). mtSSB has been shown to stimulate the DNA polymerase activity of pol γ both in the *Drosophila* and human systems (Farr *et al.* 1999, Oliveira and Kaguni 2010) and the unwinding activity of the human mtDNA helicase (*Hs*mtDNA helicase) (Korhonen *et al.* 2003, Oliveira and Kaguni 2010). In addition, human mtSSB (*Hs*mtSSB) stimulates strand-displacement DNA synthesis promoted by the combined action of the human pol γ (*Hs*pol γ) and *Hs*mtDNA helicase (Korhonen *et al.* 2004). *In vivo*, absence or depletion of mtSSB protein causes reduction of mtDNA copy number in *Drosophila* and human cells in culture (Farr *et al.* 2004, Ruhanen *et al.* 2010), and lethality at the third larval stage in developing *D. melanogaster* (Maier *et al.* 2001). Although mtSSB mutations have not thus far been documented in association with human diseases, as is the case for the genes encoding pol γ and mtDNA helicase, a recent report shows a correlation between the levels of mtSSB protein, mtDNA copy number and the aggressiveness of human osteosarcoma cells, suggesting a link between mtDNA replication and cancer progression (Shapovalov *et al.* 2011).

To date, mutagenesis studies of mtSSB have focused largely on biochemical and physiological properties of amino acid residues involved in tetramerization and/or ssDNA-binding affinities. Li and Williams (1997) demonstrated the importance of highly conserved

residues among tetrameric SSBs for protomer-protomer interactions in the mouse mtSSB, including H69 (H69, *Hs*mtSSB; H64, *Dm*mtSSB (fly)), and for ssDNA binding, including W49, W68 and F74 (W49, W68 and F74, *Hs*mtSSB; Y50, W63 and F69, *Dm*mtSSB). *Dm*mtSSB variants bearing W63A and/or F69A substitutions were defective in DNA binding *in vitro* as predicted, and the corresponding mutant genes promoted mtDNA depletion when expressed in *Drosophila* S2 cells in culture (Farr *et al.* 2004). Interestingly, these proteins were also defective in stimulating the DNA polymerase activity of *Drosophila* pol γ (*Dm*pol γ). The homologous residues in the prototypical tetrameric SSB from *Escherichia coli* (*Ec*SSB) have been implicated in similar functions (Bujalowski and Lohman 1991, Lohman and Ferrari 1994, Raghunathan *et al.* 2000), in keeping with the high degree of conservation between bacterial and mitochondrial SSBs.

We sought to investigate properties that are specific to animal mtSSBs in the context of mtDNA replication by targeting amino acid residues that are well-conserved across animal species, but differ from those in *Ec*SSB. Unlike the bacterial origin of mtSSBs, the catalytic subunit of pol γ and the mtDNA helicase share a common ancestry with the bacteriophage T7 DNA polymerase and primase-helicase enzymes, respectively (Shutt and Gray 2006). This raises the interesting question of how the bacterial-like mtSSB has evolved to function in concert with the T7-like pol γ and mtDNA helicase in the mtDNA replisome. In an earlier study, we explored biochemically the capacity of terminal deletion variants of *Hs*mtSSB to bind ssDNA and stimulate *Hs*pol γ and *Hs*mtDNA helicase (Oliveira and Kaguni 2010). We determined that the absence of the termini was not deleterious and in fact, the stimulation of *Hs*pol γ was higher in the presence of the variants than with wild-type *Hs*mtSSB. In the present report, we describe biochemical and physiological studies of additional mtSSB variants carrying amino acid

substitutions or deletions in residues that map outside of the DNA-binding groove, mostly in loop regions on the surface of the protein (Figure 13). Our findings provide insight into how mtSSB coordinates the functions of pol γ and mtDNA helicase and participates in the formation of the mtDNA replisome, a multi-protein complex in which defects caused by genetic mutations can promote aging, and culminate in a variety of human diseases (Spelbrink *et al.* 2001, Edgar and Trifunovic 2009, Stumpf and Copeland 2011, Euro *et al.* 2011).

Experimental Procedures

Nucleotides and nucleic acids

Unlabeled deoxy- and ribonucleotides were purchased from Amersham Bioscience. [α-^{32}P]dATP and [γ-^{32}P]ATP were purchased from MP Biomedicals. Wild-type M13 (6,407 nt) and pBSKS+ (2,958 nt) DNAs were prepared by standard laboratory methods. Oligodeoxynucleotides complementary to these DNAs were synthesized in an Applied Biosystems oligonucleotide synthesizer. The singly-primed M13 DNA used in DNA polymerase assays was prepared as described previously (Williams *et al.* 1993). The substrate for the DNA unwinding assays and the 48-mer oligodeoxynucleotide used in gel mobility shift assays (GMSA) were prepared as described in Oliveira and Kaguni (2010). The dsRNA used for knockdown of endogenous *Dm*mtSSB (*Dm*mtSSB$_{endo}$) in S2 cells was produced *in vitro* using MEGAscript® T7 kit (Ambion), according to manufacturer's specifications. The DNA used as template in the reaction to produce the dsRNA was generated via PCR with the following primers: 5'<u>TAATACGACTCACTATAGGGAGA</u>AATTTAAGCCCAGATCAC3' and 5'<u>TAATACGACTCACTATAGGGAGA</u>TGGAGTACGACTACGCATG3', where the underlined sequences represent the minimal promoter needed for T7 RNA polymerase

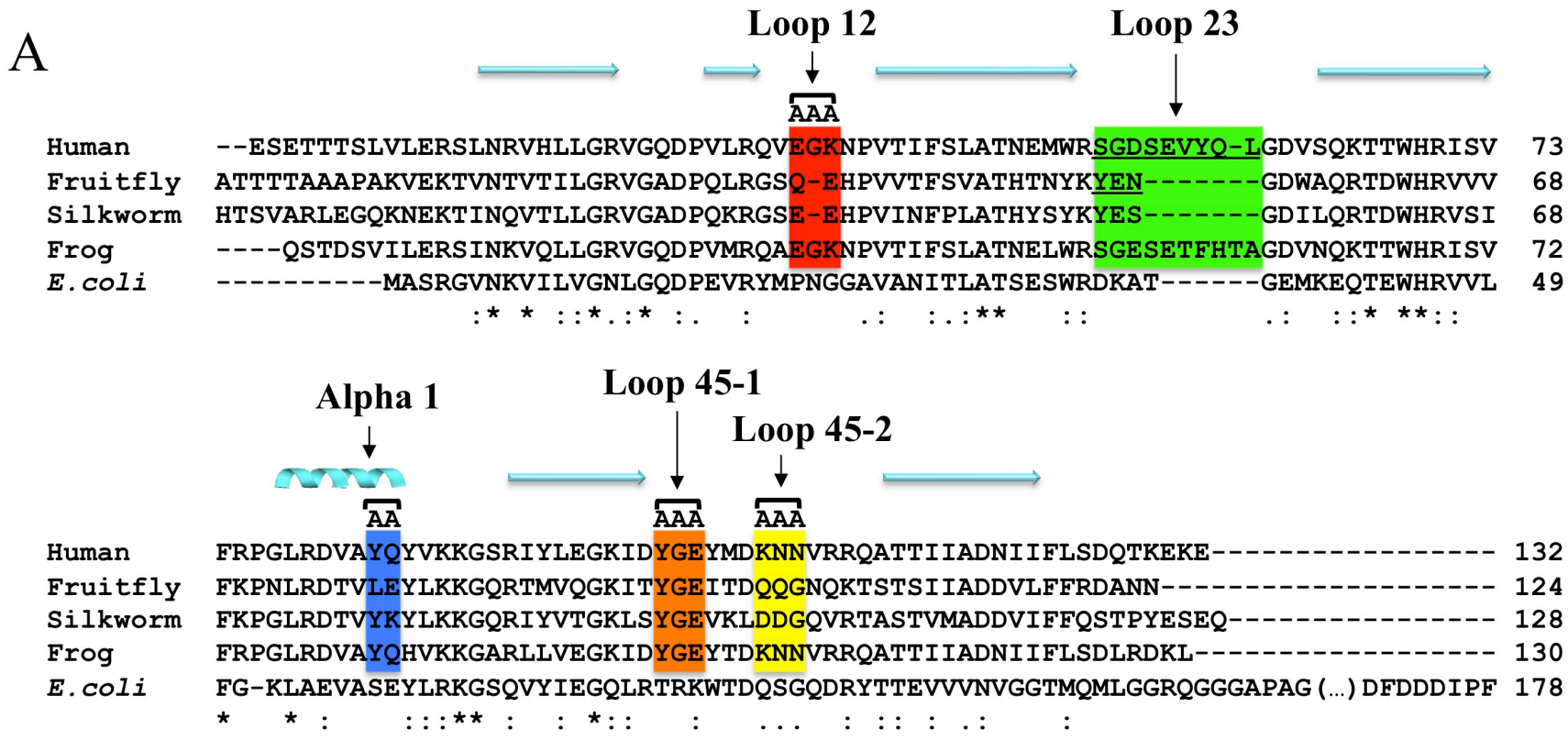
A
Loop 12
Loop 23
AAA
Human --ESETTTSLVLERSLNRVHLLGRVGQDPVLRQVEGKNPVTIFSLATNEMWRSGDSEVYQ-LGDVSQKTTWHRISV 73
Fruitfly ATTTTAAAPAKVEKTVNTVTILGRVGADPQLRGSQ-EHPVVTFSVATHTNYKYEN-------GDWAQRTDWHRVVV 68
Silkworm HTSVARLEGQKNEKTINQVTLLGRVGADPQKRGSE-EHPVINFPLATHYSYKYES-------GDILQRTDWHRVSI 68
Frog ----QSTDSVILERSINKVQLLGRVGQDPVMRQAEGKNPVTIFSLATNELWRSGESETFHTAGDVNQKTTWHRISV 72
E.coli ----------MASRGVNKVILVGNLGQDPEVRYMPNGGAVANITLATSESWRDKAT------GEMKEQTEWHRVVL 49
:* * ::*.:* :. : .: :.:** :: .: ::* **::
Alpha 1
Loop 45-1
Loop 45-2
AA
AAA
AAA
Human FRPGLRDVAYQYVKKGSRIYLEGKIDYGEYMDKNNVRRQATTIIADNIIFLSDQTKEKE----------------- 132
Fruitfly FKPNLRDTVLEYLKKGQRTMVQGKITYGEITDQQGNQKTSTSIIADDVLFFRDANN------------------- 124
Silkworm FKPGLRDTVYKYLKKGQRIYVTGKLSYGEVKLDDGQVRTASTVMADDVIFFQSTPYESEQ---------------- 128
Frog FRPGLRDVAYQHVKKGARLLVEGKIDYGEYTDKNNVRRQATTIIADNIIFLSDLRDKL------------------ 130
E.coli FG-KLAEVASEYLRKGSQVYIEGQLRTRKWTDQSGQDRYTTEVVVNVGGTMQMLGGRQGGGAPAG(...)DFDDDIPF 178
* * : :::** : : *:: : ... : :: : .: :

Figure 13.

Figure 13 (continued).

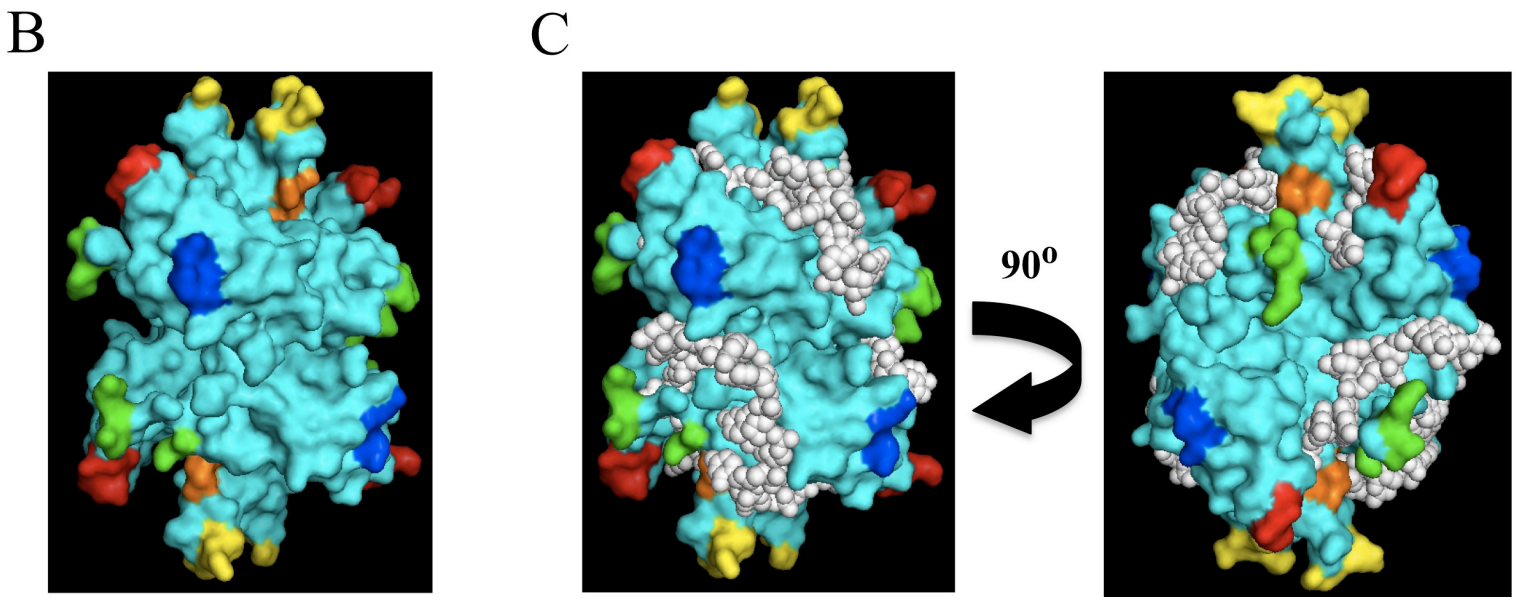

Figure 13. Mutagenesis of mtSSB and model of ssDNA binding. A, multiple sequence alignment of animal mtSSBs with *E. coli* SSB was performed as described in Oliveira and Kaguni (2010). Only the representative mtSSB sequences from humans (GenBank accession: NP_003134), fruitfly (*Drosophila melanogaster*; GenBank accession: AAF16936), silkworm (*Bombyx mori*; GenBank accession: ABF51293), and frog (*Xenopus laevis*; GenBank accession: NP_001095241) are shown. Targeted amino acid residues are highlighted in colored boxes: those indicated as "AA" or "AAA" were selected for double or triple alanine substitution mutagenesis, respectively; residues in loop 2,3 were targeted for deletion mutagenesis (underlined). **B**, mapping of targeted residues on the crystal

structure of *Hs*mtSSB (Yang *et al.* 1997). **C**, model of *Hs*mtSSB bound to ssDNA (represented as white spheres) showing that the targeted residues do not lie on the DNA-binding groove of the protein. Colored residues in **B** and **C** are the same as represented in **A**. The nomenclature adopted to describe the structural elements of *Hs*mtSSB is that used by Raghunathan *et al.* (1997) for *Ec*SSB, in which the loop regions contain the numbers of its flanking β-sheet elements (for example, loop 1,2 lies between β-sheets 1 and 2). For interpretation of the references to color in this and all other figures, the reader is referred to the electronic version of this dissertation.

transcription initiation. The amplified fragment (~120 bp) contained the entire sequence of the 3' UTR of the mRNA of *Dm*mtSSB$_{endo}$.

Mutagenesis of Hs*mtSSB and* Dm*mtSSB*

*Hs*mtSSB variants were constructed via site-directed PCR mutagenesis of the *Hs*mtSSBwt cDNA (notwithstanding the mitochondrial presequence) cloned into pET11a vector. PCRs were performed using this vector as template, *Pfu* DNA polymerase (Stratagene) and standard laboratory methods. The oligonucleotides used for PCR were: 5'TGAGACAGGTGGcAGcAgcAAATCCAGTCACAATA3' and 5'TATTGTGACTGGATTTgcTgCTgCCACCTGTCTCA3' for *Hs*mtSSBloop12; 5'CTAATGAGATGTGGCGA--GGTGATGTCAGTC3' and 5'GACTGACATCACC--TCGCCACATCTCATTAG3' for *Hs*mtSSBloop23; 5'CAGAGACGTGGCAgcTgcATATGTGAAAAAG3' and 5'CTTTTTCACATATgcAgcTGCCACGTCTCTG3' for *Hs*mtSSBα1; 5'GGGAAAATAGACgcTGcTGcATACATGGATAAAAA3' and 5'TTTTTATCCATGTATgCAgCAgcGTCTATTTTCCC3' for *Hs*mtSSBloop45-1; and 5'GTGAATACATGGATgcAgcTgcTGTGAGGCGACAAG3' and 5'CTTGTCGCCTCACAgcAgcTgcATCCATGTATTCAC3' for *Hs*mtSSBloop45-2. *Dm*mtSSB variants were constructed via site-directed PCR mutagenesis of the *Dm*mtSSBwt cDNA cloned into pMt/Hy vector. PCRs were performed using this vector as template, *Pfu* DNA polymerase (Stratagene) and standard laboratory methods. The oligonucleotides used for PCR were: 5'CCGGCACGCGGG--GTTGAAAAAACTG3' and 5'CAGTTTTTTCAAC--CCCGCGTGCCGG3' for *Dm*mtSSBΔN;

5’GCTGCGTGGATCCgcGGcGCATCCGGTGGTC3’ and 5’GACCACCGGATGCgCCgcGGATCCACGCAGC3’ for *Dm*mtSSBloop12; 5’CACCAACTACAAA--GGCGACTGGGCC3’ and 5’GGCCCAGTCGCC--TTTGTAGTTGGTG3’ for *Dm*mtSSBloop23; 5’GCGTGACACCGTGgcGGcATACTTGAAGAAGG3’ and 5’CCTTCTTCAAGTATgCCgcCACGGTGTCACGC3’ for *Dm*mtSSBα1; 5’GGGAAAGATCACCgcTGcAGcGATCACCGACCAGC3’ and 5’GCTGGTCGGTGATCgCTgCAgcGGTGATCTTTCCC3’ for *Dm*mtSSBloop45-1; 5’GAGAGATCACCGACgcGgcGGcCAACCAGAAGACT3’ and 5’AGTCTTCTGGTTGgCCgcCgcGTCGGTGATCTCTC3’ for *Dm*mtSSBloop45-2; and 5’GTTGTTTTTCCGTTAAGCCAACAACTAA3’ and 5’TTAGTTGTTGGCTTAACGGAAAAACAAC3’ for *Dm*mtSSBΔC. The lower case letters, the “--” and the underlined sequences indicate the sites where mutations were introduced to create alanine substitutions, amino acid deletions or a stop codon, respectively.

Purification of Hs*mtSSBs,* Hs*pol γ and* Hs*mtDNA helicase*

Recombinant human mtSSB proteins were prepared from bacterial cells, as described by Oliveira and Kaguni (2010). Recombinant human pol γ-α exo$^-$ and pol γ-β were prepared from *Sf*9 and bacterial cells, respectively, as described by Oliveira and Kaguni (2009). Recombinant human mtDNA helicase was prepared from *Sf*9 cells, as described by Ziebarth *et al.* (2007).

Gel mobility shift assays and DNA unwinding assays

GMSA and DNA unwinding assays were performed as described in Oliveira and Kaguni (2010). Briefly, reaction mixtures (20 μL) for GMSA contained 20 mM Tris-HCl, pH 7.5, 1 mM DTT, 4 mM $MgCl_2$, 50 mM NaCl, 36 fmol 5′-end-labeled 48-mer, and the indicated amounts of *Hs*mtSSB proteins. Samples were incubated at 20°C for 10 min prior to electrophoresis in 6% native polyacrylamide gels. For DNA unwinding assays, reaction mixtures (50 μL) contained 20 mM Tris-HCl, pH 7.5, 10% glycerol, 500 μg/mL bovine serum albumin, 10 mM DTT, 4 mM $MgCl_2$, 3 mM ATP, 50 mM KCl, 0.4 nM of DNA unwinding substrate, 4 nM of *Hs*mtDNA helicase (as hexamer), and the indicated concentrations of *Hs*mtSSB proteins. The reactions were incubated at 37°C for 30 min and then processed for analysis. DNA products were fractionated from substrate by electrophoresis in a 22% native polyacrylamide gel at 600 V for ~ 30 min. The data from GMSA and DNA unwinding assays were analyzed with Origin (OriginLab, Northampton, MA), using a sigmoidal curve fit and default parameters. The values of maximal DNA unwinding stimulation by *Hs*mtSSB variants were compared to that of *Hs*mtSSBwt using a Student's t-test.

DNA polymerase γ stimulation assays

Reaction mixtures (50 μL) contained 50 mM Tris-HCl, pH 8.5, 4 mM $MgCl_2$, 400 μg/ml bovine serum albumin, 10 mM DTT, 20-100 mM KCl, 20 μM each dGTP, dATP, dCTP and dTTP, [α-^{32}P]dATP (2 μCi), 3 μM (as nucleotide) singly-primed wild-type M13 DNA, 10 ng *Hs*pol γ-α exo$^-$ Fr IV, 48 ng *Hs*pol γ-β Fr III, and the indicated amounts of *Hs*mtSSB proteins.

Incubation was at 37^{o}C for 30 min. Samples were processed and nucleotide incorporation was quantitated in a liquid scintillation counter.

Generation of stable cell lines, knockdown of Dm*mtSSB$_{endo}$ and induction of* Dm*mtSSB variants*

Drosophila Schneider S2 cells were cultured at 25^{o}C in *Drosophila* Schneider medium supplemented with 10% fetal bovine serum, 50 U/mL penicillin G and 50 μg/mL streptomycin sulfate (Gibco-Invitrogen). For establishment of stable lines, ~1.2 x 10^{7} cells were transfected with 1 μg of pMt/Hy vector carrying *Dm*mtSSBwt or variant genes using the Effectene kit (Qiagen), according to manufacturer's specifications. Hygromycin-resistant cells were selected with 0.2 mg/mL hygromycin for at least 5 passages, before transfer to standard growth medium. For knockdown of endogenous *Dm*mtSSB protein, 3 μg of dsRNA (representing the 3' UTR of *Dm*mtSSB$_{endo}$ mRNA) were delivered to 3 x 10^{6} cells using the Effectene kit. Cells were cultured for 3 days before reduction in levels of *Dm*mtSSB$_{endo}$ protein was observed. In the experiments with EtBr, cells were treated with 0.2 μg EtBr per mL of growth medium 3 days prior to treatment with dsRNA. For induction of expression of *Dm*mtSSB variants, cells treated with dsRNA for 3 days were subjected to the indicated concentrations of $CuSO_4$ to promote appropriate expression from the metallothionein promoter (Bunch *et al.* 1988).

Immunoblotting

For *Dm*mtSSB detection, total protein extracts from S2 cells were separated in 17% SDS-polyacrylamide gels following standard laboratory methods. Proteins were transferred to

nitrocellulose membranes (Protran BA83, Whatman), which were preincubated for 1 h with 5% skim milk in Tris-buffered saline containing 0.1% Tween 20 (TBST), followed by incubation of 1 h with *Dm*mtSSB antibody (1:8000 dilution in TBST/1% milk). The membranes were washed several times with TBST for 1.5 h, incubated with horseradish peroxidase-conjugated anti-rabbit IgG (1:16000 dilution in TBST/1% milk, Bio-Rad) for 1 h, and washed again several times with TBST for 1.5 h. *Dm*mtSSB bands were visualized using ECL Western blotting reagents (Amersham Biosciences). For β-tubulin detection, a similar procedure was performed, except that protein extracts were run on 12% SDS-polycrylamide gels and the antibodies used were E7 supernatant (1:50 dilution in TBST/1% milk – DSHB, University of Iowa) and alkaline phosphatase-conjugated anti-mouse IgG (1:2000 dilution in TBST/1% milk, Bio-Rad). β-tubulin bands were visualized using alkaline phosphatase buffer (100 mM Tris-HCl, pH 9.5, 100 mM NaCl and 5 mM $MgCl_2$) containing 330 μg/mL nitro blue tetrazolium and 165 μg/mL 5-bromo-4-chloro-3-indolyl phosphate.

Quantitative real time-PCR

Total DNA was extracted from S2 cells using phenol/chloroform protocol and standard laboratory procedures. mtDNA copy number was determined by quantification of relative amounts of mtDNA to nuclear DNA via real time amplification of a fragment of the mitochondrial 16S gene (primers: 5'AAAAAGATTGCGACCTCGAT3' and 5'AAACCAACCTGGCTTACACC3') and the nuclear RpL32 gene (primers: 5'AGGCCCAAGATCGTGAAGAA3' and 5'TGTGCACCAGGAACTTCTTGAA3'). Reactions were performed using SYBR® Green JumpStart™ Taq ReadyMix™ (Sigma-Aldrich) on a

7500 Real Time PCR System instrument (Applied Biosystems), according to manufacturers' specifications.

Molecular modeling

To construct the model of *Hs*mtSSB bound to ssDNA, the crystal structure of *Hs*mtSSB (pdb code 3ULL, Yang *et al.* 1997) was aligned to the structure of *Ec*SSB bound to ssDNA (pdb code 1EYG, Raghunathan *et al.* 2000) using PyMol (The PyMOL Molecular Graphics System, Version 1.3, Schrödinger, LLC). The atomic coordinates of *Ec*SSB were then removed, causing the structure of ssDNA to fit in the DNA binding groove of *Hs*mtSSB without major atomic collisions.

Results

We selected candidate regions of the mtSSB protein for mutagenesis based on the assumption that residues important for functional and/or physical interactions with pol γ and mtDNA helicase would be well conserved among animal mtSSB sequences, and also locate on the surface of the protein structure. We avoided residues conserved between mtSSBs and *Ec*SSB, because of their essential roles in the stabilization of the tertiary/quaternary structure of the protein and/or in contacting DNA directly; disrupting such properties would be expected to cause indirect effects on the ability of the protein to stimulate its mtDNA replisome partners (Farr *et al.* 2004). The selected residues and an evaluation of their locations in a molecular model of *Hs*mtSSB bound to ssDNA that indicates none of them are likely to interact directly with ssDNA are shown in Figure 13.

Differential stimulation of Hs*pol γ and* Hs*mtDNA helicase by variants of* Hs*mtSSB*

We expressed and purified near to homogeneity recombinant wild-type *Hs*mtSSB (*Hs*mtSSBwt), and proteins bearing double- or triple-alanine substitutions mapping in loop 1,2 (E33A/G34A/K35A, *Hs*mtSSBloop12), in alpha-helix 1 (Y83A/Q84A, *Hs*mtSSBα1), and in loop 4,5 (Y100A/G101A/E102A, *Hs*mtSSBloop45-1; and K106A/N107A/N108A, *Hs*mtSSBloop45-2), or a deletion in loop 2,3 (S51-L59, *Hs*mtSSBloop23). Velocity sedimentation indicated that all the variant *Hs*mtSSB proteins retain their homotetrameric state (data not shown), whereas their ssDNA-binding affinities, as analyzed by gel mobility shift assays (GMSA), varied slightly (Figure 14A). The variants *Hs*mtSSBloop12 and *Hs*mtSSBloop23 bound to ssDNA with affinities 1.3- and 1.6-fold higher than that of *Hs*mtSSBwt, respectively; the affinities of the three other variants did not differ substantially from that of *Hs*mtSSBwt, consistent with the model presented in Figure 13C.

We then examined the ability of the *Hs*mtSSB variants and non-cognate SSBs to stimulate the dsDNA unwinding activity of *Hs*mtDNA helicase. Interestingly, helicase stimulation by *Hs*mtSSBloop12 and *Hs*mtSSBloop23 reflects their increased ssDNA binding, as maximal stimulation is achieved at lower concentrations of these variants (37 nM) as compared to *Hs*mtSSBwt (50 nM). Nevertheless, maximal stimulation by *Hs*mtSSBloop12 is reduced ~40% as compared to that by *Hs*mtSSBwt, whereas the reduction caused by *Hs*mtSSBloop23 is only ~15% (Figure 14B). In addition, *Hs*mtSSBloop45-2 also showed a ~40% reduced capacity to stimulate *Hs*mtDNA helicase *in vitro*, suggesting that residues in loop 1,2 and 4,5-2 are responsible for the functional interactions that we observed between *Hs*mtSSB and *Hs*mtDNA helicase. In comparison, we found that the maximal stimulation of the *Hs*mtDNA helicase by *Hs*mtSSBwt is similar to that contributed by the non-cognate *Dm*mtSSBwt and *Ec*SSB (Figure

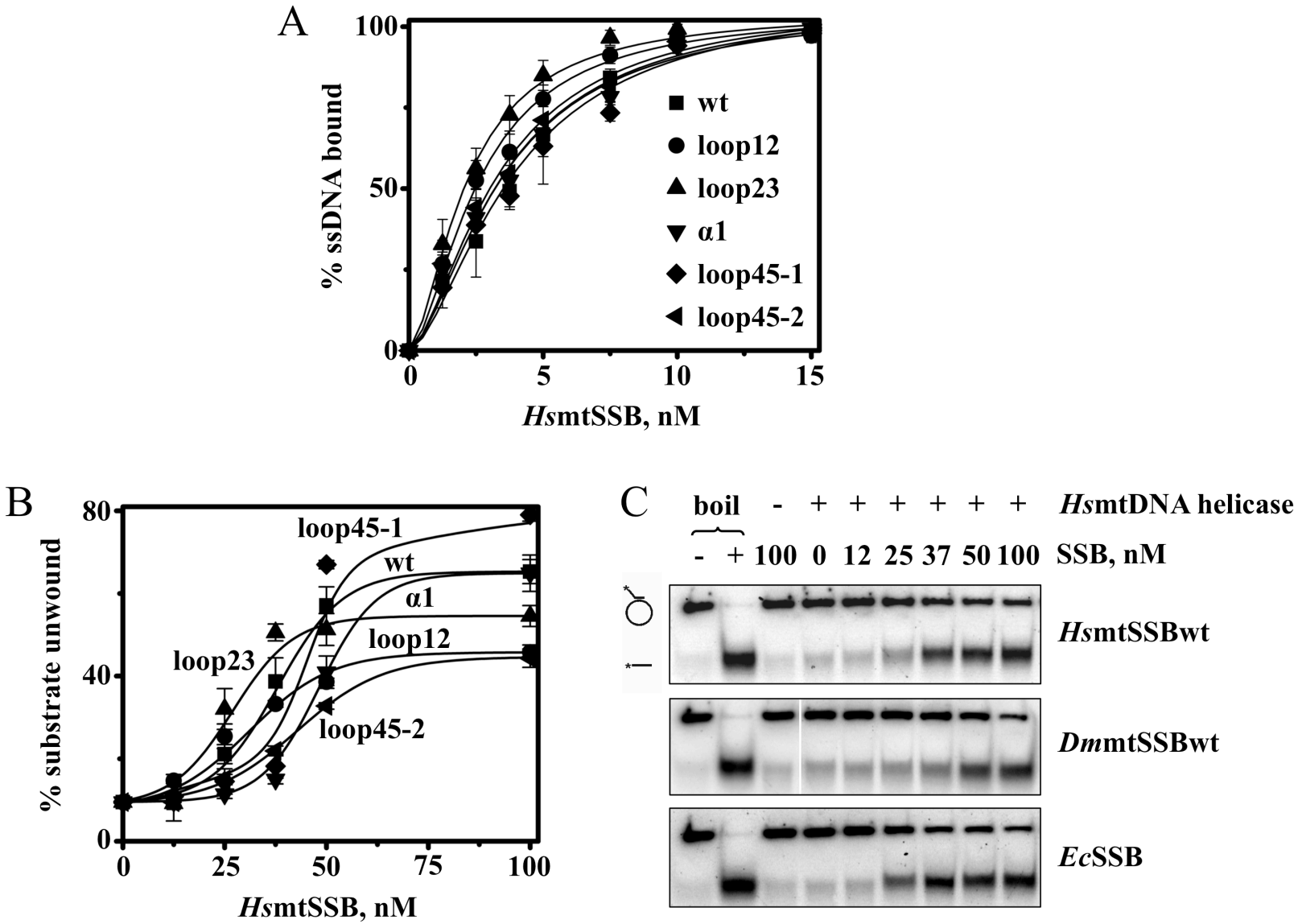

Figure 14. ssDNA-binding affinities and stimulation of *Hs*mtDNA helicase by *Hs*mtSSB variants. A, ssDNA-binding affinity was

evaluated by GMSA, as described under "Experimental Procedures". The fraction of unbound and bound oligomer was quantitated, and the data were plotted as the average percent of substrate utilized from three independent experiments. **B** and **C**, DNA unwinding assays were performed as described under "Experimental Procedures", using 3.5 nM of *Hs*mtDNA helicase (as hexamer). "–" and "+ boil" lanes represent the intact and denatured substrate (heated to 100^{o}C for 2 min prior to loading), respectively. The data in **B** represent the average of unwound substrate as percent from three independent experiments.

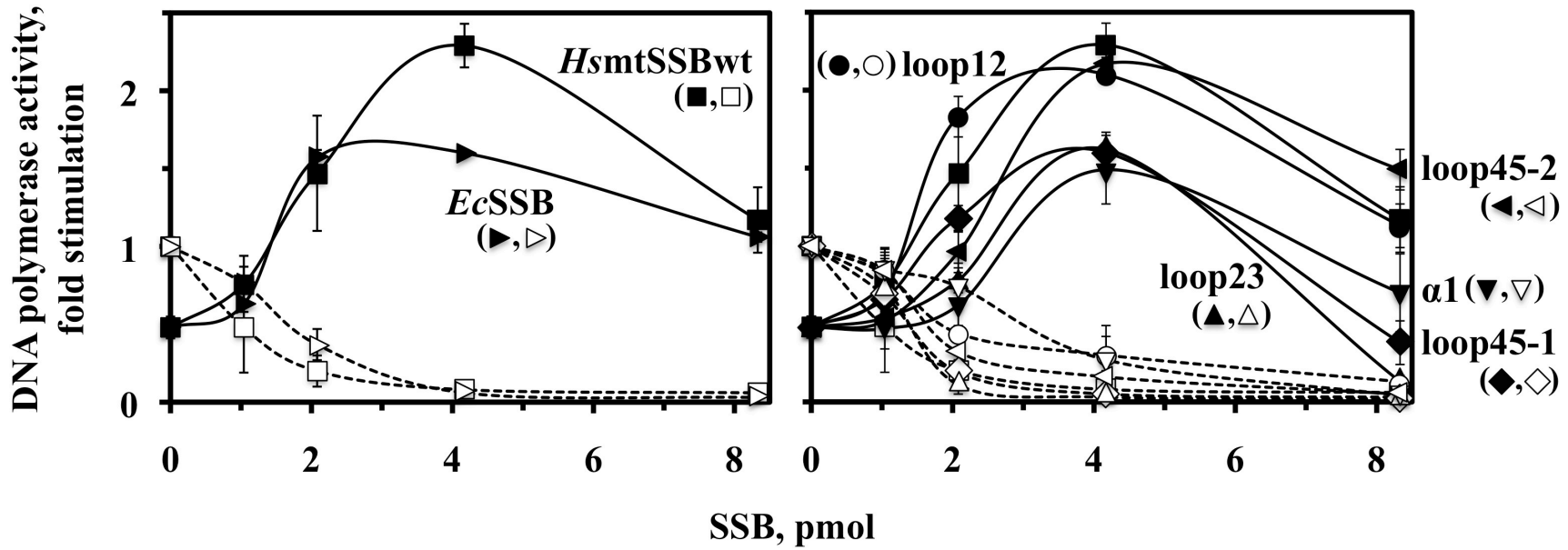

Figure 15. Variants of *Hs*mtSSB have reduced capacity to stimulate DNA polymerase activity of *Hs*pol γ. DNA polymerase assays were performed as described under "Experimental Procedures", on singly-primed M13 DNA using 60 fmol of *Hs*pol γ holoenzyme and the indicated amounts of SSB. Assays were performed at 20 mM KCl (solid lines and symbols) and at 100 mM KCl (dashed lines and open symbols). The data were normalized to the amount of nucleotide incorporated by *Hs*pol γ at 100 mM KCl in the absence of SSB (arbitrarily set to 1), and represent the average of three independent experiments.

14C), in contrast with to the results reported by Korhonen *et al.* (2003).

Next, we measured the stimulation of the DNA polymerase activity of *Hs*pol γ on a singly-primed ssDNA template. As we reported previously (Oliveira and Kaguni 2010), we observed that the DNA polymerase activity of *Hs*pol γ in the absence of *Hs*mtSSB was approximately 2-fold higher at 100 mM than at 20 mM KCl. In contrast, in the presence of the variant *Hs*mtSSBs, *Hs*pol γ was stimulated at 20 mM KCl, but inhibited completely at 100 mM KCl (Figure 15). Furthermore, the variants *Hs*mtSSBloop23, *Hs*mtSSBα1 and *Hs*mtSSBloop45-1 show a reduced capacity to stimulate DNA synthesis by *Hs*pol γ (~60% of that of *Hs*mtSSBwt), which indicates that the altered amino acid residues in these variants are important for the functional interactions between *Hs*mtSSB and *Hs*pol γ. Notably, the stimulation of *Hs*pol γ by these defective variants is similar to that observed with the non-cognate *Ec*SSB, and the *Hs*mtSSB residues identified as important for *Hs*pol γ stimulation differ from those shown to be important for stimulation of *Hs*mtDNA helicase (Figure 14B).

mtDNA depletion in cells overexpressing variants of Dm*mtSSB under conditions of mitochondrial homeostasis*

We developed a *Drosophila* S2 cell system in which we knocked down *Dm*mtSSB protein ($Dm\text{mtSSB}_{endo}$) by treatment with dsRNA homologous to the 3'-UTR of the endogenous gene and expressed an exogenous *Dm*mtSSB variant, to evaluate mtDNA maintenance and replication under various physiological conditions. dsRNA treatment depleted $Dm\text{mtSSB}_{endo}$ and mtDNA copy number to ~10% and ~40% of the levels in the control cells, respectively. In agreement with previous data from our lab (Farr *et al.* 2004), expression of an exogenous

*Dm*mtSSBwt gene promoted an increase in mtDNA copy number proportional to the level of protein induction (Figure 16A).

We also established stable cell lines carrying the genes for five *Dm*mtSSB variants equivalent to the *Hs*mtSSB variants described above (Q35A/E36A, *Dm*mtSSBloop12; ΔY52-N54, *Dm*mtSSBloop23; L68A/E69A, *Dm*mtSSBα1; Y85A/G86A/E87A, *Dm*mtSSBloop45-1; and Q91A/Q92A/G93A, *Dm*mtSSBloop45-2). Additionally, we established cell lines to express *Dm*mtSSBΔN (Δ1-11) and *Dm*mtSSBΔC (Δ121-124), which we have recently shown to modulate pol γ stimulation *in vitro* in the human system (Oliveira and Kaguni 2010). However, we observed that their induction is consistently poor (data not shown), indicating that the deletion variants are unstable in the cellular environment. Immunoblot analysis showed that expression of the other five variants occurs at high levels after 14 days of induction with 0.4 mM $CuSO_4$ (5- to 10-fold higher than *Dm*mtSSB$_{endo}$; Figure 16B, *upper panel*). Relative mtDNA copy number in cells overexpressing *Dm*mtSSBwt was unchanged, but was reduced significantly (25-60% of that of control cells) in cells overexpressing *Dm*mtSSBloop12, loop23, α1, loop45-1 and loop45-2, and in *Dm*mtSSB$_{endo}$-knockdown cells (Figure 16B, *lower panel*).

Defects in mtDNA repletion upon expression of Dm*mtSSB variants*

We then investigated mtDNA repletion in S2 cells expressing the *Dm*mtSSB variants after mtDNA depletion with ethidium bromide (EtBr). Application of low concentrations of EtBr in the cell culture (0.2 μg/mL growth media) depleted mtDNA to ~30% of that of control cells after three days of treatment, without affecting *Dm*mtSSB$_{endo}$ levels (Figure 17A). After removal of EtBr from the culture, control cells recovered completely from mtDNA depletion in

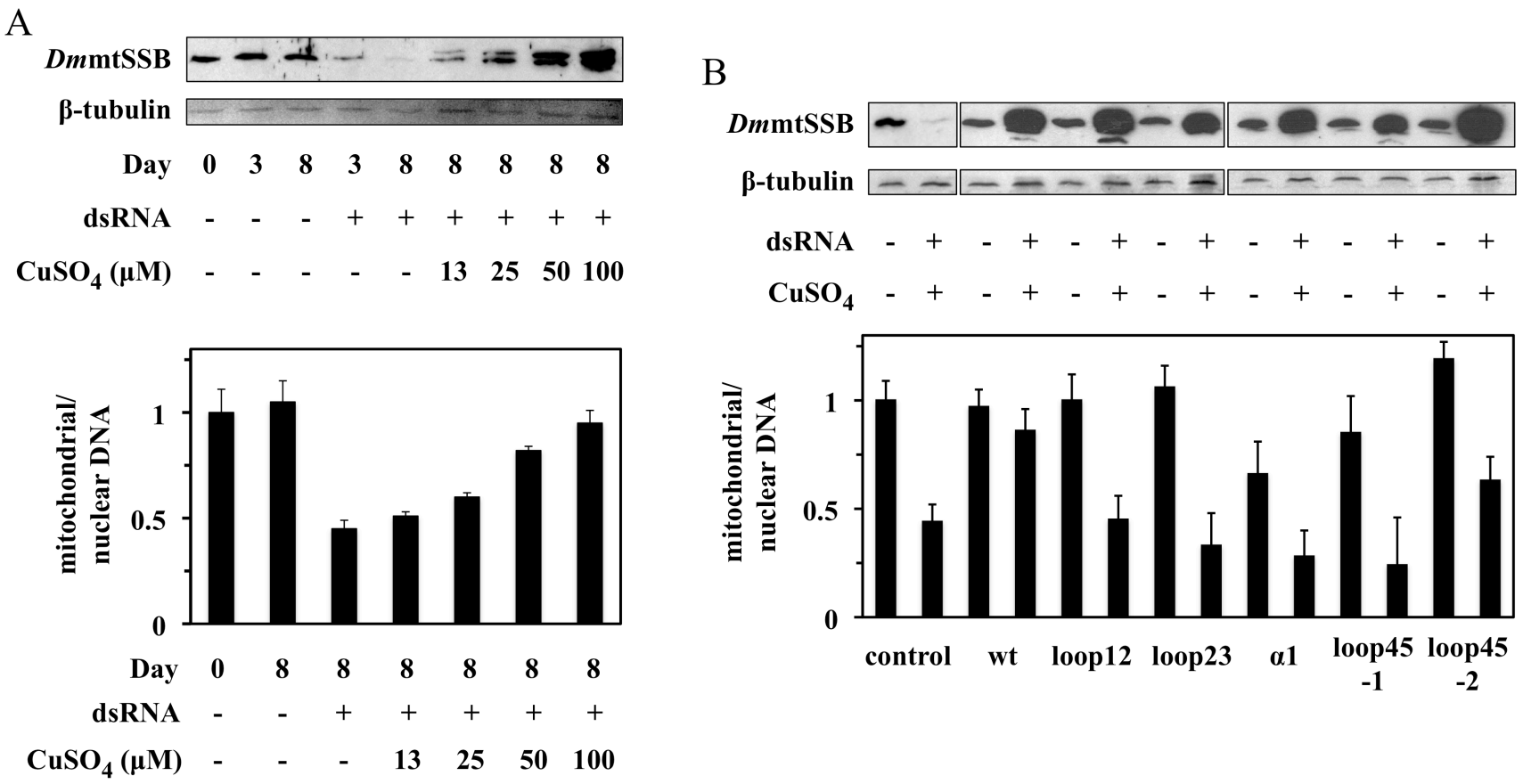

Figure 16. Knockdown of *Dm*mtSSB$_{endo}$ and overexpression of *Dm*mtSSB variants in S2 cells causes mtDNA depletion under conditions of mitochondrial homeostasis. A, cells carrying pMt/*Dm*mtSSBwt/Hy were cultured in the presence of dsRNA homologous to the 3'-UTR of *Dm*mtSSB$_{endo}$ mRNA (1 μg per 10^6 cells) and the indicated concentration of $CuSO_4$, and harvested at

the indicated time points. Immunoblotting analysis of *Dm*mtSSB and β-tubulin proteins (*upper panel*), and qPCR to measure relative mtDNA copy number (*lower panel*), were performed as described under "Experimental Procedures". The band above the exogenous *Dm*mtSSBwt (*upper panel*) represents the accumulation of the pre-processed form of the protein that contains the mitochondrial targeting signal. **B**, cells carrying pMt/Hy plasmids with the indicated *Dm*mtSSB variants were cultured for 14 days in the presence or absence of dsRNA (1 μg per 10^6 cells) and 0.4 mM $CuSO_4$. Effects of overexpression on mtDNA levels were quantitated and are shown in the *lower panel*. The data were normalized to the ratio of mitochondrial/ nuclear DNA in S2 cells without treatment (arbitrarily set to 1), and represent the average of experiments from at least two independent cell lines. Error bars represent the standard deviation among the lines. Bands below the exogenous *Dm*mtSSBwt, loop12 and loop45-1 protein bands (*upper panel*) represent proteolytic products observed upon their overexpression, and/ or in sample processing.

~9 days, whereas mtDNA levels in *Dm*mtSSB$_{endo}$-knockdown cells remained substantially lower (55% of that of control cells) for as long as 15 days. Cells carrying the exogenous *Dm*mtSSBwt gene were treated with dsRNA to knock down *Dm*mtSSB$_{endo}$, and with $CuSO_4$ to induce the expression of *Dm*mtSSBwt after EtBr treatment. When *Dm*mtSSBwt was expressed at a level comparable to *Dm*mtSSB$_{endo}$ in control cells (in the presence of 0.04 mM $CuSO_4$), recovery from mtDNA depletion also occurred in ~9 days, after a 3-day lag time. This delay may result from our experimental design, which requires $CuSO_4$ addition to the cells 3 days after the dsRNA treatment (see "Experimental Procedures" for details). In contrast to endogenous-level *Dm*mtSSBwt expression, the 3-day lag time was not observed upon *Dm*mtSSBwt overexpression, and mtDNA copy number was restored to normal levels at a faster rate (Figure 17A, *right panel*).

Next, we induced the five *Dm*mtSSB variant proteins at two expression levels after the combined EtBr and dsRNA treatments: expression levels equivalent to *Dm*mtSSB$_{endo}$ under normal growth conditions (endogenous-level) and overexpression (Figure 17B). We observed distinct phenotypes of mtDNA depletion, allowing us to categorize the variants in three groups. The first comprises *Dm*mtSSBloop12, which is the only protein that caused strong reduction of mtDNA copy number under conditions of mitochondrial homeostasis (40% of that of control cells), but showed only a small-to-moderate effect under recovery from depletion, either upon endogenous-level expression or overexpression of the protein (60-80% of that of cells expressing *Dm*mtSSBwt). The second group comprises *Dm*mtSSBloop23, which caused a clear mtDNA depletion (15-30% of that of control cells) only when high levels of the protein were expressed. The third group comprises *Dm*mtSSBα1, loop45-1 and loop45-2, which caused reduction in

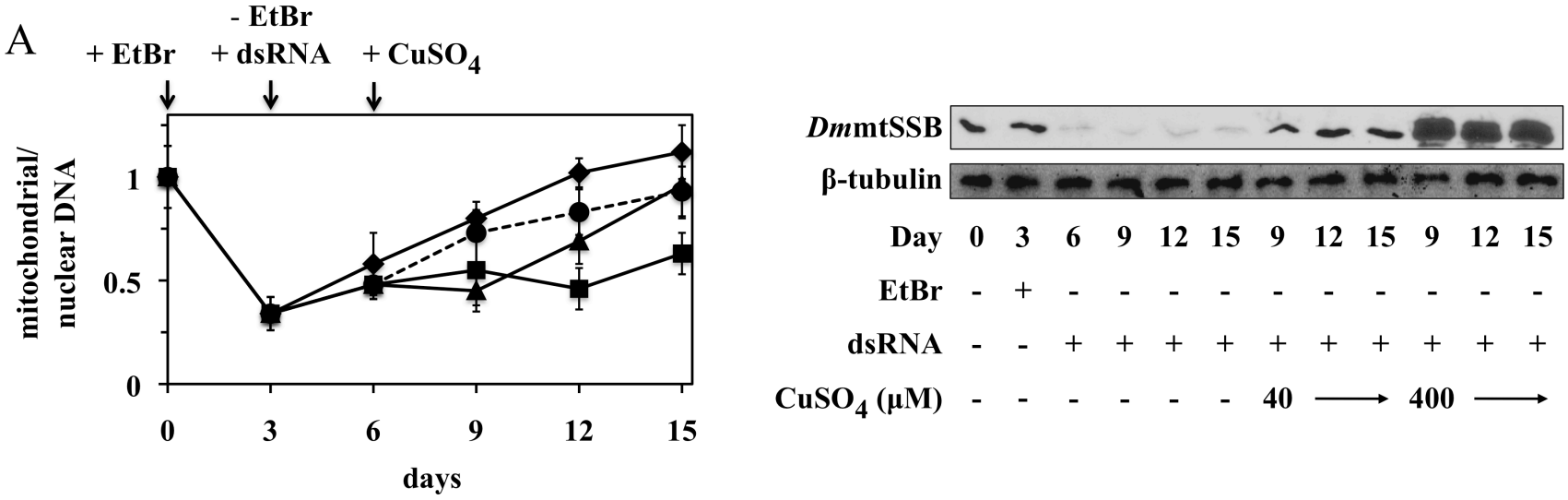
A
- EtBr
+ EtBr
+ dsRNA
+ CuSO4
mitochondrial/
nuclear DNA
1
0.5
0
0
3
6
9
12
15
days
DmmtSSB
β-tubulin
Day 0 3 6 9 12 15 9 12 15 9 12 15
EtBr - + - - - - - - - - - -
dsRNA - - + + + + + + + + + +
CuSO4 (μM) - - - - - - 40 → 400 →

Figure 17.

Figure 17 (continued).

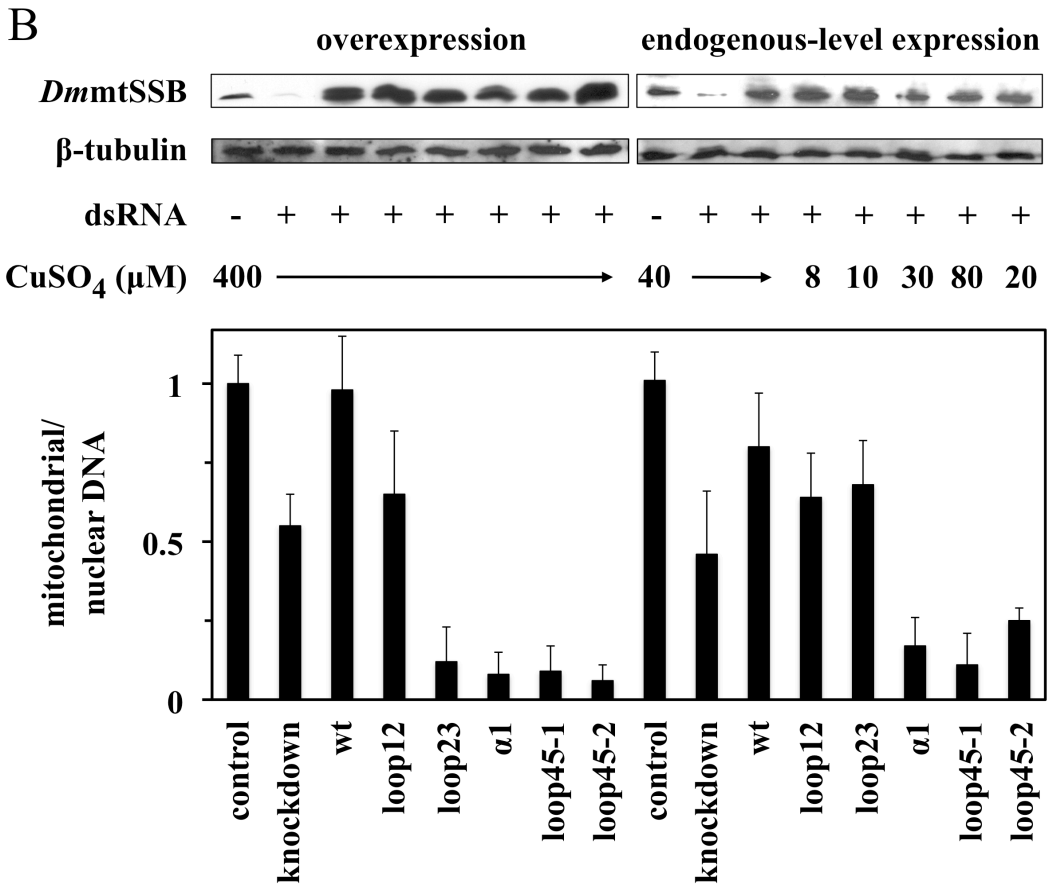

Figure 17. Expression of *Dm*mtSSB variants impedes recovery from mtDNA depletion in *Drosophila* S2 cells. A, *left panel*, 0.2 μg/mL of EtBr was applied for 3 days to the growth media of cells carrying the *Dm*mtSSBwt gene, followed by a recovery time of 12

days upon removal of EtBr. Control cells had neither dsRNA or $CuSO_4$ treatment (diamonds and solid line), whereas experimental lines were treated with dsRNA only (squares and solid line), dsRNA and 40 μM $CuSO_4$ (triangles and solid line), or dsRNA and 400 μM $CuSO_4$ (circles and dashed line). The time point in which each treatment was initiated is indicated with arrows. Relative mtDNA copy number was analyzed by qPCR, as described under "Experimental Procedures". *Right panel*, *Dm*mtSSB and β-tubulin protein levels were analyzed by immunoblotting, as described under "Experimental Procedures". **B**, the experimental design was as in **A** using cells expressing different *Dm*mtSSB variant genes. The concentrations of $CuSO_4$ used to induce the overexpression and endogenous-level expression of *Dm*mtSSB proteins are indicated. Cells were harvested at day 12 (9 days of recovery from EtBr treatment). *Upper panel*, *Dm*mtSSB and β-tubulin protein levels were analyzed by immunoblotting and by qPCR, respectively. *Lower panel*, relative mtDNA copy number was analyzed by qPCR. The data were normalized to the ratio of mitochondrial/ nuclear DNA in control S2 cells (arbitrarily set to 1), and represent the average of experiments with two independent cell lines. Error bars represent the standard deviation among the lines.

mtDNA copy number under all conditions tested (10-50% of that of control cells), with more severe phenotypes revealed upon overexpression of the protein during recovery from the EtBr treatment. Interestingly, the knockdown of *Dm*mtSSB$_{endo}$ (dsRNA treatment only) caused about the same reduction in mtDNA copy number under both homeostasis and EtBr recovery conditions (Figures. 16B and 17B).

Discussion

DNA replisomes are well-coordinated machines in which the activity of one protein component is regulated by that of the others. For example, replicative helicases from bacteria and viruses that unwind dsDNA at low catalytic rates become highly efficient when coupled to DNA polymerases and/ or SSBs (reviewed in Hamdan and Richardson 2009, Langston *et al.* 2009). At the animal mtDNA replication fork, little is known about how the three key components of the replisome function coordinately to copy the mitochondrial genome. Studies to date have focused largely on structure-function relationships in pol γ and mtDNA helicase, and their association with human diseases, such as progressive external ophthalmoplegia and Alper's syndrome (Kaguni 2004, Korhonen *et al.* 2008, Holmlund *et al.* 2009, Stumpf and Copeland 2011, Euro *et al.* 2011). Furthermore, deregulation of replisome function *in vivo* has been shown in human cell lines expressing active site mutants of pol γ and mtDNA helicase: dysfunctional pol γ mutants induced delayed lagging-DNA strand synthesis causing replication stalling, whereas defective helicases caused an increased rate of initiation of lagging-DNA strand synthesis relative to the rate of mtDNA fork progression (Wanrooij *et al.* 2007).

Here, we present a biochemical and physiological analysis of the role of mtSSB at the mtDNA replication fork. We generated five recombinant *Hs*mtSSB variants designed not to

exhibit defects in ssDNA binding, and found that two of them (*Hs*mtSSBloop12 and loop23) actually bound ssDNA with slightly higher affinity than *Hs*mtSSBwt, indicating that loops 1,2 and 2,3 in *Hs*mtSSB are either closer to the DNA-binding channel and/ or participate negatively in an alternative binding mode. We speculate that loop 2,3 of vertebrate mtSSBs, which contain a 6-7 amino acid insertion relative to this region in invertebrate mtSSBs and bacterial SSBs, can form a flexible domain that may disturb ssDNA binding in the absence of pol γ. Most of the amino acid residues in loop 2,3 are disordered in the crystal structure of *Hs*mtSSB (Yang *et al.* 1997), the loop carries a slight negative charge, as analyzed by electrostatic surface potential, and it appears to be important for pol γ stimulation *in vitro* and *in vivo*, as discussed below.

Functional interactions between pol γ and mtSSB have been shown clearly with native and recombinant forms of the *Drosophila* proteins (Thommes *et al.* 1995, Farr *et al.* 1999, 2004, Maier *et al.* 2001). Both the DNA polymerase and exonuclease activities of the *Dm*pol γ holoenzyme are stimulated 15- to 20-fold on singly primed ssDNA templates by *Dm*mtSSB over a broad range of KCl concentrations. *Dm*mtSSB increases primer recognition, DNA synthesis, processivity, and mispair hydrolysis during proofreading DNA synthesis by *Dm*pol γ. In the human system, *Hs*pol γ holoenzyme is stimulated by *Hs*mtSSB only at very low ionic strength, and the overall stimulation is only ~2.5-fold (Oliveira and Kaguni 2010, Figure 15). We showed here that *Ec*SSB can also interact functionally with *Hs*pol γ and stimulate its DNA polymerase activity ~1.5-fold at 20 mM KCl, establishing a baseline level of *Hs*pol γ stimulation *in vitro*. The ability of *Hs*mtSSB variants in loop23, α1 and loop45-1 to stimulate the mitochondrial replicase was no better than that of *Ec*SSB, suggesting possible defects in pol γ-mtSSB interactions. We found that *Dm*mtSSBα1 and loop45-1 caused mtDNA depletion in S2 cells under all conditions tested, whereas *Dm*mtSSBloop23 only reduced mtDNA copy number when

expressed >50-fold higher than *Dm*mtSSB$_{endo}$. Residual *Dm*mtSSB$_{endo}$, and mixed *Dm*mtSSB$_{endo}$-*Dm*mtSSBloop23 tetramers in cells expressing *Dm*mtSSBloop23 at levels equivalent to the endogenous level (resulting in a ratio of ~10 *Dm*mtSSBloop23 to 1 *Dm*mtSSB$_{endo}$) appear to be sufficient to maintain mtDNA at the same level as in *Dm*mtSSB$_{endo}$-knockdown cells (40-50% of control S2 cells). Thus, at endogenous-level expression, the increased ssDNA-binding ability of *Dm*mtSSBloop23 may compensate for the loss of native pol γ-mtSSB interactions. However, as indicated above, loop 2,3 is one of the most variable regions among animal mtSSBs, suggesting that the biochemical results observed with *Hs*mtSSBloop23 and the physiological response observed with *Dm*mtSSBloop23 are likely species-specific effects that represent distinct mechanisms of pol γ regulation. In fact, as we have speculated previously (Oliveira and Kaguni 2010), the presence of a dimeric accessory subunit exclusive to vertebrate pol γs might increase DNA synthesis by the mitochondrial replicase to a level that makes the contribution of mtSSB to the overall rate of DNA synthesis only moderate. By comparison, the substantial stimulation of *Dm*mtSSB on the DNA polymerase activity of *Dm*pol γ holoenzyme appears to correlate with the presence of a monomeric accessory subunit in insect pol γs, and to a short loop 2,3 in mtSSBs.

Our group and others have shown that *Hs*mtSSBwt interacts functionally with *Hs*mtDNA helicase using a preformed fork-like substrate to stimulate its dsDNA unwinding activity (Korhonen *et al.* 2003, Oliveira and Kaguni 2010). On such a simple substrate one might predict that the helicase would be stimulated *in vitro* by any SSB capable of preventing reannealing of the unwound DNA. Indeed, we show here that both *Ec*SSB and *Dm*mtSSB can stimulate the activity of *Hs*mtDNA helicase similarly to *Hs*mtSSBwt. In contrast, Korhonen *et al.* (2003)

failed to show a stimulation by *Ec*SSB and interpreted their findings as a specific interaction between *Hs*mDNA helicase and *Hs*mtSSBwt. Though we cannot document conclusively an explanation for the different observations discussed here, we note that the stimulation of *Hs*mtDNA helicase by *Hs*mtSSBwt reported by Korhonen *et al.* (2003) was only moderate (~2.5-fold), whereas our data show a ~7-fold effect (Oliveira and Kaguni 2010, Figure 14B) that may allow an evaluation of specificity.

Our studies of fly and human mtSSB variants suggest that residues in loop 1,2 and loop 4,5 serve important but distinct roles in interacting with the mtDNA helicase. Interestingly, loop 1,2 of *Dm*mtSSB appears to be involved only in mtDNA homeostasis in S2 cells, whereas *Dm*mtSSBloop45-2 induces moderate and severe mtDNA depletion under homeostasis and EtBr recovery conditions, respectively. During recovery from EtBr treatment, mtDNA replication is apparently stimulated and may occur by a different mechanism and/ or more independently from the cell cycle than under homeostasis conditions. We speculate that loop 4,5-2 provides the primary point of interaction between mtSSB and mtDNA helicase that promotes efficient dsDNA unwinding during mtDNA replication. Loop 1,2 may also contact the helicase, perhaps facilitating enzyme function only to maintain mtDNA at normal levels under homeostasis conditions. This hypothesis correlates with our findings that *Hs*mtSSBloop45-2 shows the lowest stimulation of *Hs*mtDNA helicase *in vitro*, even at protein levels 3-fold higher than that required to saturate the ssDNA substrate (data not shown). Alternatively, disruption of loop 4,5 may cause a primary biochemical defect that we have not yet tested but that results in reduced DNA polymerase and/ or helicase stimulation *in vitro*, and depletion of mtDNA in cultured cells. Though cooperativity in ssDNA binding is debated in mtSSBs (Curth *et al.* 1994, Thommes *et al.* 1995), loss of this property would represent a plausible explanation, because loop 4,5 of

*Ec*SSB has been implicated in cooperative DNA binding in the bacterial protein (Raghunathan *et al.* 2000).

Takamatsu *et al.* (2002) have estimated that the molecular ratio of mtSSB to mtDNA in human HeLa cells is approximately 3000: 1 (or 750 tetrameric mtSSBs to 1 mtDNA molecule). Our treatment with dsRNA in S2 cells knocked down *Dm*mtSSB$_{endo}$ to ~10% of its endogenous level, decreasing the ratio to ~190 mtSSB tetramers to 1 mtDNA (assuming *Drosophila* S2 cells have a similar mtSSB: mtDNA ratio); this resulted in depletion of mtDNA to 40% of initial levels under homeostasis conditions. This ratio is similar to those used in our *in vitro* assays for maximal stimulation of *Hs*pol γ and *Hs*mtDNA helicase (~180:1 and ~125:1, respectively). Because mtSSB is clearly abundant in mitochondria, we postulate that the residual *Dm*mtSSB$_{endo}$ in dsRNA-treated cells can still form functional replisomes to maintain mtDNA at sufficient levels. This is supported further by the data from EtBr treatment in which the mtSSB: mtDNA ratio in *Dm*mtSSB$_{endo}$-knockdown cells during the initial recovery from mtDNA depletion is ~250:1, but decreases to ~140:1 as mtDNA copy number increases from 30 to 55% of that of control cells in 12 days. In fact, recovery of mtDNA copy number is reduced only when a dysfunctional mtSSB is expressed after EtBr treatment.

Although physical interaction data are not presented here, our findings suggest that mtSSB uses a repertoire of structural elements in stimulating pol γ and mtDNA helicase to ensure proper mtDNA maintenance in animal cells. Its functional properties may result from multiple sites of physical interaction that may also be associated with different mtDNA replication modes *in vivo*. In any case, it is evident that the mechanisms by which mtSSBs function at the mtDNA replication fork are distinct from those that bacterial, viral and nuclear

eukaryotic SSBs employ in their respective replisomes, despite their shared features in ssDNA binding (Shamoo *et al.* 1995, Bochkarev *et al.* 1997, Raghunathan *et al.* 1997, Yang *et al.* 1997, Hollis *et al.* 2001). Further biochemical, structural and physiological studies are clearly needed to test the relevant hypotheses, and to help understand the mechanisms of mtDNA replication in healthy cells and in myriad disease states.

CHAPTER 5

PERSPECTIVES AND FUTURE DIRECTIONS: MODELING POL γ-mtSSB INTERACTION, EXPLORING mtDNA HELICASE STIMULATION BY mtSSB, AND INVESTIGATING mtDNA REPLICATION INTERMEDIATES

Summary

In this chapter, I present a series of experiments that explore some of the unanswered questions raised in the previous chapters regarding the functions of the mitochondrial single-stranded DNA-binding protein (mtSSB) in promoting mitochondrial DNA (mtDNA) replication in animal cells. First, we developed a molecular model in which the crystal structure of the human mtSSB was docked onto that of human pol γ to investigate mtSSB-pol γ interactions from a structural point of view. The model agrees with the bulk of biochemical data reported in Chapters 3 and 4, and with other published results from our lab. Notably, the model also suggests that a cluster of mutations in pol γ associated with various human diseases is located at the putative point of physical interactions between mtSSB and pol γ, and that the disruption of such interactions may cause and/ or aggravate the disease state. Second, we investigated further the functional interactions between mtSSB and mtDNA helicase by studying the biochemical properties of a C-terminally truncated form of the human helicase. The variant enzyme exhibited salt-dependent DNA unwinding activity and significantly lower stimulation by human mtSSB as compared to the wild-type helicase, suggesting that the C-terminal tail is important for helicase function and for interactions at the mtDNA replication fork. Third, we analyzed the mtDNA replication intermediates (RIs) from *Drosophila* S2 cells in culture overexpressing variants of mtDNA helicase and mtSSB. Defective variants frequently promoted the accumulation of RIs associated with regions of replication stalling, indicating that these genomic regions in particular compromise the progression of the mtDNA replisome *in vivo*. Although the data presented here can potentially explain many features of the mtDNA replisome, future biochemical, physiological and structural experiments are needed to test the hypotheses raised to help us understand mtDNA replication in healthy and perturbed cells.

Molecular Model of pol γ-mtSSB Interaction

We tested if the biochemical and physiological data presented in Chapter 4 can be further supported by structural data. Our biochemical data suggests that *Hs*mtSSB proteins bearing mutations in loop 2,3, alpha-helix 1 and loop 4,5-1 are not capable of proper stimulation of the DNA polymerase activity of *Hs*pol γ (Figure 4.3). We developed a computer model using the ClusPro 2.0 server (Kozakov *et al.* 2010), in which we docked the crystal structure of *Hs*mtSSB (Yang *et al.* 1997) onto the structure of *Hs*pol γ (Lee *et al.* 2009). Our model (Figure 18) yields important predictions of how loop 2,3 and alpha-helix 1 of *Hs*mtSSB interact with the catalytic subunit of the mitochondrial replicase. In particular, loop 2,3 makes physical contacts with the IP subdomain (in the spacer region domain) and the fingers subdomain (in the DNA polymerase domain) (Figure 19). We observed potential electrostatic and/ or hydrogen bonding interactions involving residues D53, E55 and D61 in loop 2,3 with residues N736 and K755 in the IP subdomain, and R964 and R972 in the fingers subdomain (Figure 19B-D). In addition, V56 in loop 2,3 makes potential hydrophobic interactions with L779 in the IP subdomain (Figure 19E). Residues in alpha-helix 1 of *Hs*mtSSB interact exclusively with the fingers subdomain of *Hs*pol γ-α: favorable interactions are observed involving Y83, Q84 and K87 of alpha-helix 1 and K1035 and E1042 of the fingers (Figure 20). We did not obtain any evidence of protein-protein interactions involving loop 4,5-1 of *Hs*mtSSB in this model or in any other model generated with other software (data not shown).

We observed that the amino acid residues G619, W620 and Y622 of *Hs*pol γ-α locate close to the point of interaction of the IP subdomain with loop 2,3 of *Hs*mtSSB (Figure 21A). Our group showed previously that *Dm*pol γ variants bearing G575A/W576A/F578A substitutions had reduced stimulation by *Dm*mtSSB *in vitro* (Luo and Kaguni 2005). Most notably, amino acid

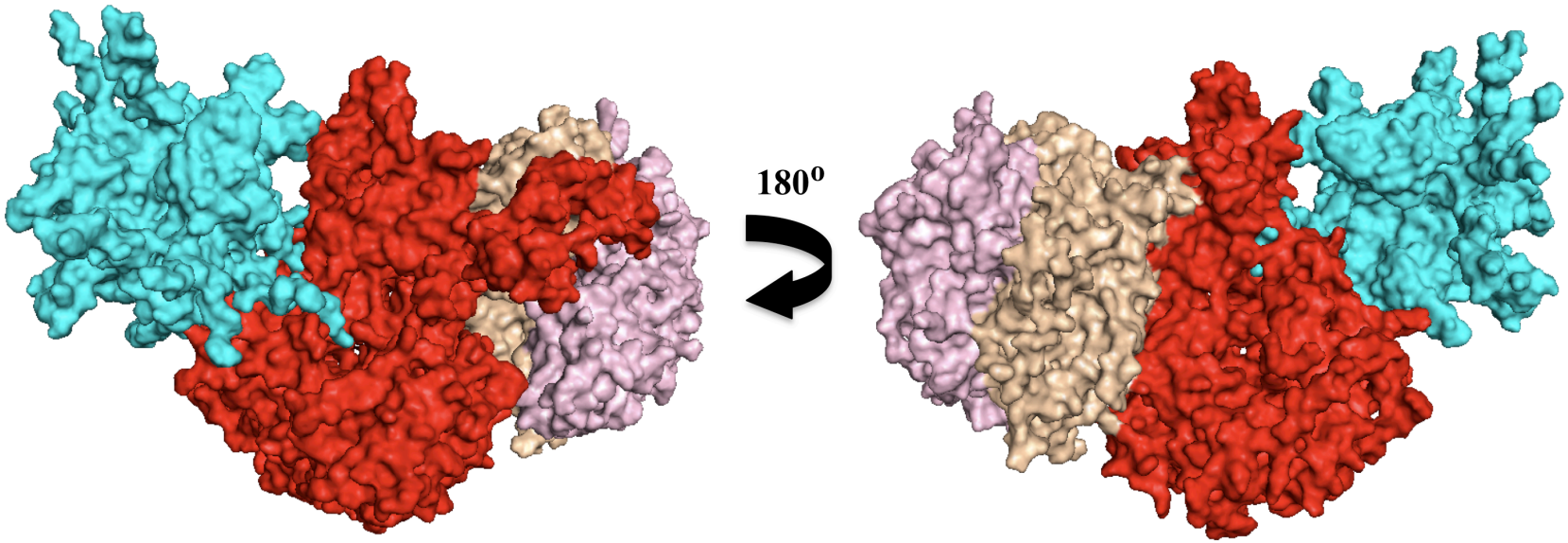

Figure 18. General view of the structural model of pol γ-mtSSB interaction. The model was generated by docking the crystal structure of *Hs*mtSSB (Yang *et al.* 1997) onto that of the *Hs*pol γ holoenzyme (Lee *et al.* 2009), using the software ClusPro 2.0 server. *Hs*mtSSB tetramer is depicted in cyan; the catalytic subunit, and the proximal and the distal protomers of the accessory subunit of *Hs*pol γ are shown in red, wheat and pink, respectively.

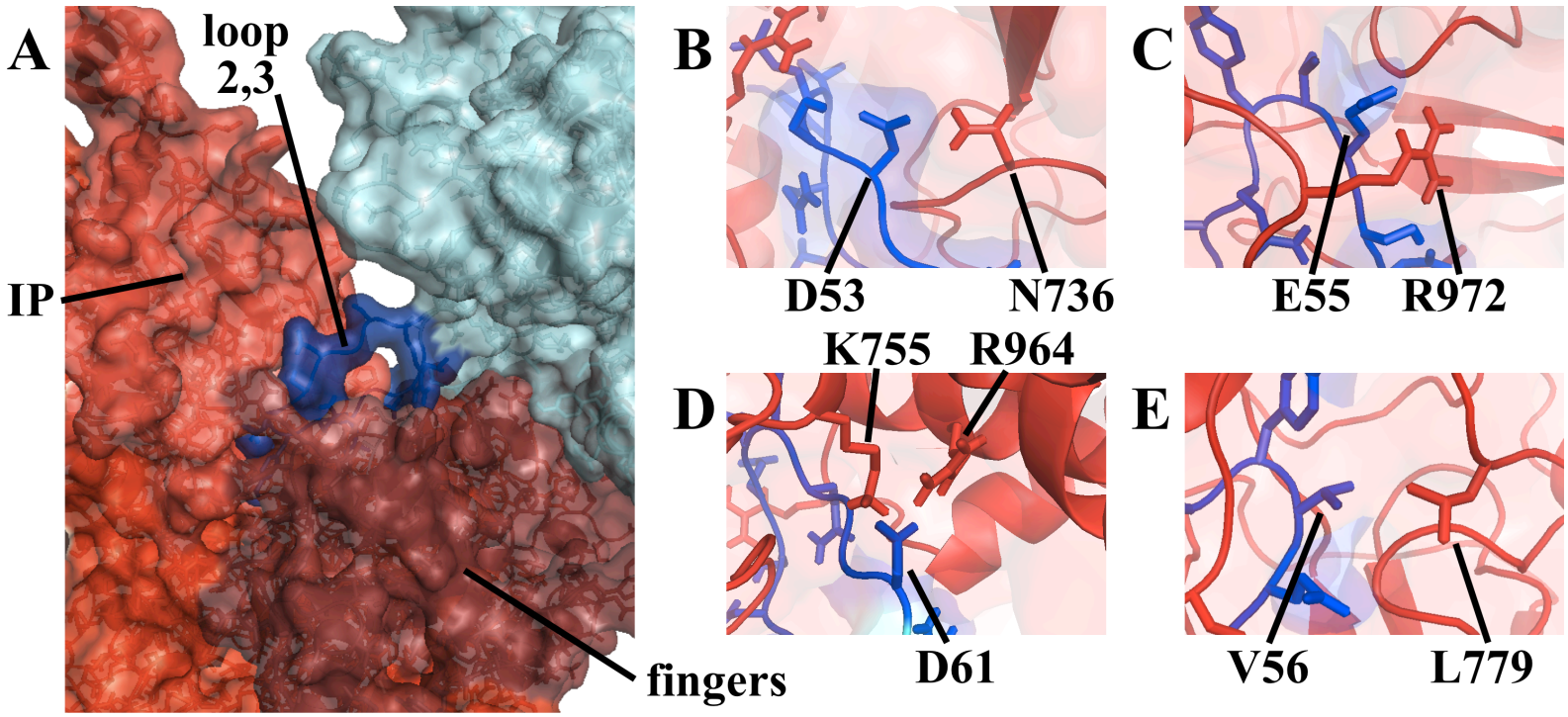

Figure 19. Loop 2,3 of *Hs*mtSSB is proposed to interact with the IP and the fingers subdomains of *Hs*pol γ. A, detailed view of the interaction of loop 2,3 of *Hs*mtSSB with *Hs*pol γ-α, according to the docking model. Specific residues involved in this interaction are depicted in **B-E** (see text for details). Residues in loop 2,3 of *Hs*mtSSB are represented in blue; the IP and the fingers subdomains of *Hs*pol γ are represented in light and dark red, respectively.

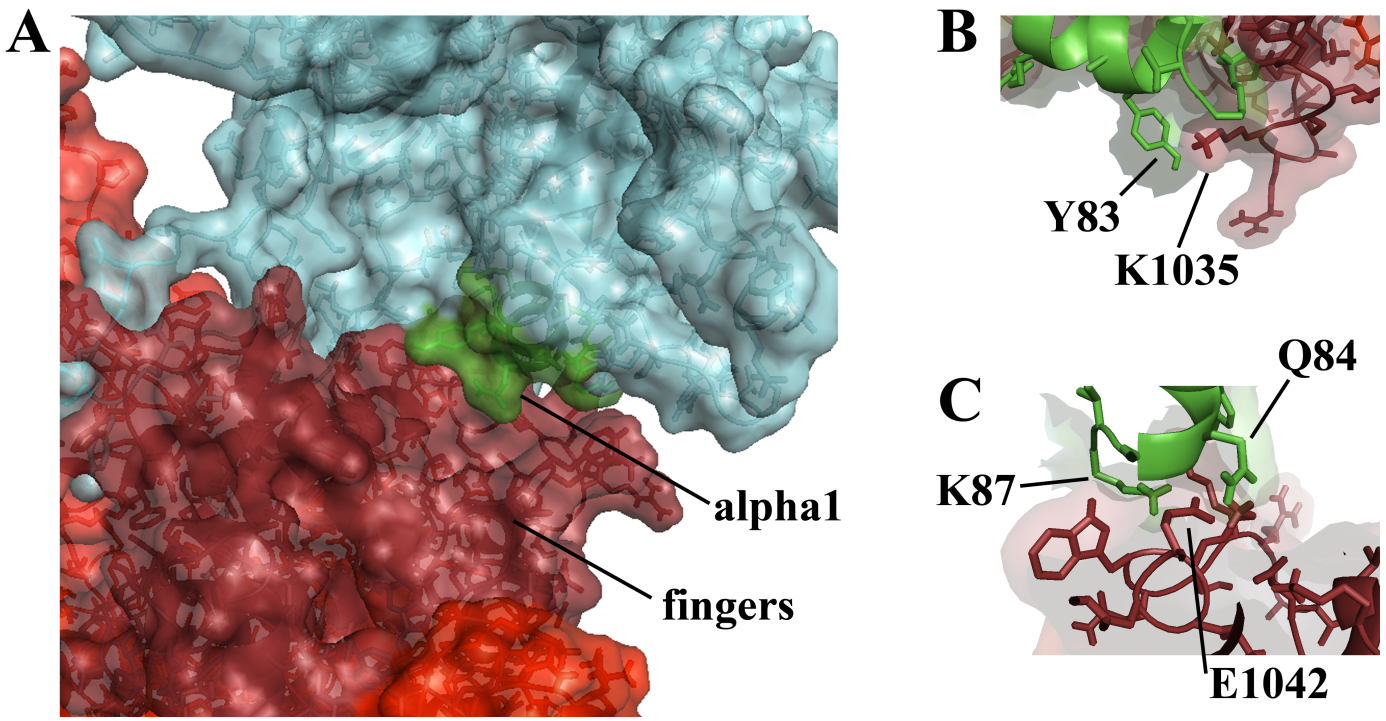

Figure 20. Alpha-helix 1 of *Hs*mtSSB is proposed to interact with the fingers subdomain of *Hs*pol γ. A, detailed view of the interaction of alpha-helix 1 of *Hs*mtSSB with *Hs*pol γ-α, according to the docking model. Specific residues involved in this interaction are depicted in **B** and **C** (see text for detail). Residues in alpha-helix 1 of *Hs*mtSSB are represented in green; the fingers subdomain of *Hs*pol γ is represented in dark red.

substitutions in *Hs*pol γ-α alleles that are associated with cases of Alpers, Parkinson, Charcot-Marie Tooth, Progressive External Ophthalmoplegia (PEO) and Ataxia-Neuropathy diseases in human patients (Davidzon *et al.* 2006, Nguyen *et al.* 2006, Yamanaka *et al.* 2007, Zsurka *et al.* 2008, Bortot *et al.* 2009, Euro *et al.* 2011, Stumpf and Copeland 2011) are found in the vicinity of the region of potential interaction between *Hs*mtSSB and *Hs*pol γ (Figure 21B). We speculate that the mtDNA depletion and/or deletions observed in tissue samples of the patients carrying *Hs*pol γ-α alleles G737R, F749S, L752P, K755E, R964C or L966R can be explained partially by defects in *Hs*pol γ stimulation by *Hs*mtSSB. The primary biochemical defect of most disease mutants is likely associated with DNA binding, DNA polymerase and/or exonuclease activities of *Hs*pol γ *per se*; the lack or reduction of potential interactions with *Hs*mtSSB may in fact enhance such defects under certain physiological states, ultimately causing disease conditions. For example, *Hs*pol γ-α allele R964C has been implicated in defects of nucleotide selectivity and impairment of DNA polymerase activity (Bailey *et al.* 2009); the same residue appears to interact directly with loop 2,3 of *Hs*mtSSB (Figures 19D and 21B).

Our structural model also suggests that *Hs*mtSSB is able to modulate the partitioning loop of *Hs*pol γ, a recently identified structural element that appears to be specific to pol γs and is postulated to coordinate the balance between DNA polymerase and exonuclease activities by positioning the primer-template DNA at the appropriate active site of the enzyme (Euro *et al.* 2011). It uses a steric mechanism that excludes the primer-template DNA containing lesions and/ or mispairs from the pol active site, faciliting substrate utilization by the exo active site. Residues K1035 and E1042 of the fingers subdomain of *Hs*pol γ-α, which we propose to make contact with the alpha-helix 1 of *Hs*mtSSB, are in fact in close proximity to the alpha-helix that contains the first ten residues of the partitioning loop (Figure 22). Interestingly, our group has

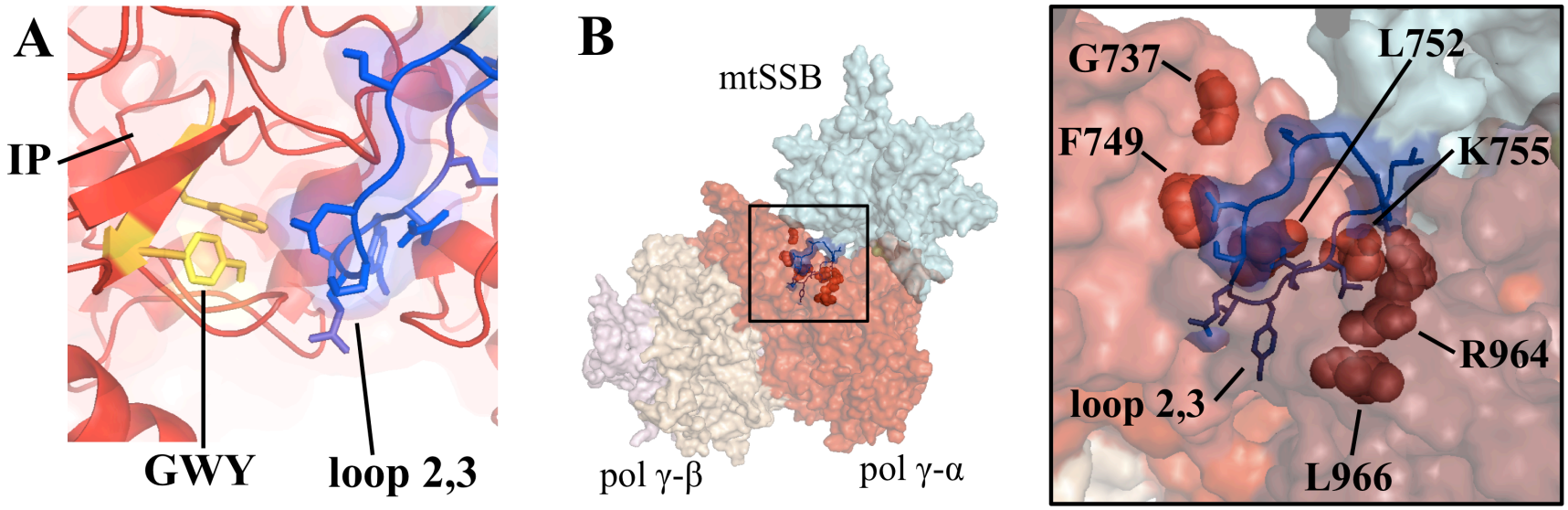

Figure 21. Biochemical mutations of *Dm*pol γ and disease-associated mutations of *Hs*pol γ map in the vicinity of the proposed interaction site between pol γ and mtSSB. A, detailed view of the interaction of loop 2,3 of *Hs*mtSSB with *Hs*pol γ-α, showing the position of G619, W620 and Y622 (GWY, yellow). Alanine substitutions of these residues in *Dm*pol γ affected DNA polymerase stimulation by *Dm*mtSSB (Luo and Kaguni 2005). **B,** location of residues of *Hs*pol γ that have been found associated with various human diseases. *Left panel*, general view of the *Hs*pol γ-*Hs*mtSSB model showing the clustering of disease mutations around loop 2,3 of *Hs*mtSSB (inside box). *Right panel*, detailed view of the clustering. The disease allele G737R is associated with PEO, Alpers, Parkinson and Charcot Marie Tooth diseases; F749S, L752P, K755E and L966R are found in patients with Alpers disease; and R964C is found in Ataxia-Neuropathy (reviewed in Stumpf and Copeland 2011). Residues in loop 2,3 of *Hs*mtSSB are represented in blue; the IP and the fingers subdomains of *Hs*pol γ are represented in light and dark red.

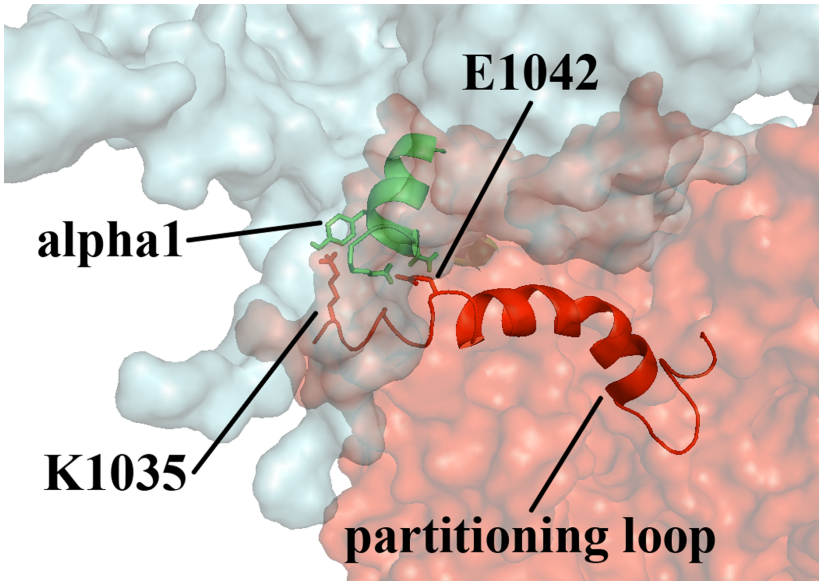

Figure 22. *Hs*mtSSB may modulate the partitioning loop of *Hs*pol γ. The alpha-helix 1 of *Hs*mtSSB may interact with residues K1035 and E1042 of *Hs*pol γ-α, which map in close proximity to the partitioning loop. This recently identified structural element is proposed to function by sensing misincorporated nucleotides and positioning the primer-template DNA either at the DNA polymerase or exonuclease active sites for proper function of the mitochondrial replicase (Euro *et al.* 2011). *Hs*mtSSB is depicted in cyan, with the exception of residues in alpha-helix 1, which are represented in green; *Hs*pol γ is represented in red.

demonstrated that *Dm*mtSSB can stimulate the exonuclease activity of *Dm*pol γ up to 15-fold (Farr *et al.* 1999). We speculate that the magnitude of this effect is accomplished in part by modulation of the partitioning loop of pol γ by mtSSB. However, it is not apparent that mtSSB increases mispair specificity by pol γ, indicating that the proposed modulation needs to be evaluated more carefully.

We reported in Chapter 3 that the N- and C-termini of *Hs*mtSSB modulate negatively the DNA polymerase activity of *Hs*pol γ *in vitro*. As illustrated in Figure 23A, the molecular model suggests that either of the negatively-charged termini of *Hs*mtSSB may partially occupy the positively-charged DNA-binding pocket of the mitochondrial replicase in the absence of DNA. In the presence of primer-template DNA, the termini might disrupt the progression of DNA synthesis by dislodging the DNA from the pol active site of pol γ (Figure 23B). *Hs*mtSSB proteins lacking either or both termini would then render the holoenzyme readily available for DNA binding, thus promoting increased DNA synthesis (Figure 3.6). The reasons why such a putative control mechanism may operate is as yet unclear, but we propose that it may be related to the coordination of the DNA polymerase and exonuclease activities of pol γ by mtSSB. Unfortunately, *Dm*mtSSB variants lacking the N- or C-terminus are not stable when expressed in *Drosophila* S2 cells (Chapter 4), which prevents us from exploring further this phenomenon in a physiological context. Nonetheless, the analysis of the model of protein-protein interactions between pol γ and mtSSB presented here explains partially the biochemical data our lab has reported to date relevant to understanding the functional roles of pol γ-mtSSB interactions in mtDNA replication. The model has also created testable hypotheses, especially in regard to the involvement of mtSSB in the development and progression of human diseases.

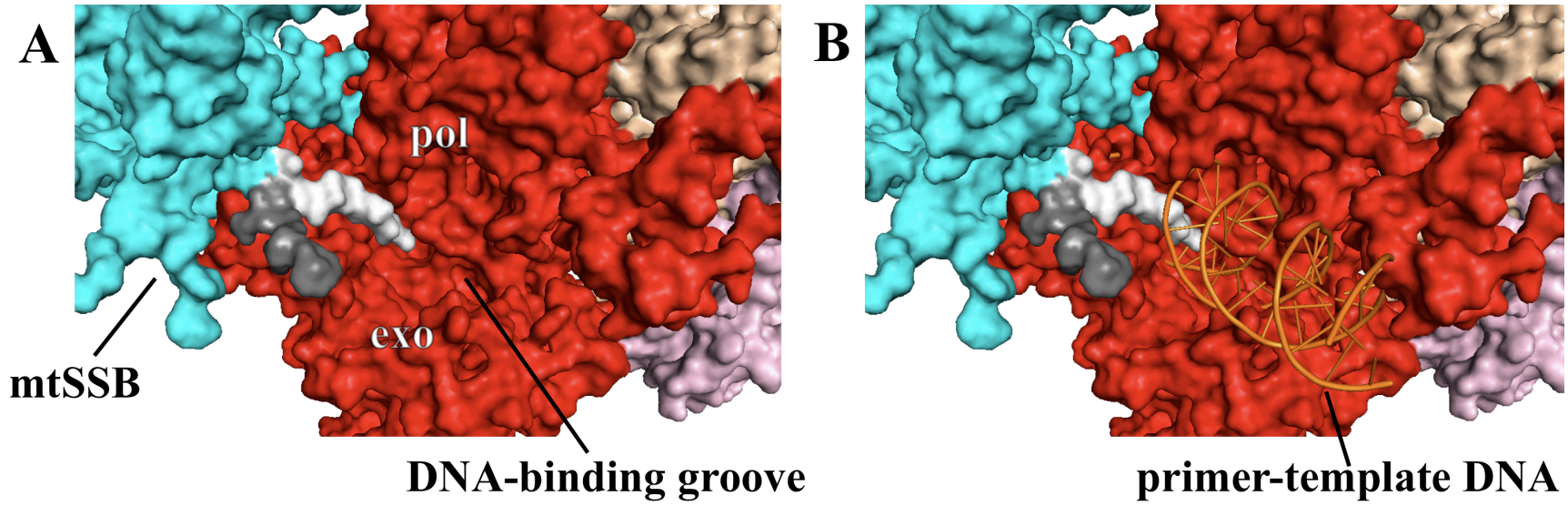

Figure 23. The terminal regions of *Hs*mtSSB may modulate the DNA polymerase activity of *Hs*pol γ by disrupting binding of primer-template DNA. A, detailed view of the positioning of the N- (light gray) and C-termini (dark gray) of *Hs*mtSSB in relation to the DNA-binding groove of *Hs*pol γ-α, based upon the docking model. Because the termini are disordered in the crystal structure of *Hs*mtSSB (Yang *et al.* 1997), we modeled their residues using the software MODELLER (Sali *et al.* 1995) prior to docking *Hs*mtSSB onto the *Hs*pol γ structure. **B**, model of primer-template binding by *Hs*pol γ (courtesy of Greg Farnum; Euro *et al.* 2011) and the possible interference by the *Hs*mtSSB termini. *Hs*mtSSB is represented in cyan. *Hs*pol γ-α is represented in red, with the DNA polymerase (pol) and exonuclease (exo) domains as indicated in **A**. The proximal and the distal protomers of the accessory subunit of *Hs*pol γ are shown in wheat and pink, respectively.

Methods

To construct the model of *Hs*pol γ-*Hs*mtSSB interaction, we first used the software MODELLER (Sali *et al.* 1995) at default parameters to evaluate the three regions of *Hs*mtSSB that are disordered in the crystal structure (pdb code: 3ULL, Yang *et al.* 1997): E1-V9 (N-terminus), S54-L59 (loop 2,3) and D126-E132 (C-terminus). The tetrameric *Hs*mtSSB structure containing the modeled termini and loop 2,3 was submitted to the software ClusPro 2.0 (Kozakov *et al.* 2010) for docking into the crystal structure of *Hs*pol γ holoenzyme (pdb code: 3IKM, Lee *et al* 2009) at default parameters. This software calculates surface complementarities and also evaluates electrostatic attractions between regions of the two proteins of interest. Notably, electrostatic attractions appear to be important for the functional interactions between *Hs*pol γ and *Hs*mtSSB (Oliveira and Kaguni 2010). The model presented here has been selected among all the output models because it agrees with the bulk of the biochemical and physiological data reported in Chapter 4 and in the published literature (see previous section for details). All of the figures were generated and the model was analyzed using the software PyMol (The PyMOL Molecular Graphics System, Version 1.3, Schrödinger, LLC.).

Stimulation of *Hs*mtDNA helicase and its truncation variant P66 by *Hs*mtSSB

P66 is a recombinant form of a proteolytic fragment of *Hs*mtDNA helicase that lacks 44 residues from the C-terminus. Our lab showed previously that P66 has a DNA-dependent ATPase activity that is ~2-fold greater than that of the full-length protein (Ziebarth *et al* 2007). P66 is purified as a hexameric protein, and is apparently stabilized by cofactors, such as Mg^{+2} and ATP, similarly to full-length *Hs*mtDNA helicase (data not shown). Here we investigate the

dsDNA unwinding activity of the full-length and P66 helicases, and their stimulation by *Hs*mtSSBwt protein.

P66 activity is salt-dependent and is not stimulated by Hs*mtSSB*

We performed DNA unwinding assays with increasing concentrations of *Hs*mtDNA helicase and P66 at 20 and 100 mM KCl (Figure 24). At 20 mM KCl, the unwinding activity of P66 was ~2.3-fold higher than that of the full-length protein (Figure 24A, *upper panel*), consistent with the ATPase activity data reported by Ziebarth *et al.* (2007) at a similar salt concentration. However, P66 unwinding activity decreased substantially when the assays were performed at 100 mM KCl (Figure 24A, *lower panel*, *lanes* 17-20), reaching only ~10% of the total substrate unwound at the highest protein concentration. The activity of the full-length helicase was slightly better at 100 than at 20 mM KCl, possibly because of the effect of higher salt on mtDNA helicase stability, yet a corresponding increased stability due to higher salt conditions does not explain the poor activity of P66 at 100 mM KCl.

Next, we performed DNA unwinding assays at 20 and 100 mM KCl with *Hs*mtDNA helicase and P66 in the presence of *Hs*mtSSBwt (Figure 25). *Hs*mtSSBwt was able to stimulate the unwinding activity of the full-length helicase up to 5-fold. We detected no significant difference between *Hs*mtDNA helicase stimulation by *Hs*mtSSBwt at 20 and 100 mM KCl, consistent with our previous results (Oliveira and Kaguni 2010). On the other hand, *Hs*mtSSBwt did not stimulate the unwinding activity of P66 at 20 mM KCl, and it promoted only a slight increase in the poor activity of P66 at 100 mM KCl, bringing it to the level of the full-length helicase activity alone (Figure 25). Such an effect appears to be independent of *Hs*mtSSBwt concentration.

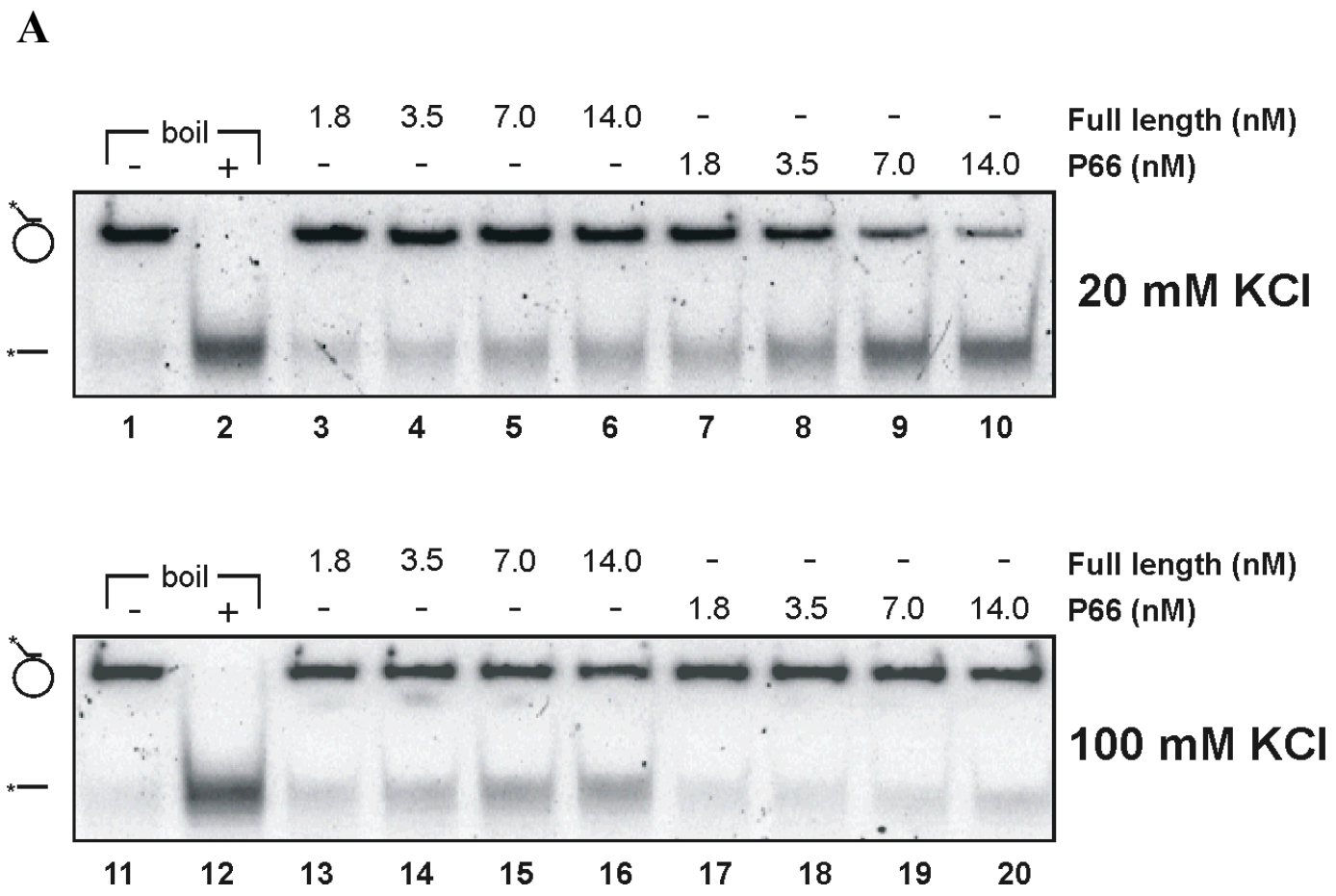
A
boil
- + - - - - 1.8 3.5 7.0 14.0
1.8 3.5 7.0 14.0 - - - - Full length (nM)
P66 (nM)
20 mM KCl
1 2 3 4 5 6 7 8 9 10
boil
- + - - - - 1.8 3.5 7.0 14.0
1.8 3.5 7.0 14.0 - - - - Full length (nM)
P66 (nM)
100 mM KCl
11 12 13 14 15 16 17 18 19 20

Figure 24.

Figure 24 (continued).

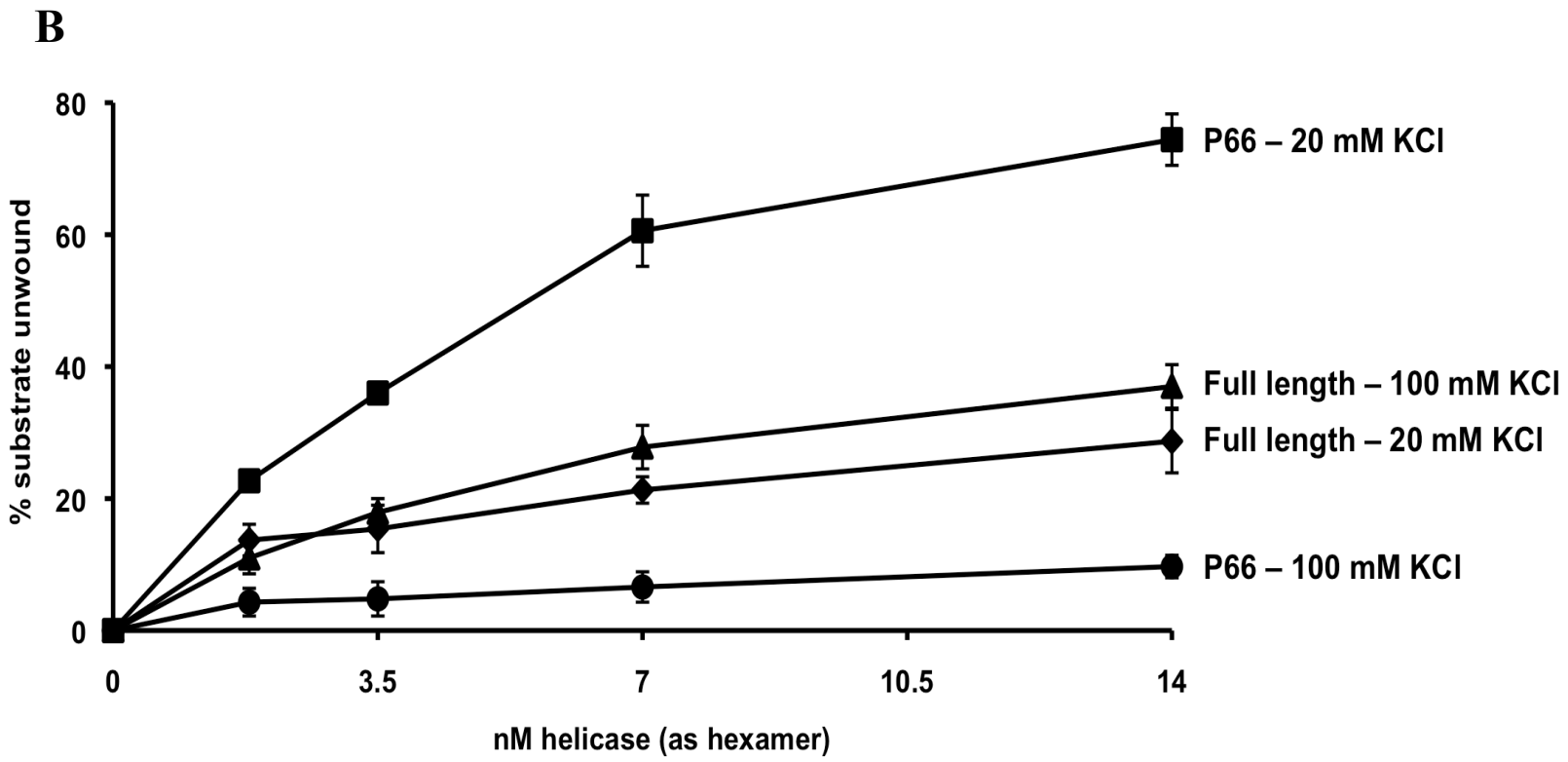

Figure 24. dsDNA unwinding activity of P66 is dependent on salt concentration. A, DNA unwinding assays were performed as described under "Methods". *Lanes 1* and *11*, intact substrate ("– boil"); *2* and *12*, denatured substrate (100^{o}C for 2 min – "+ boil"). The concentration of helicase used is indicated above each lane. **B**, analysis of the data shown in **A** combined with that from two other experiments. The points represent the average of unwound substrate as percent, and the error bars represent the standard deviation.

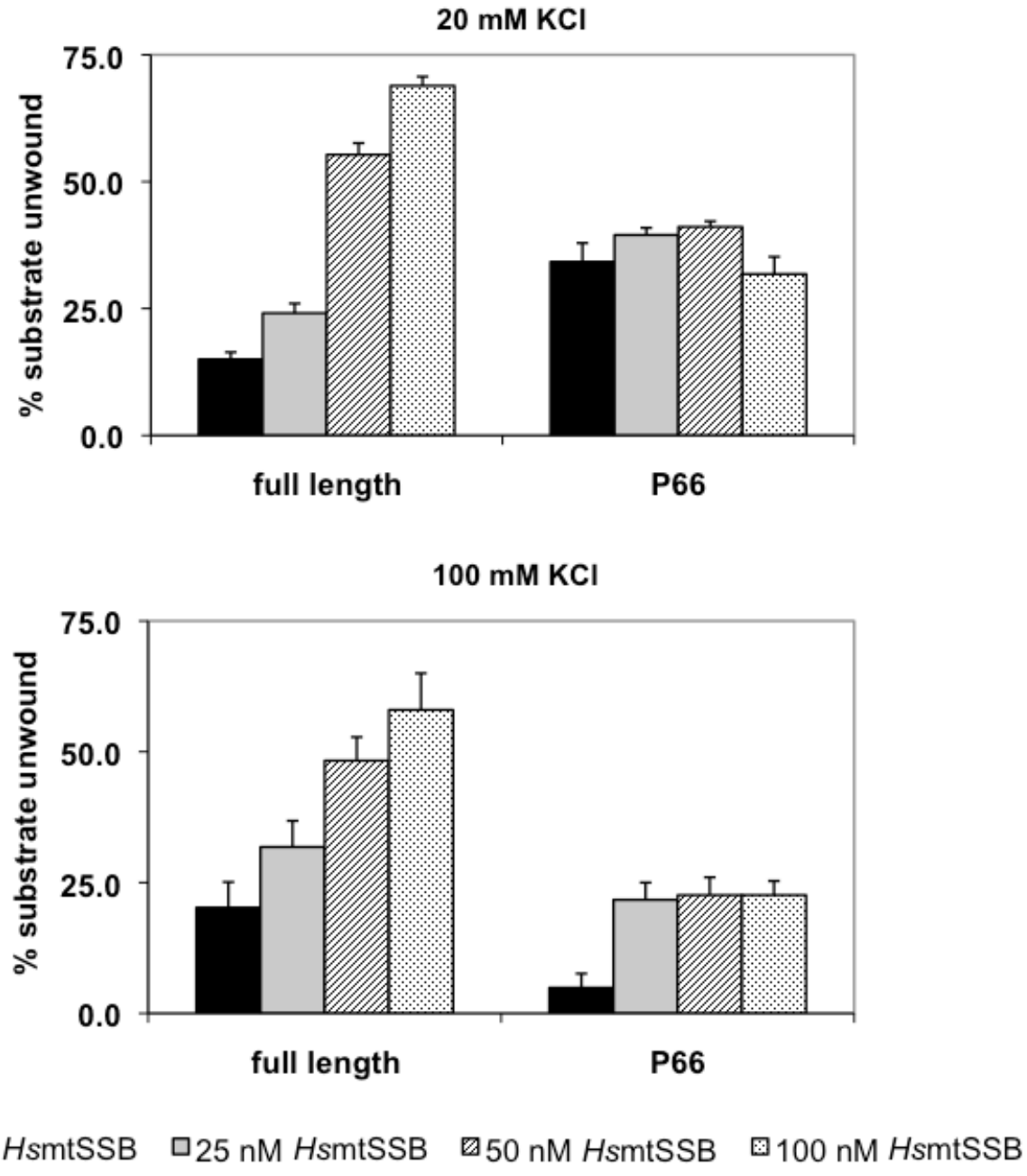

Figure 25. *Hs*mtSSB does not stimulate the unwinding activity of P66. DNA unwinding assays were performed as described under "Methods", using 3.5 nM helicase (as hexamer) and the indicated concentrations of *Hs*mtSSBwt. The assays were performed at 20 mM (*upper panel*) and 100 mM KCl (*lower panel*). The bars represent the average values of unwound substrate as percent from three independent experiments, and the error bars represent the standard deviation.

Discussion

Multiple sequence alignment and secondary structure prediction showed significant sequence and structural similarity between the C-terminal helicase domain of the mtDNA helicase and the bacteriophage T7 primase-helicase gp4 (Spelbrink *et al.* 2001, Korhonen *et al.* 2003, Matsushima & Kaguni 2007, Ziebarth *et al.* 2007). However, distinct amino acid sequences are found at the extreme C-terminal region (Figure 26). In T7 gp4, the last 17 amino acids comprise a highly-negative region that is important for physical interactions with T7 DNA Pol holoenzyme. The C-terminal truncated gp4 promotes no strand displacement DNA synthesis in the presence of T7 Pol, despite primer synthesis, nucleotide hydrolysis, and dsDNA unwinding activities of the primase-helicase enzyme not being affected (Notarnicola *et al.* 1997, Lee *et al.* 2006). By comparison with T7 gp4, the extreme C-terminal region of *Hs*mtDNA helicase is longer (44 amino acids), positively charged, and contains no aromatic residues. The deletion of this region alters nucleotide hydrolysis significantly *in vitro* (Ziebarth *et al.* 2007) and dsDNA unwinding activities (Figure 24) in a salt dependent manner. At salt conditions closer to the physiological state (100 mM KCl), P66 is unable to unwind dsDNA efficiently, even in the presence of *Hs*mtSSB. At 20 mM KCl, its efficiency increases on average 7.5-fold; compared to the full-length protein, P66 activity is ~2.3-fold higher. The full-length mtDNA helicase, on the other hand, unwinds dsDNA similarly at 20 and 100 mM KCl, and its activity is stimulated ~5-fold by *Hs*mtSSBwt, independent of salt concentration. These results suggest functional coordination at the replication fork of the unwinding activity of the mtDNA helicase by its C-terminal region under the fluctuating ionic conditions that can occur *in vivo* (Hackenbrock 1968). Recently, we have shown that the overexpression of a C-terminal deletion mutant of the *Drosophila* mtDNA helicase analogous to P66 causes no effects on the mtDNA levels of S2 cells

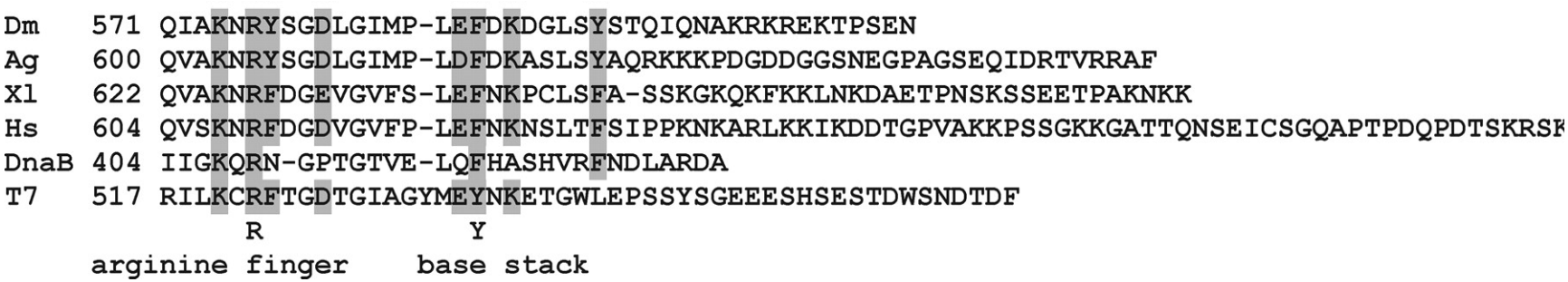

Figure 26. Sequence alignment of the C-terminal region of animal mtDNA helicases, bacterial DnaB and T7 gp4. *Dm*, mtDNA helicase of the fly; *Ag*, mosquito; *Xl*, frog; *Hs*, human; *DnaB*, *Thermus aquaticus* DnaB helicase; *T7*, bacteriophage T7 gp4 primase-helicase. Conserved amino acid residues are indicated in *gray*. The positions of residues important for ATPase activity, such as the arginine finger and base stack, are indicated below the alignment. Adapted from Matsushima *et al.* (2008).

(Matsushima *et al.* 2008). However, the fact that the deletion mutant was overexpressed in the presence of the endogenous full-length protein leaves the possibility for formation of functional heterohexamers that are able to maintain replication. It is also important to point out that the extreme C-terminus of the *Drosophila* mtDNA helicase is not conserved with the human homologue in terms of amino acid sequence, although it is also positively charged (Matsushima *et al.* 2008).

In addition to our demonstration of salt sensitivity, our results show that P66 does not interact functionally with *Hs*mtSSB *in vitro* (Figure 25). In the T7 system, it has been shown that the gp2.5 SSB protein interacts physically with gp4 primase-helicase and modulates its multiple functions, such as primer synthesis, nucleotide hydrolysis and dsDNA unwinding (Kim & Richardson 1994, He & Richardson 2004). The C-terminal region of another superfamily 4 helicase, RepA, also appears to be involved in interactions with the replisome of the plasmid RSF1010 (Ziegelin *et al.* 2003). Furthermore, the C-terminus of the bacteriophage T4 gp41 helicase is the point of physical contact with the gp59 helicase loader/ gp32 SSB complex (Delagoutte and von Hippel 2005). This, in combination with the data presented in Chapter 4, suggests that the stimulation of the *Hs*mtDNA helicase by *Hs*mtSSB occurs via protein-protein interactions involving the C-terminal region of the helicase, and loops 1,2 and 4,5-2 of *Hs*mtSSB. Further physical interaction experiments will be important to understand helicase-mtSSB function at the mtDNA replication fork.

Methods

dsDNA unwinding assays – Reaction mixtures (50 µL) contained 20 mM Tris-HCl, pH 7.5, 10% glycerol, 500 µg/mL bovine serum albumin, 10 mM dithiothreitol, 4 mM $MgCl_2$, 3

mM ATP, 0.4 nM of unwinding substrate (Oliveira and Kaguni 2010), and the indicated concentrations of KCl, and full-length mtDNA helicase, P66, and *Hs*mtSSB. Reactions were pre-incubated at 37^{O}C for 5 min prior to the addition of the helicase, and then incubated further at 37^{O}C for 30 min, and stopped by the addition of 5 μL of 10x stop solution (6% SDS, 100 mM EDTA, pH 8.0), followed by 5 μL of 10x loading buffer (50% glycerol, 0.25% bromophenol blue). DNA products were separated from substrate by electrophoresis in a 22% polyacrylamide gel (59:1 acrylamide/bisacrylamide) using 1x TBE (90 mM Tris-HCl-borate, 2 mM EDTA), at 600 V until the dye had traveled 3 cm (~ 30 min). After electrophoresis, the gel was dried under vacuum with heat, and exposed to a Phosphor Screen (Amersham Biosciences), which was scanned using the Storm 820 Scanner (Amersham Biosciences). The volume of each band was determined and background subtracted by computer integration analysis, using the ImageQuant software version 5.2 (Amersham Biosciences). Unwinding is defined as the fraction of radiolabeled DNA species that is single-stranded (product), as follows: % unwinding = (V_P / (V_S + V_P)) x 100, in which V_P represents the volume of the product and V_S the volume of non-unwound substrate.

mtDNA Replication Intermediates in *Drosophila* Cells with Defects in mtDNA Replication

The use of two-dimensional agarose gel electrophoresis (2DAGE) to analyze mtDNA replication intermediates (RIs) from mammalian cells and tissues expressing variant forms of pol γ, mtDNA helicase, or other proteins involved in mtDNA transactions has contributed largely to the current understanding of animal mtDNA replication *in vivo*. Although *Drosophila melanogaster* has been a very useful model organism for studies of mitochondrial biology, little

is known about the mechanisms of mtDNA replication in *Drosophila* cells. Our lab in collaboration with Howard Jacobs's lab (University of Tampere) has started addressing this issue using the 2DAGE technique and nucleic acid material extracted from mitochondria of different *Drosophila* tissues. Preliminary analysis of mtDNA RIs from S2 cells in culture indicates that insect mitochondrial genomes replicate unidirectionally from a single origin mapped within the A+T-rich region (see Figure 1.1 for genome map), with coupled leading and lagging DNA strand synthesis (Figure 27 and data not shown), and no clear evidence of RITOLS (RNA incorporated throughout the lagging strand; see Chapter 1 for review of the models of mtDNA replication in mammals). Unpublished data from the Jacobs's lab demonstrate that the transcription termination factor DmTTF has a major impact on regulating mtDNA replication in *Drosophila*, by promoting stalling of the replisome and accumulation of mtDNA RIs at DmTTF binding sites (Priit Joers, unpublished data). Additionally, a "pausing region" characterized by the accumulation of RIs throughout an ~6 Kb region that lies between the second DmTTF binding site and the replication termination site (A+T-rich region) in *D. melanogaster* mtDNA, has been described in control cells cultured under standard growth conditions (Figure 27). Here, we present additional evidence that the DmTTF binding sites and the "pausing region" in *Drosophila* mtDNA are associated with abnormal replication and mtDNA depletion in S2 cells expressing variants of the mtDNA helicase and mtSSB.

Overexpression of wild-type and ATPase-deficient mtDNA helicases generates aberrant mtDNA replication intermediates

We established S2 cell lines carrying the gene encoding the wild-type *Dm*mtDNA helicase and the variant Y595A under the control of the metallothionein promoter.

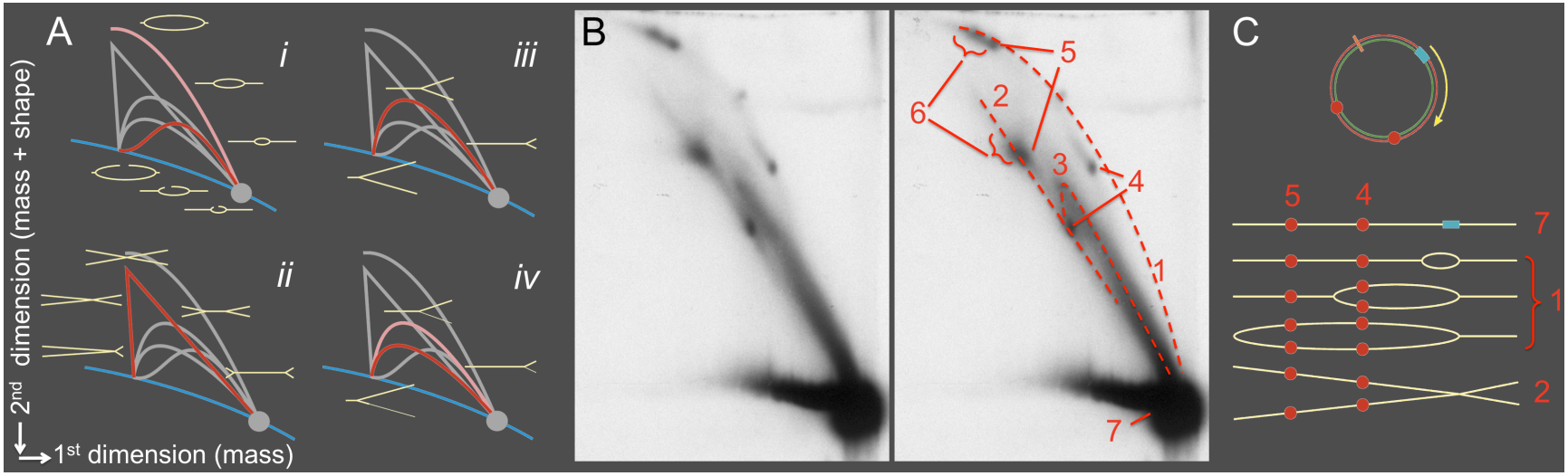

Figure 27. Unidirectional theta replication of *Drosophila melanogaster* mtDNA in S2 cells. A, schematic patterns of typical replication intermediates (RIs) separated by 2D-AGE. The blue arc in each of the panels represents non-replicating DNA molecules. In *i*, the pink arc represents the pattern obtained when a fragment with a centered origin of replication is probed. When one of the strands that constitute the bubble ruptures, the molecules migrate more rapidly, as represented by the red arc. In *ii*, when two forks approach each other (double Y), when a fixed replication terminus is present, or when recombination takes place (X arc), the different DNA structures would fall along the red arc. A complete simple Y arc resulting from a fragment that is replicated passively from an outside origin is represented in red in panel *iii* and in pink in panel *iv*. The red arc in panel *iv* represents a sub-Y structure, in which single-strandedness is present in the fragment. **B**, *left panel* shows a representative autoradiograph of mtDNA RIs obtained from

sucrose-gradient purified mitochondria of *Drosophila* S2 cells cultured under standard growth conditions. mtDNA was linearized with the single-cleaving restriction endonuclease *Eco*RV and hybridized to a 16S rDNA probe. *Right panel,* identification of replication intermediates: the bubble, double-Y and Y arcs (1 to 3*,* respectively) are represented with dashed lines; 4 and 5 represent RIs accumulated at the DmTTF binding sites; 6 depicts the "pausing region" (see text for details); and 7 represents the non-replicating mtDNA molecules. **C**, interpretation of the data from **B** and from mtDNA treated with additional restriction endonucleases and DNA- or RNA-modifying enzymes (data not shown). The orange line marks the *Eco*RV restriction site in *Drosophila* mtDNA, the blue box represents the A+T-rich region, and the red dots (4 and 5) are DmTTF binding sites. 1, 2 and 7 are examples of molecules comprising the bubble arc, the double-Y arc and the non-replicating mtDNA, as shown in **B**.

Overexpression of the wild-type protein in S2 cells causes increase of ~30% in mtDNA copy number, as compared to the control cells (Matsushima and Kaguni 2007, 2009, Matsushima *et al.* 2008). Matsushima *et al.* (2008) showed that the overexpression of the mtDNA helicase variant Y595A causes severe mtDNA depletion in S2 cells and that the recombinant human homologue (F628A, Figure 26) is defective in ATP hydrolysis. We overexpressed these proteins under conditions of mitochondrial homeostasis for 7 days and analyzed the mtDNA RIs by 2DAGE (Figure 28). The overexpression of wild-type *Dm*mtDNA helicase appears to reduce the accumulation of RIs associated with the DmTTF binding sites and the "pausing region", suggesting that the amount of mtDNA helicase in normal cells is a limiting factor that causes the replisome to stall transiently when replicating these regions. Overexpression of the Y595A helicase resulted in clear accumulation of RIs at the same genomic regions, suggesting that the ATPase activity of *Dm*mtDNA helicase is absolutely necessary for the progression of the replication fork beyond those sites. We speculate that the presence of DmTTF itself bound to the mtDNA of *Drosophila* interferes with replication by a mechanism similar to that suggested for mTERF1 in human mitochondria (Hyvärinen *et al.* 2007), and that secondary structure within the genome is responsible for the observation of the "pausing region". The additional wild-type helicase present upon overexpression may help the replisome to advance through the physical barriers imposed by DmTTF binding and the DNA hairpins, therefore increasing mtDNA copy number; on the other hand, defective helicases might not be able to displace DmTTF or resolve secondary structures efficiently, causing replisome stalling, aberrant mtDNA molecules and consequent mtDNA depletion. This hypothesis is supported by the fact that the largest cluster of tRNA genes in insect mitochondrial genomes, which can potentially form several hairpin structures on both DNA strands, is found adjacent to the second DmTTF binding site in

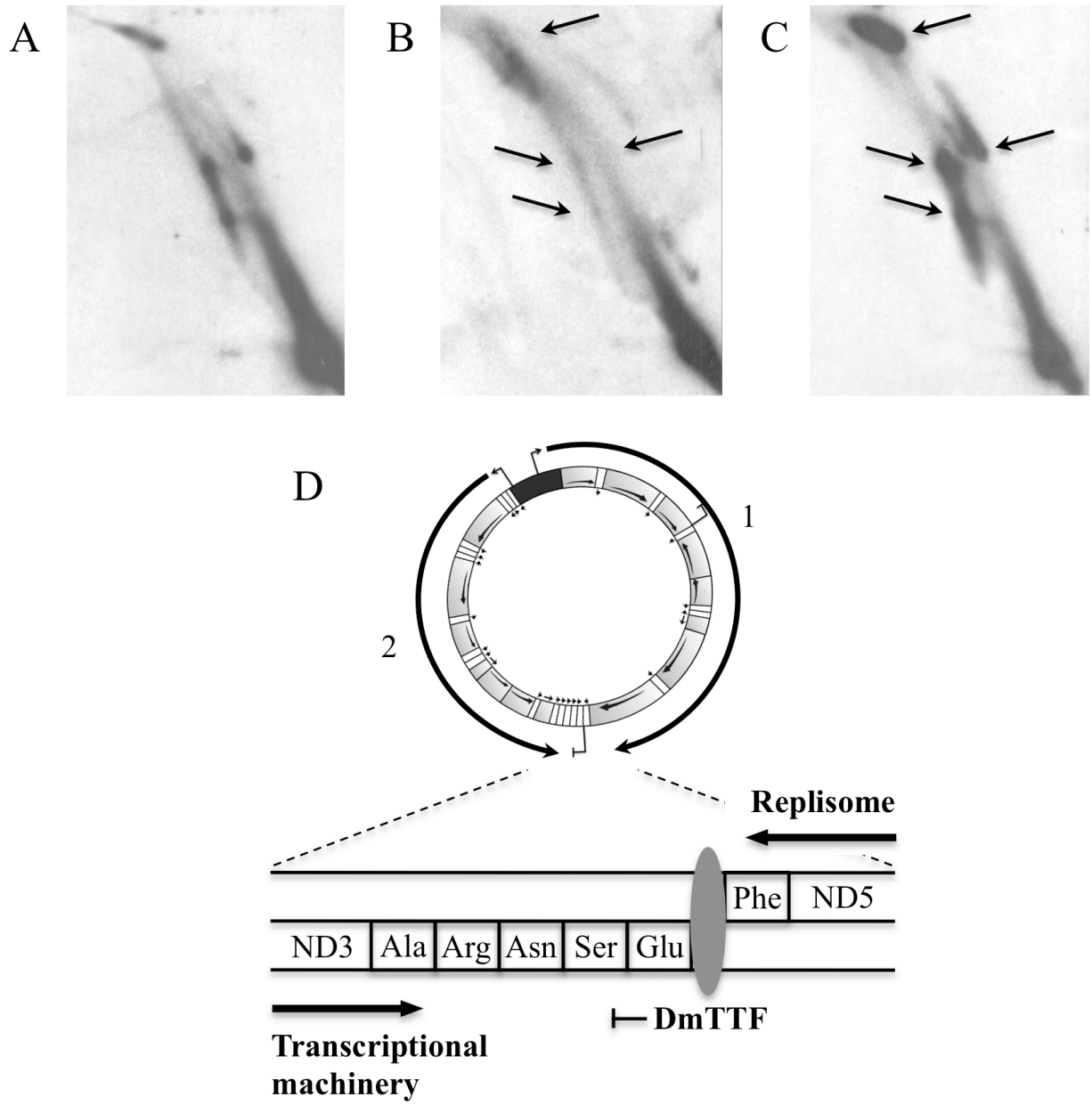

Figure 28. Aberrant mtDNA replication intermediates from S2 cells overexpressing *Dm*mtDNA helicases. mtDNA was purified from crude mitochondrial extracts of control S2 cells (**A**), and cells overexpressing wild-type *Dm*mtDNA helicase (**B**) or the Y595A variant (**C**), digested with *Eco*RV prior to 2D electrophoresis and hybridized with mtDNA probe, as described under "Methods". Arrows indicate the decrease (**B**) and increase (**C**) of RIs associated with the DmTTF binding sites and the "pausing region". **D**, schematic representation of the fly

mitochondrial genome showing the second DmTTF binding site flanked by a cluster of six tRNA genes, where the replisome may encounter the transcriptional machinery moving in the opposite direction. 1, nature of the RI of *Drosophila* mtDNA at the time that the replication fork encounters the transcription bubble; 2, primary polycistronic transcript that is terminated at the second DmTTF binding site. Initiation of mtDNA replication and transcription is believed to occur within the A+T-rich region (black region in the mitochondrial genome).

Drosophila mtDNA (Figure 28D). Alternatively, the "pausing region" may be generated by the encounter of the replisome with the transcriptional machinery, which progresses in the opposite direction in that region of the fly mitochondrial genome. The stalling of DNA replication forks by transcription bubbles appears to occur very frequently in bacterial genomes and is most likely a universal phenomenon (reviewed in Langston *et al.* 2009). Future experiments will help test the hypotheses presented here, and establish the roles for DmTTF and the significance of the "pausing region" in regulating mtDNA copy number in *Drosophila*.

Overexpression of mtSSB variants is associated with phenotypes of mtDNA replication stalling

We next analyzed mtDNA RIs from S2 cell lines that were treated with dsRNA to knock down *Dm*mtSSB$_{endo}$, and with $CuSO_4$ to overexpress various *Dm*mtSSB variants under conditions of mitochondrial homeostasis. We reported in Chapter 4 that mtDNA copy number is reduced in cells overexpressing *Dm*mtSSBloop12, loop23, α1, loop45-1 and loop45-2, and in *Dm*mtSSB$_{endo}$-knockdown cells (Figure 4.4). The cells were cultured for 14 days under these conditions and mtDNA RIs were analyzed by 2DAGE (Figure 29). The pattern of RIs from cells overexpressing *Dm*mtSSBwt is similar to that of the control cells (Figure 29A, *panels iii* and *i*, respectively), consistent with the fact that mtDNA levels do not vary between these cell lines. Unlike the overexpression of *Dm*mtDNA helicase Y595A, none of the cell lines overexpressing *Dm*mtSSB variants and treated with dsRNA exhibit phenotypes of severe mtDNA replication stalling. Evidence of mild replication defects is observed for *Dm*mtSSB$_{endo}$-knockdown cells and cells overexpressing *Dm*mtSSBloop23 (Figure 29B, *panels ii* and *v*, respectively). In both cases, there appears to be a decrease in RIs associated with the DmTTF binding sites (1 and 2),

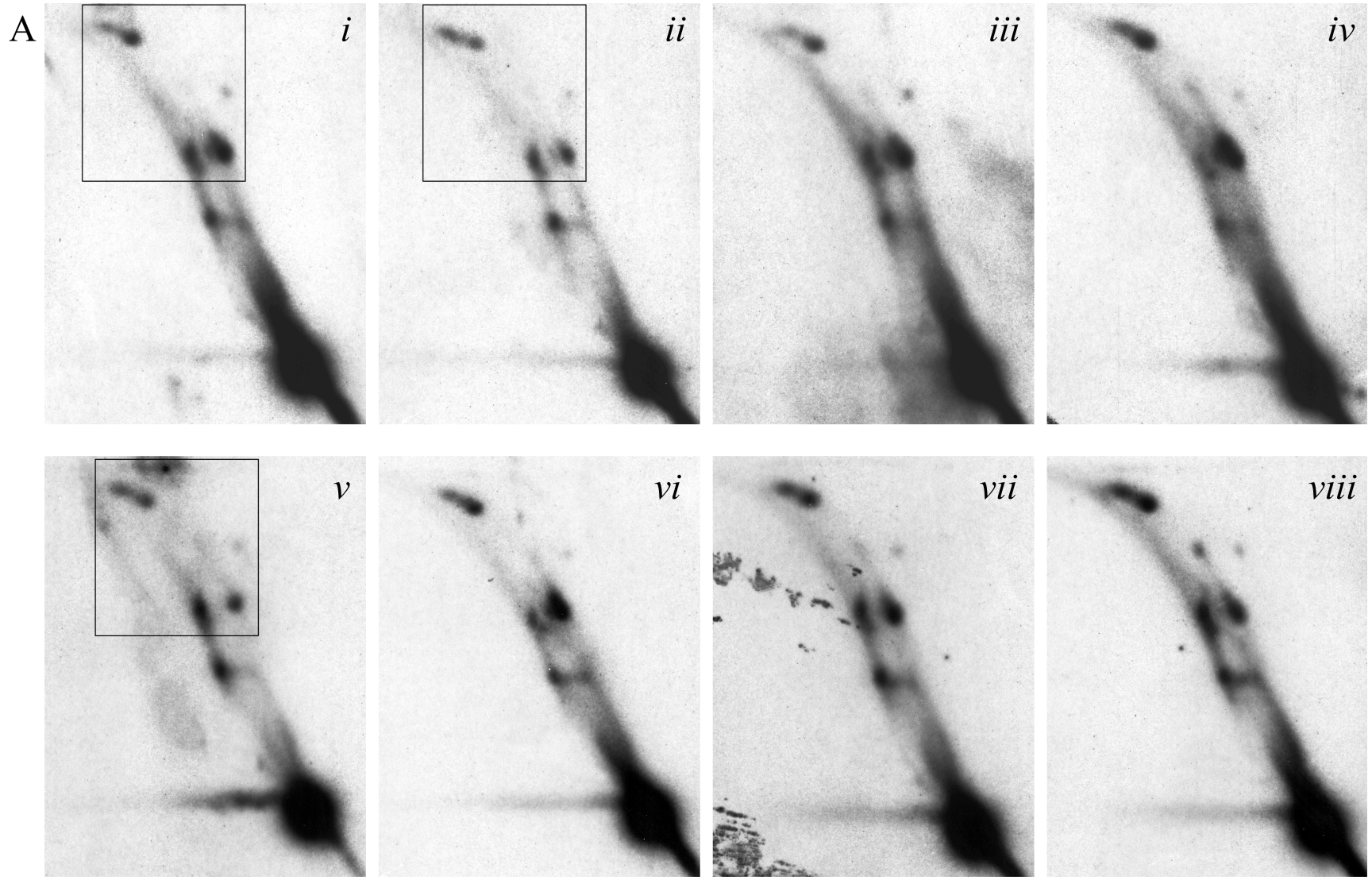

Figure 29.

Figure 29 (continued).

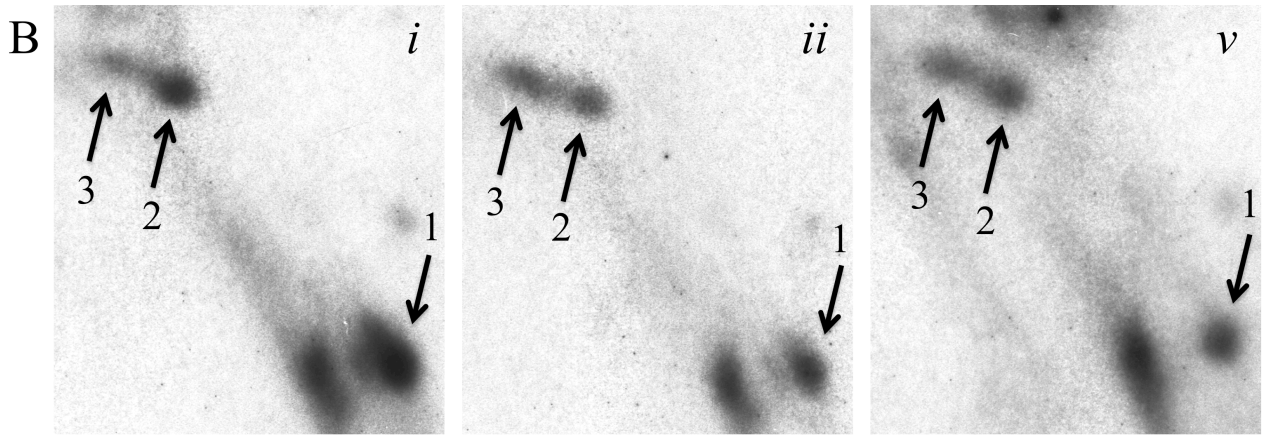

Figure 29. mtDNA RIs from S2 cells overexpressing *Dm*mtSSB variants under conditions of mitochondrial homeostasis. A, mtDNA was purified from crude mitochondrial extracts of control S2 cells (*i*), cells treated with dsRNA to knock down *Dm*mtSSB$_{endo}$ (*ii*), and cells overexpressing *Dm*mtSSBwt (*iii*), *Dm*mtSSBloop12 (*iv*), *Dm*mtSSBloop23 (*v*), *Dm*mtSSBα1 (*vi*), *Dm*mtSSBloop45-1 (*vii*) or *Dm*mtSSBloop45-2 (*viii*). Samples were processed as described under "Methods". Boxes in *i*, *ii* and *v* are enlarged in **B** to show the relative abundance of the RIs representing the first (1) and second (2) DmTTF binding sites, and the "pausing region" (3).

and an increase in those associated with the "pausing region" (3). The lack of apparent aberrant mtDNA RIs in cells overexpressing the *Dm*mtSSB variants may relate to the limited severity of the defects they cause: under conditions of mitochondrial homeostasis, none of the mtSSB variants cause reduction in mtDNA copy number as severe as that caused by the ATPase-deficient mtDNA helicase, which resulted in cell lethality within 4 weeks (Matsushima *et al.* 2008), presumably because the mtSSB variants maintain their efficient ssDNA-binding abilities. In addition, as we showed in Chapter 4, mtSSB appears to interact functionally and/ or physically with pol γ or mtDNA helicase using two or three distinct structural regions on the protein surface, suggesting that the function of the replisome is not abolished completely when mtSSB variants bearing altered amino acid residues only in one particular structural element are expressed *in vivo*.

Although the analysis of the entire linearized mitochondrial genome can provide a general picture of the RIs, replication defects associated with specific genomic regions are only shown clearly when the defect is severe, as is the case for the overexpression of *Dm*mtDNA helicase Y595A. Further investigation of alterations in the RIs associated with the "pausing region" and the DmTTF binding sites when *Dm*mtSSB$_{endo}$ is knocked down and/ or the *Dm*mtSSB variants are expressed, may require the analysis of the genomic regions of interest using a 2D gel system that provides increased resolution of the mtDNA molecules. For example, the second DmTTF binding site and the "pausing region" can be isolated with the restriction endonucleases *Hpa*I and *Bsr*BI prior to the two-dimensional electrophoresis, allowing the analysis of a ~6.4 Kb region that does not contain the origin of replication or the termination site. Similarly, the endonuclease *Cla*I would generate an ~5 Kb mtDNA fragment containing the first binding site of DmTTF. In addition, exacerbation of the replication defects caused by mtSSB

variants may be required to observe the accumulation of RIs by 2DAGE. This could be accomplished by expressing the variant proteins during mtDNA repletion, similarly to the experiments in Chapter 4 evaluating the recovery from ethidium bromide treatment. The ideas presented here can be pursued experimentally using the same S2 cell system we have developed, and will help us document more completely how mtSSB functions in *Drosophila* mtDNA replication.

Methods

S2 cell lines carrying the genes for wild-type *Dm*mtDNA helicase and the Y595A variant were generated and cultured as described by Matsushima *et al* (2008). S2 cell lines carrying the genes for *Dm*mtSSBwt and the *Dm*mtSSB variants were generated and cultured as described in Chapter 4. To extract mtDNA, cells were washed once with 1X phosphate-saline buffer and immediately resuspended in 0.1X homogenization buffer (4 mM Tris-HCl, pH 7.5, 2.5 mM NaCl, 0.5 mM $MgCl_2$. After 9 min of incubation on ice, cells were homogenized in a glass Dounce homogenizer with 20 strokes of a tight-fitting pestle. One-ninth volume of 10X homogenization buffer was added, followed by two centrifugations at 1000 x *g* for 5 min at 4^oC to collect nuclei and cell debris. The supernatant was centrifuged at 16000 x *g* for 5 min at 4^oC to collect mitochondria, which were then resuspended in nucleic acid extraction buffer containing 25 mM HEPES, pH 7.5, 25 mM EDTA, pH 8.0, 75 mM NaCl, 1% sodium dodecyl-sulphate, and 0.2 μg/mL Proteinase K, followed by incubation at 37^oC for 1 h. mtDNA was extracted with phenol-chloroform-isoamyl alcohol (25:24:1), and precipitated with ammonium acetate and cold ethanol, following standard laboratory protocols.

Purified mtDNA (~20 μg) was digested with the restriction endonuclease *Eco*RV (NEB), which cleaves the *Drosophila* mtDNA once at position 1362. Linearized mtDNA was loaded onto a 0.28% agarose gel (first dimension) and electrophoresed for 24 h at 32 V (1.7 V/cm) in 1X TBE buffer. Individual lanes were cut out and rotated 90^{o}, and a 0.58% agarose gel containing 300 ng/μL ethidium bromide (second dimension), pre-cooled to 55^{o}C, was cast around the samples from the first dimension gel. The second dimension gel was electrophoresed for 67 h at 56 V (1.8 V/cm) in 1X TBE buffer containing 300 ng/μL ethidium bromide. mtDNA was transferred from the second dimension gel to a Hybond N+ membrane (GE Healthcare) by a standard Southern blotting protocol, and crosslinked to the membrane using ultra-violet light. The membranes were hybridized with radiolabeled probes created by PCR using as template a fragment of the *Drosophila* mtDNA (positions 3777-4100), and exposed to a Kodak X-ray film overnight at -80^{o}C.

Concluding Remarks

Mechanistic studies of mtDNA replication have been hampered by the lack of functional and physical interaction data among the components of the mtDNA replisome. Although significant effort has been made towards the characterization of pol γ, mtDNA helicase and mtSSB variants with defects in their primary activities, such as DNA polymerase and exonuclease, dsDNA unwinding and ATP hydrolysis, and ssDNA binding, respectively, few reports to date have demonstrated biochemical and/ or physiological defects associated solely or partially with reduced protein-protein interactions at the mtDNA replication fork. I believe that the work presented in this thesis provides a major contribution to the field by addressing the

question of how the bacterial-like mtSSB functions coordinately to stimulate the bacteriophage T7-like pol γ and mtDNA helicase, and to promote mtDNA replication in animal cells. We suggest that mtSSB accomplishes this by using a repertoire of structural elements that are not shared with bacterial SSBs, representing evolutionary novelties acquired after the symbiotic event that gave rise to the mitochondrion. We summarized the biochemical, physiological and structural properties of the mtSSB variants that helped us draw such conclusions in Table 2. Interestingly, some of the novel elements of mtSSB are proposed to interact physically with a region of pol γ where a group of mutations associated with various human diseases are mapped. Unfortunately, similar structural analyses and modeling predictions cannot currently be performed reliably for mtSSB interactions with mtDNA helicase, because of the lack of structural information for the latter. However, I suspect it is a matter of time until new biochemical and structural data are published suggesting that mtDNA helicase alleles associated with human cases of PEO are defective in interacting with mtSSB or pol γ.

Although the data presented in Chapter 5 on the pol γ-mtSSB model, the stimulation of P66 helicase by mtSSB, and the analysis of mtDNA RIs from *Drosophila* cells do support the roles we propose for mtSSB, the results are still speculative and/ or preliminary, stressing the need for further experimentation to provide a clear picture of the interactions that occur at the mtDNA replication fork. Experiments to complement these data and test the hypotheses that we have generated can most likely be pursued without extensive technical difficulties. The main challenges remaining in studying mtDNA replisome function include the development of experimental conditions to test physical interactions among pol γ, mtDNA helicase and mtSSB *in vitro*, the optimization of a strand-displacement DNA synthesis assay to test the concerted action of the recombinant components of the mtDNA replisome and their variants, and the discovery

and characterization of new components of the mtDNA replisome. Overcoming these technical obstacles must be prioritized.

The scientific community is still far from understanding the link between mtDNA replication and the myriad cellular processes in which the mitochondrion is involved, with animal development, human diseases and aging, but it is clear to me that substantial progress has been made. Although the research presented in this thesis represents a basic research perspective, I hope that it will contribute to such progress directly, and pave the way for future work that will focus on the interplay of the various mitochondrial functions.

Table 2. Summary of the biochemical, physiological and structural properties of mtSSB variants as compared to those of wild-type mtSSB

mtSSB protein	tetramer formation	ssDNA-binding affinity	pol γ stimulation	mtDNA helicase stimulation	mtDNA copy number	supporting structural data
ΔN	+	wt*	increased	wt	NA**	+
ΔC	+	wt	increased	wt	NA	+
ΔNΔC	+	wt	increased	wt	NA	+
loop12	+	increased	wt	reduced	reduced	NA
loop45-2	+	wt	wt	reduced	reduced	NA
loop23	+	increased	reduced	wt	reduced	+
α1	+	wt	reduced	wt	reduced	+
loop45-1	+	wt	reduced	wt	reduced	-

* wt indicates that the activity of the mtSSB variant did not differ significantly from that of the wild-type mtSSB.

** NA indicates that the property of the mtSSB variant was not determined.

APPENDIX 1

LIST OF PUBLICATIONS

Oliveira, MT & Kaguni, LS (2011) Reduced stimulation of recombinant pol γ and mtDNA helicase by variants of mitochondrial single-stranded DNA-binding protein (mtSSB) correlates with defects in mtDNA replication in animal cells. Journal of Biological Chemistry, submitted.

Oliveira, MT & Kaguni, LS (2010) Functional roles for the N- and C-terminal regions of the human mitochondrial single-stranded DNA-binding protein. PLoS ONE, 5(10): e15379. doi: 10.1371/journal.pone.0015379.

Oliveira, MT, Garesse, R & Kaguni, LS (2010) Animal models of mitochondrial DNA transactions in disease and ageing. Experimental Gerontology, 45: 489-502.

Dallmann, HG, Tomer, G, Fackelmayer, OJ, Chen, J, Wiktor-Becker, A, Ferrara, T, **Oliveira, MT**, Burgers, PMJ, Kaguni, LS & McHenry, CS (2010) Parallel multiplicative target screening against diverse bacterial replicases: identification of specific inhibitors with broad spectrum potential. Biochemistry, 49: 2551-2562.

Oliveira, MT & Kaguni, LS (2009) Comparative purification strategies for *Drosophila* and human mitochondrial DNA replication proteins: DNA polymerase g and mitochondrial single-stranded DNA-binding protein. Methods in Molecular Biology, 554: 37-58.

Oliveira, MT, Barau, JG, Junqueira, ACM, Feijão, PC, da Rosa, AC, Abreu, CF, Azeredo-Espin, AML & Lessinger, AC (2008) Structure and evolution of the mitochondrial genomes of *Haematobia irritans* and *Stomoxys calcitrans*: the Muscidae (Diptera: Calyptratae) perspective. Molecular Phylogenetics and Evolution, 48: 850-857.

Oliveira, MT, Azeredo-Espin, AML & Lessinger, AC (2007) The mitochondrial DNA control region of Muscidae flies: evolution and structural conservation in a Dipteran context. Journal of Molecular Evolution, 64: 519-527.

Oliveira, MT, da Rosa, AC, Azeredo-Espin, AML & Lessinger, AC (2006) Improving access to the control region and tRNA gene clusters of dipteran mitochondrial DNA. Journal of Medical Entomology, 43: 636-639.

Oliveira, MT, Azeredo-Espin, AML & Lessinger, AC (2005) Evolutionary and structural analysis of cytochrome c oxidase subunit I (COI) gene from *Haematobia irritans*, *Stomoxys calcitrans* and *Musca domestica* mitochondrial DNA. DNA Sequence, 16: 156-160.

REFERENCES

REFERENCES

Achanta, G., Sasaki, R., Feng, L., Carew, J.S., Lu, W., Pelicano, H., Keating, M.J., Huang, P. 2005. Novel role of p53 in maintaining mitochondrial genetic stability through interaction with DNA pol gamma. EMBO J. 24, 3482-3492.

Adán, C., Matsushima, Y., Hernández-Sierra, R., Marco-Ferreres, R., Fernández-Moreno, M.A., González-Vioque, E., Calleja, M., Aragón, J.J., Kaguni, L.S., Garesse, R. 2008. Mitochondrial transcription factor B2 is essential for metabolic function in *Drosophila melanogaster* development. J. Biol. Chem. 283, 12333-12342.

Alam, T.I., Kanki, T., Muta, T., Ukaji, K., Abe, Y., Nakayama, H., Takio, K., Hamasaki, N., Kang, D. 2003. Human mitochondrial DNA is packaged with TFAM. Nucleid Acids Res. 31, 1640-1645.

Andres-Mateos, E., Perier, C., Zhang, L., Blanchard-Fillion, B., Greco, T.M., Thomas, B., Ko, H.S., Sasaki, M., Ischiropoulos, H., Przedborski, S., Dawson, T.M., Dawson, V.L. 2007. DJ-1 gene deletion reveals that DJ-1 is an atypical peroxiredoxin-like peroxidase. Proc. Natl. Acad. Sci. USA 104, 14807-14812.

Ashley, N., Poulton, J. 2009. Anticancer DNA intercalators cause p53-dependent mitochondrial DNA nucleoid re-modelling. Oncogene 28, 3880-3891.

Bacman, S.R., Williams, S.L., Moraes, C.T. 2009. Intra- and inter-molecular recombination of mitochondrial DNA after in vivo induction of multiple double-strand breaks. Nucleic Acids Res. 37, 4218-4226.

Bae, S.H., Seo, Y.S. 2000. Characterization of the enzymatic properties of the yeast dna2 helicase/ endonuclease suggests a new model for Okazaki fragment processing. J. Biol. Chem. 277, 26632-26641.

Bandy, B., Davidson, A.J. 1990. Mitochondrial mutations may increase oxidative stress: implication for carcinogenesis and ageing? Free Radical Biol. Med. 8, 523-539.

Baqri, R.M., Turner, B.A., Rheuben, M.B., Hammond, B.D., Kaguni, L.S., Miller, K.E. 2009. Disruption of mitochondrial DNA replication in *Drosophila* increases mitochondrial fast axonal transport in vivo. PLoS ONE 4, e7874.

Bailey, C.M., Kasiviswanathan, R., Copeland, W.C., Anderson, K.S. 2009. R964C mutation of DNA polymerase γ imparts increased stavudine toxicity by decreasing nucleoside analog discrimination and imparing polymerase activity. Antimicrob. Agents Chemother. 53, 2610-2612.

Bailey, L.J., Cluett, T.J., Reyes, A., Prolla, T.A., Poulton, J., Leeuwenburgh, C., Holt, I.J. 2009.

Mice expressing an error-prone DNA polymerase in mitochondria display elevated replication pausing and chromosomal breakage at fragile sites of mitochondrial DNA. Nucleic Acids Res. 37, 2327-2335.

Bochkarev, A., Pfuetzner, R.A., Edwards, A.M., Frappier, L. 1997 Structure of the single-stranded-DNA-binding domain of replication protein A bound to DNA. Nature 385, 176-181.

Bogenhagen, D.F. 2009. Does mtDNA nucleoid organization impact aging? Exp. Gerontol. doi: 10.1016/j.exger.2009.12.002.

Bogenhagen, D.F., Clayton, D.A. 2003a. The mitochondrial DNA replication bubble has not burst. Trends Biochem. Sci. 28, 357-360.

Bogenhagen, D.F., Clayton, D.A. 2003b. Concluding remarks: The mitochondrial DNA replication bubble has not burst. Trends Biochem. Sci. 28, 404-405.

Bogenhagen, D.F., Rousseau, D., Burke, S. 2008. The layered structure of human mitochondrial DNA nucleoids. J. Biol. Chem. 283, 3665-3675.

Bonawitz, N.D., Clayton, D.A., Shadel, G.S. 2006. Initiation and beyond: multiple functions of the human mitochondrial transcription machinery. Mol. Cell 24, 813-825.

Boore, J.L. 1999. Animal mitochondrial genomes. Nucleic Acids Res. 27, 1767-1780.

Bortot, B., Barbi, E., Biffi, S., Lunazzi, G., Bussani, R., Burlina, A., Norbedo, S., Ventura, A., Carrozzi, M., Severini, G.M. 2009. Dig. Liver Dis. 41, 494-499.

Bourdon, A., Minai, L., Serre, V., Jais, J.P., Sarzi, E., Aubert, S., Chretien, D., de Lonlay, P., Paquis-Flucklinger, V., Arakawa, H., Nakamura, Y., Munnich, A., Rotig, A. 2007. Mutation of RRM2B, encoding p53-controlled ribonucleotide reductase (p53R2), causes severe mitochondrial DNA depletion. Nat. Genet. 39, 776-780.

Brown, W.M., George, M., Wilson, A.C. 1979. Rapid evolution of animal mitochondrial DNA. Proc. Natl. Acad. Sci. USA 76, 1967-1971.

Bujalowski, W., Lohman, T.M. 1991. Monomer-tetramer equilibrium of the *Escherichia coli ssb-1* mutant single strand binding protein. J. Biol. Chem. 266, 1616-1626.

Bunch, T.A., Grinblat, Y., Goldstein, L.S. 1988. Characterization and use of the *Drosophila* metallothionein promoter in cultured *Drosophila melanogaster* cells. Nucleic Acids Res. 16, 1043-1061.

Burger, G., Gray, M.W., Lang, B.F. 2003. Mitochondrial genomes: anything goes. Trends Genetics 19, 709-716.

Burke, R.L., Alberts, B.M., Hosoda, J. 1980. Proteolytic removal of the COOH terminus of the T4 gene 32 helix-destabilizing protein alters the T4 *in vitro* replication complex. J. Biol. Chem. 255, 11484-11493.

Carew, J.S., Huang, P. 2002. Mitochondrial defects in cancer. Mol. Cancer 1, 9.

Cha, G.H., Kim, S., Park, J., Lee, E., Kim, M., Lee, S.B., Kim, J.M., Chung, J., Cho, K.S., 2005. Parkin negatively regulates JNK pathway in the dopaminergic neurons of Drosophila. Proc. Natl. Acad. Sci. USA 102, 10345-10350.

Chatterjee, A., Mambo, E., Zhang, Y., DeWeese, T., Sidransky, D. 2006. Targeting of mutant hOGG1 in mammalian mitochondria and nucleus: effect on cellular survival upon oxidative stress. BMC Cancer 6, 235.

Chipuk, J.E., Kuwana, T., Bouchier-Hayes, L., Droin, N.M., Newmeyer, D.D., Schuler, M., Green, D.R. 2004. Direct activation of Bax by p53 mediates mitochondrial membrane permeabilization and apoptosis. Science 303, 1010-1014.

Clayton, D.A. 1982. Replication of animal mitochondrial DNA. Cell 28, 693-705.

Copeland, W.C. 2008. Inherited mitochondrial diseases of DNA replication. Annu. Rev. Med. 59, 131-146.

Copeland, W.C., Wachsman, J.T., Johnson, F.M., Penta, J.S. 2002. Mitochondrial DNA alterations in cancer. Cancer Invest. 20, 557-569.

Cotney, J.L., Shadel, G.S. 2006. Evidence for an early gene duplication event in the evolution of the mitochondrial transcription factor B family and maintenance of rRNA methyltransferase activity in human mtTFB1 and mtTFB2. J. Mol. Evol. 63, 707-717.

Cotney, J.L., Wang, Z., Shadel, G.S. 2007. Relative abundance of the human mitochondrial transcription system and distinct roles for h-mtTFB1 and h-mtTFB2 in mitochondrial biogenesis and gene expression. Nucleic Acids Res. 35, 4042-4054.

Curth, U., Genschel, J., Urbanke, C., Greipel, J. 1996. *In vitro* and *in vivo* function of the C-terminus of *Escherichia coli* single-stranded DNA binding protein. Nucleic Acids Res. 24, 2706-2711.

Curth, U., Urbanke, C., Greipel, J., Gerberding, H., Tiranti, V., *et al.* 1994. Single-stranded-DNA-binding proteins from human mitochondria and *Escherichia coli* have analogous physicochemical properties. Eur. J. Biochem. 221, 435-443.

D'Aurelio, M., Gajewski, C.D., Lin, M.T., Mauck, W.M., Shao, L.Z., Lenaz, G., Moraes, C.T., Manfredi, G. 2004. Heterologous mitochondrial DNA recombination in human cells. Hum. Mol. Genet. 13, 3171-3179.

Davidzon, G., Greene, P., Mancuso, M., Klos, K.J., Ahlskog, J.E., Hirano, M., DiMauro, S. 2006. Early-onset familial Parkinsonism due to *POLG* mutations. Ann. Neurol. 59, 859-862.

Delagoutte, E., von Hippel, P.H. 2005. Mechanistic studies of the T4 DNA (gp41) replication helicase: functional interactions of the C-terminal tail of the helicase subunits with the T4 (gp59) helicase loader protein. J. Mol. Biol. 347, 257-275.

Di Re, M., Sembongi, H., He, J., Reyes, A., Yasukawa, T., Martinsson, P., Bailey, L.J., Goffart, S., Boyd-Kirkup, J.D., Wong, T.S., Fersht, A.R., Spelbrink, J.N., Holt, I.J. 2009. The accessory subunit of mitochondrial DNA polymerase γ determines the DNA content of mitochondrial nucleoids in human cultured cells. Nucleic Acids Res. doi: 10.1093/nar/gkp614.

Dobson, A.W., Xu, Y., Kelley, M.R., LeDoux, S.P., Wilson, G.L. 2000. Enhanced mtDNA repair and cellular survival following oxidative stress by targeting the hOGG repair enzyme to mitochondria. J. Biol. Chem. 275, 37518-37523.

Druzhyna, N.M., Hollensworth, S.B., Kelley, M.R., Wilson, G.L., LeDoux, S.P. 2003. Targeting human 8-oxoguanine glycosylase to mitochondria of oligodendrocytes protects against menadione-induced oxidative stress. Glia 42, 370-378.

Druzhyna, N.M., Musiyenko, S.I., Wilson, G.L., LeDoux, S.P. 2005. Cytokines induce NO-mediated mtDNA damage and apoptosis in oligodendrocytes. Protective role of targeting 8-oxoguanine glycosylase to mitochondria. J. Biol. Chem. 280, 21673-21679.

Druzhyna, N.M., Wilson, G.L., LeDoux, S.P. 2008. Mitochondrial DNA repair in ageing and disease. Mech. Ageing Dev. 129, 383-390.

Duxin, J.P., Dao, B., Martinsson, P., Rajala, N., Guittat, L., Campbell, J.L., Spelbrink, J.N., Stewart, S.A. 2009. Human Dna2 is a nuclear and mitochondrial DNA maintenance protein. Mol. Cell. Biol. 29, 4274-4282.

Edgar, D., Shabalina, I., Camara, Y., Wredenberg, A., Calvaruso, M.A., Nijtmans, L., Nedergaard, J., Cannon, B., Larsson, N.G., Trifunovic, A. 2009. Random point mutations with major effects on protein-coding genes are the driving force behind premature ageing in mtDNA mutator mice. Cell Metab. 10, 131-138.

Edgar, D., Trifunovic, A. 2009. The mtDNA mutator mouse: dissecting mitochondrial involvement in aging. Aging 1, 1028-1032.

Ekstrand, M.I., Terzioglu, M., Galter, D., Zhu, S., Hofstetter, C., Lindqvist, E., Thams, S., Bergstrand, A., Hansson, F.S., Trifunovic, A., Hoffer, B., Cullheim, S., Mohammed, A.H., Olson, L., Larsson, N.G. 2007. Progressive parkinsonism in mice with respiratory-chain-deficient dopamine neurons. Proc. Natl. Acad. Sci. 104, 1325-1330.

Englander, E.W., Hu, Z., Sharma, A., Lee, H.M., Wu, Z.H., Greeley, G.H. 2002. Rat MYH, a glycosylase for repair of oxidatively damaged DNA, has brain-specific isoforms that localize to neuronal mitochondria. J. Neurochem. 83, 1471-1480.

Euro, L., Farnum, G.A., Palin, E., Suomalainen, A., Kaguni, L.S. 2011. Clustering of Alpers disease mutations and catalytic defects in biochemical variants reveal new features of molecular mechanism of the human mitochondrial replicase, Pol γ. Nuc. Acid. Res., *in press*.

Falkenger, M., Gaspari, M., Rantanen, A., Trifunovic, A., Larsson, N.G., Gustafsson, C.M. 2002. Mitochondrial transcription factors B1 and B2 activate transcription of human mtDNA. Nat. Genet. 31, 289-294.

Falkenberg, M., Larsson, N.G., Gustafsson, C.M. 2007. DNA replication and transcription in mammalian mitochondria. Annu. Rev. Biochem. 76, 679-699.

Fan, L., Kaguni, L.S. 2001. Multiple regions of subunit interaction in *Drosophila* mitochondrial DNA polymerase: three functional domains in the accessory subunit. Biochemistry 40, 4780-4791.

Fan, L., Kim, S., Farr, C. L., Schaefer, K. T., Randolph, K. M., Tainer, J. A., Kaguni, L. S. 2006. A novel processive mechanism for DNA synthesis revealed by structure, modeling and mutagenesis of the accessory subunit of human mitochondrial DNA polymerase. J. Mol. Biol. 358, 1229-1243.

Fan, W., Waymire, K.G., Narula, N., Li, P., Rocher, C., Coskun, P.E., Vannan, M.A., Narula, J., Macgregor, G.R., Wallace, D.C. 2008. A mouse model of mitochondrial disease reveals germline selection against severe mtDNA mutations. Science 319, 958-962.

Fansler, B.S., Loeb, L.A. 1974. Sea urchin nuclear DNA polymerase. Methods Enzymol. 29, 53-70.

Farr, C.L., Kaguni, L.S. 2002a. Purification strategies for *Drosophila* mtDNA replication proteins in native and recombinant form. DNA polymerase γ. Methods Mol. Biol. 197, 273-283.

Farr, C.L., Kaguni, L.S. 2002b. Purification strategies for *Drosophila* mtDNA replication proteins in native and recombinant form. Mitochondrial single-stranded DNA-binding protein. Methods Mol. Biol. 197, 285-294.

Farr, C.L., Matsushima, Y., Lagina III, A.T., Luo, N., Kaguni, L.S. 2004. Physiological and biochemical defects in functional interactions of mitochondrial DNA polymerase and DNA-binding mutants of single-stranded DNA-binding protein. J. Biol. Chem. 279, 17047-17053.

Farr, C.L., Wang, Y., Kaguni, L.S. 1999. Functional interactions of mitochondrial DNA polymerase and single-stranded DNA-binding protein: template-primer DNA binding and initiation and elongation of DNA strand synthesis. J. Biol. Chem 274, 14779-14785.

Fernández-Moreno, M.A., Farr, C.L., Kaguni, L.S., Garesse, R. 2006. *Drosophila melanogaster* as a model system to study mitochondrial function. Methods Mol. Biol. 372, 33-49.

Fernandez-Silva, P., Martinez-Azorin, F., Micol, V., Attardi, G. 1997. The human mitochondrial transcription termination factor (mTERF) is a multizipper protein but binds to DNA as a monomer, with evidence pointing to intramolecular leucine zipper interactions. EMBO J. 16, 1066-1079.

Fukui, H., Moraes, C.T. 2009. Mechanisms of formation and accumulation of mitochondrial DNA deletions in ageing neurons. Hum. Mol. Gen. 18, 1028-1036.

Garrido, N., Griparic, L., Jokitalo, E., Wartiovaara, J., van der Bliek, A.M., Spelbrink, J.N. 2003. Composition and dynamics of human mitochondrial nucleoids. Mol. Biol. Cell 14, 1583-1596.

Gaspari, M., Falkenberg, M., Larsson, N.G., Gustafsson, C.M. 2004. The mitochondrial RNA polymerase contributes critically to promoter specificity in mammalian cells. EMBO J. 23, 4606-4614.

Gilkerson, R.W., Schon, E.A. 2008. Nucleoid autonomy: an underlying mechanism of mitochondrial genetics with therapeutic potential. Commun. Integr. Biol. 1, 34–36.

Goddard, J.M., Wolstenholme, D.R. 1980. Origin and direction of replication in mitochondrial DNA molecules from genus *Drosophila*. Nucleic Acids Res. 8, 741-757.

Goffart, S., Cooper, H.M., Tyynismaa, H., Wanrooij, S., Suomalainen, A., Spelbrink, J.N. 2009. Twinkle mutations associated with autosomal dominant progressive external ophthalmoplegia lead to impaired helicase function and in vivo mtDNA replication stalling. Hum. Mol. Genet. 18, 328-340.

Goldberg, M.S., Fleming, S.M., Palacino, J.J., Cepeda, C., Lam, H.A., Bhatnagar, A., Meloni, E.G., Wu, N., Ackerson, L.C., Klapstein, G.J., Gajendiran, M., Roth, B.L., Chesselet, M.F., Maidment, N.T., Levine, M.S., Shen, J. 2003. Parkin-deficient mice exhibit nigrostriatal deficits but not loss of dopaminergic neurons. J. Biol. Chem. 278, 43628-43635.

Goto, A., Matsushima, Y., Kadowaki, T., Kitagawa, Y. 2001. *Drosophila* mitochondrial transcription factor A (*d*-TFAM) is dispensable for the transcription of mitochondrial DNA in Kc167 cells. Biochem. J. 354, 243-248.

Gray, M.W., Burger, G., Lang, B.F. 1999 Mitochondrial evolution. Science 283, 1476-1481.

Greene, J.C., Whitworth, A.J., Kuo, I., Andrews, L.A., Feany, M.B., Pallanck, L.J. 2003. Mitochondrial pathology and apoptotic muscle degeneration in Drosophila parkin mutants. Proc. Natl. Acad. Sci. USA 100, 4078-4083.

Hackenbrock, C.R. 1968. Chemical and physical fixation of isolated mitochondria in low-energy and high-energy states. Proc. Natl. Acad. Sci. U.S.A. 61, 598-605.

Hainaut, P., Wiman, K.G. 2009. 30 years and a long way into p53 research. Lancet Oncol. 10, 913-919.

Hamdam, S.M., Richardson C.C. 2009. Motors, switches, and contacts in the replisome. Annu. Rev. Biochem. 78, 205-243.

Harman, D. 1972. The biologic clock: the mitochondria? J. Am. Geriatr. Soc. 20, 145-147.

He, Z.G., Rezende, L.F., Willcox, S., Griffith, J.D., Richardson, C.C. 2003. The carboxyl-terminal domain of bacteriophage T7 single-stranded DNA-binding protein modulates DNA binding and interaction with T7 DNA polymerase. J. Biol. Chem. 278, 29538-29545.

He, Z.G., Richardson, C.C. 2004. Effect of single-stranded DNA-binding proteins on the helicase and primase activities of the bacteriophage T7 gene 4 protein. J. Biol. Chem. 279, 22190-22197.

Heyne, K., Mannebach, S., Wuertz, E., Knaup, K.X., Mahyar-Roemer, M., Roemer, K. 2004. Identification of a putative p53 binding sequence within the human mitochondrial genome. FEBS Lett. 578, 198-202.

Ho, R., Rachek, L.I., Xu, Y., Kelley, M.R., LeDoux, S.P., Wilson, G.L. 2007. Yeast apurinic/ apyrimidinic endonuclease Apn1 protects mammalian neuronal cell line from oxidative stress. J. Neurochem. 102, 13-24.

Hollensworth, B.S., Shen, C., Sim, J.E., Spitz, D.R., Wilson, G.L., LeDoux, S.P. 2000. Glial cell type-specific responses to menadione-induced oxidative stress. Free Radical Biol. Med. 28, 1161-1174.

Hollis, T., Stattel, J.M., Walther, D.S., Richardson, C.C., Ellenberger, T. 2001. Structure of the gene 2.5 protein, a single-stranded DNA binding protein encoded by bacteriophage T7. Proc. Natl. Acad. Sci. U.S.A. 98, 9557-9562.

Holmlund, T., Farge, G., Pande, V., Korhonen, J., Nilsson, L., Falkenberg, M. 2009. Structure-function defects of the Twinkle amino-terminal region in progressive external ophthalmoplegia. Biochim. Biophys. Acta 1792, 132-139.

Holt, I.J. 2009. Mitochondrial DNA replication and repair: all a flap. Trends Biochem. Sci. 34, 358-365.

Holt, I.J., Jacobs, H.T. 2003. Response: The mitochondrial DNA replication bubble has not burst. Trends Biochem. Sci. 28, 355-356.

Holt, I.J., Lorimer, H.E., Jacobs, H.T. 2000. Coupled leading- and lagging-strand synthesis of mammalian mitochondrial DNA. Cell 100, 515-524.

Hyland, E.M., Rezende, L.F., Richardson, C.C. 2003. The DNA binding domain of the gene 2.5 single-stranded DNA-binding protein of bacteriophage T7. J. Biol. Chem. 278, 7247-7256.

Hyvärinen, A.K., Pohjoismäki, J.L.O., Reyes, A., Wanrooij, S., Yasukawa, T., Karhunen, P.J., Spelbrink, J.N., Holt, I.J., Jacobs, H.T. 2007. The mitochondrial transcription terminator factor mTERF modulates replication pausing in human mitochondrial DNA. Nucleic Acids Res. 35, 6458-6474.

Insdorf, N.F., Bogenhagen, D.F. (1989). DNA polymerase gamma from *Xenopus laevis*. I. The identification of a high molecular weight catalytic subunit by a novel DNA polymerase photolabeling procedure. J. Biol. Chem. 264, 21491-21497.

Iyengar, B., Luo, N., Farr, C.L., Kaguni, L.S., Campos, A.R. 2002. The accessory subunit of DNA polymerase γ is essential for mitochondrial DNA maintenance and development in *Drosophila melanogaster*. Proc. Natl. Acad. Sci. USA 99, 4483-4488.

Iyengar, B., Roote, J., Campos, A.R. 1999. The *tamas* gene, identified as a mutation that disrupts larval behavior in *Drosophila melanogaster*, codes for the mitochondrial DNA polymerase catalytic subunit (DNApol-γ125). Genetics 153, 1809-1824.

Jaiswal, M., LaRusso, N. F., Nishioka, N., Nakabeppu, Y., Gores, G. J. (2001). Human Ogg1, a protein involved in the repair of 8-oxoguanine, in inhibited by nitric oxide. Cancer Res. 61, 6388-6393.

Jang, Y.C., Van Remmen, H. 2009. The mitochondrial theory of ageing: insights from transgenic and knockout mouse models. Exp. Gerontol. 44, 256-260.

Kaguni, L.S. 2004. DNA polymerase γ, the mitochondrial replicase. Annu. Rev. Biochem. 73, 293-320.

Kaguni, L.S., Olson, M.W. (1989). Mismatch-specific 3'----5' exonuclease associated with the mitochondrial DNA polymerase from *Drosophila* embryos. Proc. Natl. Acad. Sci. USA 86, 6469-6473.

Kajander, O.A., Karhunen, P.J., Holt, I.J., Jacobs, H.T. 2001. Prominent mitochondrial DNA recombination intermediates in human heart muscle. EMBO Rep. 2, 1007-1012.

Kanki, T., Nakayama, H., Sasaki, N., Takio, K., Alam, T.I., Hamasaki, N., Kang, D. 2004. Mitochondrial nucleoid and transcription factor A. Ann. NY Acad. Sci. 1011, 61-68.

Kaufman, B.A., Durisic, N., Mativetsky, J.M., Costantino, S., Hancock, M.A., Grutter, P., Shoubridge, E.A. 2007. The mitochondrial transcription factor TFAM coordinates the

assembly of multiple DNA molecules into nucleoid-like structures. Mol. Biol. Cell 18, 3225-3236.

Khrapko, K., Kraytsberg, Y., de Grey, A.D.N.J., Schon, E.A. 2006. Does premature aging of the mtDNA mutator mouse prove that mtDNA mutations are involved in natural aging? Aging Cell 5, 279-282.

Kim, Y.T., Richardson, C.C. 1993. Bacteriophage T7 gene 2.5 protein: an essential protein for DNA replication. Proc. Natl. Acad. Sci. U.S.A. 90, 10173-10177.

Kim, Y.T., Richardson, C.C. 1994. Acidic carboxyl-terminal domain of gene 2.5 protein of bacteriophage T7 is essential for protein-protein interactions. J. Biol. Chem. 269, 5270-5278.

Kim, Y.T., Tabor, S., Bortner, C., Griffith, J.D., Richardson, C.C. 1992. Purification and characterization of the bacteriophage T7 gene 2.5 protein. A single-stranded DNA-binding protein. J. Biol. Chem. 267, 15022-15031.

Korhonen, J.A., Gaspari, M., Falkenberg, M. 2003. TWINKLE has 5'→3' DNA helicase activity and is specifically stimulated by mitochondrial single-stranded DNA-binding protein. J. Biol. Chem. 278, 48627-48632.

Korhonen, J.A., Pham, X.H., Pellegrini, M., Falkenberg, M. 2004. Reconstitution of a minimal mtDNA replisome *in vitro*. EMBO J. 23, 2423-2429.

Korhonen, J.A., Pande, V., Holmlund, T., Farge, G., Pham, X.H., Nilsson, L., Falkenberg, M. 2008. Structure-function defects of the Twinkle linker region in progressive external ophthalmoplegia. J. Mol. Biol. 377, 691-705.

Kornberg, A., Baker, T.A. 1992. DNA replication. New York: Freeman. xiv, 931 s. p.

Kozakov, D., Hall, D.R., Beglov, D., Brenke, R., Comeau, S.R., Shen, Y., Li, K., Zheng, J., Vakili, P., Paschalidis, I.C., Vajda, S. 2010. Achieving reliability and high accuracy in automated protein docking: ClusPro, PIPER, SDU, and stability analysis in CAPRI rounds 13-19. Proteins 78, 3124-3130.

Kozlov, A.G., Cox, M.M., Lohman, T.M. 2010. Regulation of single-stranded DNA binding by the C termini of *Escherichia coli* single-stranded DNA-binding (SSB) protein. J. Biol. Chem. 285, 17246-17252.

Krassa, K.B., Green, L.S., Gold, L. 1991. Protein-protein interactions with the acidic COOH terminus of the single-stranded DNA-binding protein of the bacteriophage T4. Proc. Natl. Acad. Sci. U.S.A. 88, 4010-4014.

Kraytsberg, Y., Simon, D.K., Turnbull, D.M., Khrapko, K. 2009. Do mtDNA deletions drive premature aging in mtDNA mutator mice? Aging Cell 8, 502-506.

Krishnan, K.J., Reeve, A.K., Samuels, D.C., Chinnery, P.F., Blckwood, J.K., Taylor, R.W., Wanrooij, S., Spelbrink, J.N., Lightowlers, R.N., Turnbull, D.M. 2008. What causes mitochondrial DNA deletions in human cells? Nat. Genet. 40, 275-279.

Kujoth, G.C., Hiona, A., Pugh, T.D., Someya, S., Panzer, K., Wohlgemuth, S.E., Hofer, T., Seo, A.Y., Sullivan, R., Jobling, W.A., Morrow, J.D., Van Remmen, H., Sedivy, J.M., Yamasoba, T., Tanokura, M., Weindruch, R., Leeuwenburgh, C., Prolla, T.A. 2005. Mitochondrial DNA mutations, oxidative stress, and apoptosis in mammalian ageing. Science 309, 481-484.

Kunkel, T.A., Soni, A. (1988). Exonucleolytic proofreading enhances the fidelity of DNA synthesis by chick embryo DNA polymerase-gamma. J. Biol. Chem. 263, 4450-4459.

Lakshmipathy, U., Campbell, C. 1999. The human DNA ligase III gene encodes nuclear and mitochondrial proteins. Mol. Cell. Biol. 19, 3869-3876.

Lakshmipathy, U., Campbell, C. 2001. Antisense-mediated decrease in DNA ligase III expression results in reduced mitochondrial DNA integrity. Nucleic Acids Res. 29, 668-676.

Langston, L.D., Indiani, C., O'Donnell, M. 2009. Whither the replisome: emerging perspectives on the dynamic nature of the DNA replication machinery. Cell Cycle 8, 2686-2691.

Larsson, N.G., Wang, J., Wilhelmsson, H., Oldfors, A., Rustin, P., Lewandoski, M., Barsh, G.S., Clayton, D.A. 1998. Mitochondrial transcription factor A is necessary for mtDNA maintenance and embryogenesis in mice. Nat. Genet. 18, 231-236.

Lebedeva, M.A., Eaton, J.S., Shadel, G.S. 2009. Loss of p53 causes mitochondrial DNA depletion and altered mitochondrial reactive oxygen species homeostasis. Biochim. Biophys. Acta 1787, 328-334.

LeDoux, S.P., Shen, C., Grishko, V.I., Fields, P.A., Gard, A.L., Wilson, G.L. 1998. Glial cell-specific differences in response to alkylation damage. Glia 24, 304-312.

Lee, S.J., Marintcheva, B., Hamdan, S.M., Richardson, C.C. 2006. The C-terminal residues of bacteriophage T7 gene 4 helicase-primase coordinate helicase and DNA polymerase activities. J. Biol. Chem. 281, 25841-25849.

Lee, Y.S., Kennedy, W.D., Yin, Y.W. 2009. Structural insight into processive human mitochondrial DNA synthesis and disease-related polymerase mutations. Cell 139, 312-324.

Lee, Y.S., Lee, S., Demeler, B., Molineux, I.J., Johnson, K.A., *et al.* 2010. Each monomer of the dimeric accessory protein for human mitochondrial DNA polymerase has a distinct role in conferring processivity. J. Biol. Chem. 285, 1490-1499.

Lefai, E., Calleja, M., Ruiz de Mena, I., Lagina III, A.T., Kaguni, L.S., Garesse, R. 2000. Overexpression of the catalytic subunit of DNA polymerase γ results in depletion of mitochondrial DNA in *Drosophila melanogaster*. Mol. Gen. Genet. 264, 37-46.

Li, K., Williams, R.S. 1997. Tetramerization and single-stranded DNA binding properties of the native and mutated forms of murine mitochondrial single-stranded DNA-binding proteins. J. Biol. Chem. 272, 8686-8694.

Lim, S.E., Longley, M.J., Copeland, W.C. 1999. The mitochondrial p55 accessory subunit of human DNA polymerase gamma enhances DNA binding, promotes processive DNA synthesis, and confers N-ethylmaleimide resistance. J. Biol. Chem. 274, 38197-38203.

Linder, T., Park, C.B., Asin-Cayuela, J., Pellegrini, M., Larsson, N.G., Falkenberg, M., Samuelsson, T., Gustafsson, C.M. 2005. A family of putative transcription termination factors shared amongst metazoans and plants. Curr. Genet. 48, 265-269.

Liu, Y., Kao, H.I., Bambara, R.A. 2004. Flap endonuclease 1: a central component of DNA metabolism. Annu. Rev. Biochem. 73, 589-615.

Liu, P., Qian, L., Sung, J.S., de Souza-Pinto, N.C., Zheng, L., Bogenhagen, D.F., Bohr, V.A., Wilson, D.M., Shen, B., Demple, B. 2008. Removal of oxidative DNA damage via FEN1-dependent long-patch base excision repair in human cell mitochondria. Mol. Cell. Biol. 28, 4975-4987.

Lohman, T.M., Ferrari, M.E. 1994. *Escherichia coli* single-stranded DNA-binding protein: multiple DNA-binding modes and cooperativities. Annu. Rev. Biochem. 63, 527-570.

Longley, M.J., Graziewicz, M.A., Bienstock, R.J., Copeland, W.C. 2005. Consequences of mutations in human DNA polymerase γ. Gene 354, 125-131.

Longley, M.J., Prasad, R., Srivastava, D.K., Wilson, S.H., Copeland, W.C. 1998. Identification of 5'-deoxyribose phosphate lyase activity in human DNA polymerase γ and its role in mitochondrial base excision repair. Proc. Natl. Acad. Sci. USA 95, 12244-12248.

Luo, N., Kaguni, L.S. 2005. Mutations in the spacer region of *Drosophila* mitochondrial DNA polymerase affect DNA binding, processivity, and the balance between Pol and Exo function. J. Biol. Chem. 280, 2491-2497.

Luoma, P.T., Luo, N., Löscher, W.N., Farr, C.L., Horvath, R., Wanschitz, J., Kiechl, S., Kaguni, L.S., Suomalainen, A. 2005. Functional defects due to spacer-region mutations of human mitochondrial DNA polymerase in a family with an ataxia-myopathy syndrome. Hum. Mol. Genet. 14, 1907-1920.

Ma, W., Sung, H.J., Park, J.Y., Matoba, S., Hwang, P.M. 2007. A pivotal role for p53: balancing aerobic respiration and glycolysis. J. Bioenerg. Biomembr. 39, 243-246.

Maier, D., Farr, C.L., Poeck, B., Alahari, A., Vogel, M., Fischer, S., Kaguni, L.S., Schneuwly, S. 2001. Mitochondrial single-stranded DNA-binding protein is required for mitochondrial DNA replication and development in *Drosophila melanogaster*. Mol. Biol. Cell 12, 821-830.

Marintcheva, B., Marintchev, A., Wagner, G., Richardson, C.C. 2008. Acidic C-terminal tail of the ssDNA-binding protein of bacteriophage T7 and ssDNA compete for the same binding surface. Proc. Natl. Acad. Sci. U.S.A. 105, 1855-1860.

Martin, M., Cho, J., Cesare, A.J., Griffith, J.D., Attardi, G. 2005. Termination factor-mediated DNA loop between termination and initiation sites drives mitochondrial rRNA synthesis. Cell 123, 1227-1240.

Martínez-Azorín, F., Calleja, M., Hernández-Sierra, R., Farr, C.L., Kaguni, L.S., Garesse, R., 2008. Over-expression of the catalytic core of mitochondrial DNA (mtDNA) polymerase in the nervous system of *Drosophila melanogaster* reduces median life span by inducing mtDNA depletion. J. Neurochem. 105, 165-176.

Matsushima, Y., Adán, C., Garesse, R., Kaguni, L.S. 2005. *Drosophila* mitochondrial transcription factor B1 modulates mitochondrial translation but not transcription or DNA copy number in Schneider cells. J. Biol. Chem. 280, 16815-16820.

Matsushima, Y., Farr, C.L., Fan, L., Kaguni, L.S. 2008. Physiological and biochemical defects in carboxyl-terminal mutants of mitochondrial DNA helicase. J. Biol. Chem. 283, 23964-23971.

Matsushima, Y., Garesse, R., Kaguni, L.S. 2004. *Drosophila* mitochondrial transcription factor B2 regulates mitochondrial DNA copy number and transcription in Schneider cells. 279, 26900-26905.

Matsushima, Y., Kaguni, L.S. 2007. Differential phenotypes of active site and human autosomal dominant progressive external ophthalmoplegia mutations in *Drosophila* mitochondrial DNA helicase expressed in Schneider cells. J. Biol. Chem. 282, 9436-9444.

Matsushima, Y., Kaguni, L.S. 2009. Functional importance of the conserved N-terminal domain of the mitochondrial replicative DNA helicase. Biochim. Biophys. Acta. 1787, 290-295.

Matsushima, Y., Matsumura, K., Ishii, S., Inagaki, H., Suzuki, T., Matsuda, Y., Beck, K., Kitagawa, Y. 2003. Functional domains of chicken mitochondrial transcription factor A for the maintenance of mitochondrial DNA copy number in lymphoma cell line DT40. J. Biol. Chem. 278, 31149-31158.

Metodiev, M.D., Lesko, N., Park, C.B., Cámara, Y., Shi, Y., Wibom, R., Hultenby, K., Gustafsson, C.M., Larsson, N.G. 2009. Methylation of 12S rRNA is necessary for in vivo stability of the small subunit of the mammalian mitochondrial ribosome. Cell Metab. 9, 386-397.

McCulloch, V., Seidel-Rogol, B.L., Shadel, G.S. 2002. A human mitochondrial transcription factor is related to RNA adenine methyltransferases and bind S-adenosylmethionine. Mol. Cell. Biol. 22, 1116-1125.

Miller, K.E., Sheetz, M.P. 2004. Axonal mitochondrial transport and potential are correlated. J. Cell Sci. 117, 2791-2804.

Modica-Napolitano, J. Singh, K.K. 2004. Mitochondrial dysfunction in cancer. Mitochondrion 4, 755-762.

Mootha, V.K., Bunkenborg, J., Olsen, J.V., Hjerrild, M., Wisniewski, J.R., Stahl, E., Bolouri, M.S., Ray, H.N., Sihag, S., Kamal, M., Patterson, N., Lander, E.S., Mann, M. 2003. Integrated analysis of protein composition, tissue diversity, and gene regulation in mouse mitochondria. Cell 115, 629-640.

Morel, F., Renoux, M., Lachaume, P., Alziari, S. 2008. Bleomycin-induced double-strand breaks in mitochondrial DNA of *Drosophila* cells are repaired. Mutat. Res. 637, 111-117.

Nakai, H., Richardson, C.C. 1988. The effect of the T7 and *Escherichia coli* DNA-binding proteins at the replication fork of bacteriophage T7. J. Biol. Chem. 263, 9831-9839.

Nguyen, K.V., Sharief, F.S., Chan, S.S., Copeland, W.C., Naviaux, R.X. 2006. Molecular diagnosis of Alpers syndrome. J. Hepatol. 45, 108-116.

Nishioka, K., Ohtsubo, T., Oda, H., Fujiwara, T., Kang, D., Sugimachi, K., Nakabeppu, Y. 1999. Expression and differential intracellular localization of two major forms of human 8-oxoguanine DNA glycosylase encoded by alternatively spliced OGG1 mRNAs. Mol. Biol. Cell 10, 1637-1652.

Notarnicola, S.M., Mulcahy, H.L., Lee, J., Richardson, C.C. 1997. The acidic carboxyl terminus of the bacteriophage T7 gene 4 helicase/primase interacts with T7 DNA polymerase. J. Biol. Chem. 272, 18425-18433.

Oliveira, M.T., Kaguni, L.S. 2009. Comparative purification strategies for *Drosophila* and human mitochondrial DNA replication proteins: DNA polymerase gamma and mitochondrial single-stranded DNA-binding protein. Methods Mol. Biol. 554, 37-58.

Oliveira, M.T., Kaguni, L.S. 2010. Functional roles of the N- and C-terminal regions of the human mitochondrial single-stranded DNA-binding protein. PLoS ONE 5, e15379.

Palacino, J.J., Sagi, D., Goldberg, M.S., Krauss, S., Motz, C., Wacker, M., Klose, J., Shen, J. 2004. Mitochondrial dysfunction and oxidative damage in parkin-deficient mice. J. Biol. Chem. 279, 18614-18622.

Park, C.B., Asin-Cayuela, J., Cámara, Y., Shi, Y., Pellegrini, M., Gaspari, M., Wibom, R., Hultenby, K., Erdjument-Bromage, H., Tempst, P., Falkenberg, M., Gustafsson, C.M., Larsson, N.G. 2007. MTERF3 is a negative regulator of mammalian mtDNA transcription. Cell 130, 273-285.

Park, J., Kim, Y., Chung, J. 2009. Mitochondrial dysfunction and Parkinson's disease genes: insights from Drosophila. Dis. Model Mech. 2, 336-340.

Pesah, Y., Pham, T., Burgess, H., Middlebrooks, B., Verstreken, P., Zhou, Y., Harding, M., Bellen, H., Mardon, G. 2004. Drosophila parkin mutants have decreased mass and cell size and increased sensitivity to oxygen radical stress. Development 131, 2183-2194.

Pohjoismäki, J.L.O., Goffart, S., Tyynismaa, H., Willcox, S., Ide, T., Kang, D., Suomalainen, A., Karhunen, P.J., Griffith, J.D., Holt, I.J., Jacobs, H.T. 2009. Human heart mitochondrial DNA is organized in complex catenated networks containing abundant four-way junctions and replication forks. J. Biol. Chem. 284, 21446-21457.

Pohjoismäki, J.L.O., Wanrooij, S., Hyvärinen, A.K., Goffart, S., Holt, I.J., Spelbrink, J.N., Jacobs, H.T. 2006. Alterations to the expression level of mitochondrial transcription factor A, TFAM, modify the mode of mitochondrial DNA replication in cultured human cells. Nucleic Acids Res. 34, 5815-5828.

Polosa, P.L., Deceglie, S., Roberti, M., Gadaleta, M.N., Cantatore, P. 2005. Contra-helicase activity of the mitochondrial transcription factor terminator mtDBP. Nuclei Acids Res. 33, 3812-3820.

Pridgeon, J.W., Olzmann, J.A., Chin, L.S., Li, L. 2007. PINK1 protects against oxidative stress by phosphorylating mitochondrial chaperone TRAP1. PLoS Biol. 5, e172.

Rachek, L.I., Grishko, V.I., Musiyenko, S.I., Kelley, M.R., LeDoux, S.P., Wilson, G.L. 2002. Conditional targeting of the DNA repair enzyme hOGG1 into mitochondria. J. Biol. Chem. 277, 44932-44937.

Radyuk, S.N., Michalak, K., Rebrin, I., Sohal, R.S., Orr, W.C. 2006. Effects of ectopic expression of *Drosophila* DNA glycosylases dOgg1 and RpS3 in mitochondria. Free Radical Biol. Med. 41, 757-764.

Raghunathan, S., Ricard, C.S., Lohman, T.M., Waksman, G. 1997. Crystal structure of the homo-tetrameric DNA binding domain of *Escherichia coli* single-stranded DNA-binding protein determined by multiwavelength x-ray diffraction on the selenomethionyl protein at 2.9-A resolution. Proc. Natl. Acad. Sci. U.S.A. 94, 6652-6657.

Raghunathan, S., Kozlov, A.G., Lohman, T.M., Waksman, G. 2000. Structure of the DNA binding domain of *E. coli* SSB bound to ssDNA. Nat. Struct. Biol. 7, 648-652.

Reyes, A., Yang, M.Y., Bowmaker, M., Holt, I.L. 2005. Bidirectional replication initiates at sites throughout the mitochondrial genome of birds. J. Biol. Chem. 280, 3242-3250.

Roberti, M., Bruni, F., Polosa, P.L., Manzari, C., Gadaleta, M.N., Cantatore, P. 2006. MTERF3, the most conserved member of the mTERF-family, is a modular factor involved in mitochondrial protein synthesis. Biochem. Biophys. Acta 1757, 1199-1206.

Roberti, M., Fernandez-Silva, P., Polosa, L.P., Fernandez-Vizarra, E., Bruni, F., Deceglie, S., Montoya, J., Gadaleta, M.N., Cantatore, P. 2005. In vitro transcription termination activity of the *Drosophila* mitochondrial DNA-binding protein DmTTF. Biochem. Biophys. Res. Commun. 331, 357-362.

Roberti, M., Polosa, P.L., Bruni, F., Manzari, C., Deceglie, S., Gadaleta, M.N., Cantatore, P. 2009. The MTERF family proteins: mitochondrial transcription regulators and beyond. Biochim. Biophys. Acta 1787, 303-311.

Rothfuss, O., Fisher, H., Hasegawa, T., Maisel, M., Leitner, P., Miesel, F., Sharma, M., Bornemann, A., Berg, D., Gasser, T., Patenge, N. 2009. Parkin protects mitochondrial genome integrity and supports mitochondrial DNA repair. Hum. Mol. Genet., Epub ahead of print, ddp327v1-ddp327.

Ruhanen, H., Borrie, S., Szabadkai, G., Tyynismaa, H., Jones, A.W., *et al.* 2010. Mitochondrial single-stranded DNA binding protein is required for maintenance of mitochondrial DNA and 7S DNA but is not required for mitochondrial nucleoid organisation. Biochim. Biophys. Acta 1803, 931-939.

Sali, A., Potterton, L., Yuan, F., van Vlijmen, H., Karplus, M. 1995. Evaluation of comparative protein modeling by MODELLER. Proteins 23, 318-326.

Shamoo, Y., Friedman, A.M., Parsons, M.R., Konigsberg, W.H., Steitz, T.A. 1995. Crystal structure of a replication fork single-stranded DNA binding protein (T4 gp32) complexed to DNA. Nature 376, 362-366.

Shapovalov, Y., Hoffman, D., Zuch, D., de Mesy Bentley, K.L., Eliseev, R.A. 2011. Mitochondrial dysfunction in cancer cells due to aberrant mitochondrial replication. J. Biol. Chem. 286, 22331-22338.

Shereda, R.D., Kozlov, A.G., Lohman, T.M., Cox, M.M., Keck, J.L. 2008. SSB as an organizer/mobilizer of genome maintenance complexes. Crit. Rev. Biochem. Mol. Biol. 43, 289-318.

Shereda, R.D., Reiter, N.J., Butcher, S.E., Keck, J.L. 2009. Identification of the SSB binding site on *E. coli* RecQ reveals a conserved surface for binding SSB's C terminus. J. Mol. Biol. 386, 612-625.

Shoubridge, E.A., Wai, T. 2007. Mitochondrial DNA and the mammalian oocyte. Curr. Top. Dev. Biol. 77, 87-111.

Shutt, T.E., Gray, M.W. 2006. Bacteriophage origins of mitochondrial replication and transcription proteins. Trends Genet. 22, 90-95.

Silva, J.P., Kohler, M., Graff, C., Oldfors, A., Magnuson, M.A., Berggren, P.O., Larsson, N.G. 2000. Impaired insulin secretion and β-cell loss in tissue-specific knockout mice with mitochondrial diabetes. Nat. Genet. 26, 336-340.

Slupphaug, G., Markussen, F.H., Olsen, L.C., Aasland, R., Aarsaether, N., Bakke, O., Krokan, H.E., Helland, D.E. 1993. Nuclear and mitochondrial forms of human uracil-DNA glycosylase are encoded by the same gene. Nucleic Acids Res. 21, 2579-2584.

Spelbrink, J.N., Li, F.Y., Tiranti, V., Nikali, K., Yuan, Q.P., Tariq, M., Wanrooij, S., Garrido, N., Comi, G., Morandi, L., Santoro, L., Toscano, A., Fabrizi, G.M., Somer, H., Croxen, R., Beeson, D., Poulton, J., Suomalainen, A., Jacobs, H.T., Zeviani, M., Larsson, C. 2001. Human mitochondrial DNA deletions associated with mutations in the gene encoding Twinkle, a phage T7 gene 4-like protein localized in mitochondria. Nat. Genet. 28, 223-231.

Srere, P.A. 1980. The infrastructure of the mitochondrial matrix. Trends Biochem. Sci. 5, 120-121.

Srivastava, S., Moraes, C.T. 2005. Double-strand breaks of mouse muscle mtDNA promote large deletions similar to multiple mtDNA deletions in humans. Hum. Mol. Genet. 14, 893-902.

Stumpf, J.D., Copeland, W.C. 2011. Mitocondrial DNA replication and disease: insights from DNA polymerase γ mutations. Cell. Mol. Life Sci. 68, 219-233.

Takamatsu, C., Umeda, S., Ohsato, T., Ohno, T., Abe, Y., Fukuoh, A., Shinagawa, H., Hamasaki, N., Kang, D. 2002. Regulation of mitochondrial D-loops by transcription factor A and single-stranded DNA-binding protein. EMBO Rep. 3, 451-456.

Tang, Y., Manfredi, G., Hirano, M., Schon, E.A. 2000. Maintenance of human rearranged mitochondrial DNAs in long-term cultured transmitochondrial cell lines. Mol. Biol. Cell. 11, 2349-2358.

Thömmes, P., Farr, C.L., Marton, R.F., Kaguni, L.S., Cotterill, S. 1995. Mitochondrial single-stranded DNA-binding protein from *Drosophila* embryos. Physical and biochemical characterization. J. Biol. Chem. 270, 21137-21143.

Thompson, J.D., Gibson, T.J., Plewniak, F., Jeanmougin, F., Higgins, D.G. 1997. The CLUSTAL_X windows interface: flexible strategies for multiple sequence alignment aided by quality analysis tools. Nucleic Acids Res. 25, 4876-4882.

Thompson, L.V. 2006. Oxidative stress, mitochondria and mtDNA-mutator mice. Exp. Gerontol. 41, 1220–1222.

Thyagarajan, B., Padua, R.A., Campbell, C. 1996. Mammalian mitochondria possess homologous DNA recombination activity. J. Biol. Chem. 271, 27536-27543.

Tomaska, L., Nosek, J., Kucejova, B. 2001. Mitochondrial single-stranded DNA-binding proteins: in search for new functions. Biol. Chem. 382, 179-186.

Tomkinson, A.E., Bonk, R.T., Linn, S. 1988. Mitochondrial endonuclease activities specific for apurinic/ apyrimidinic sites in DNA from mouse cells. J. Biol. Chem. 263, 12532-12537.

Trifunovic, A., Wredenberg, A., Falkenberg, M., Spelbrink, J.N., Rovio, A.T., Bruder, C.E., Bohlooly-Y, M., Gidlöf, S., Oldfors, A., Wibom, R., Törnell, J., Jacobs, H.T., Larsson, N.G. 2004. Premature ageing in mice expressing defective mitochondrial DNA polymerase. Nature 429, 417-423.

Tyynismaa, H., Mjosund, K.P., Wanrooij, S., Lappalainen, I., Ylikallio, E., Jalanko, A., Spelbrink, J.N., Paetau, A., Suomalainen, A. 2005. Mutant mitochondrial helicase Twinkle causes multiple mtDNA deletions and a late-onset mitochondrial disease in mice. Proc. Natl. Acad. Sci. USA 102, 17687-17692.

Van Dyck, E., Foury, F., Stillman, B., Brill, S.J. 1992. A single-stranded DNA binding protein required for mitochondrial DNA replication in *S. cerevisiae* is homologous to *E. coli* SSB. EMBO J. 11, 3421-3430.

Vermulst, M., Bielas, J.H., Kujoth, G.C., Ladiges, W.C., Rabinovitch, P.S., Prolla, T.A., Loeb, L.A. 2007. Mitochondrial point mutations do not limit the natural lifespan of mice. Nat. Genet. 39, 540-543.

Vermulst, M., Wanagat, J., Kujoth, G.C., Bielas, J.H., Rabinovitch, P.S., Prolla, T.A., Loeb, L.A. 2008. DNA deletions and clonal mutations drive premature ageing in mitochondrial mutator mice. Nat. Genet. 40, 392-394.

Vousden, K.H., Ryan, K.M. 2009. p53 and metabolism. Nat. Rev. Cancer doi:10.1038/nrc2715.

Wallace, D.C. 2005. A mitochondrial paradigm of metabolic and degenerative diseases, ageing, and cancer: a dawn for evolutionary medicine. Annu. Rev. Gen. 39, 359-407.

Wallace, D.C. 2008. Mitochondria as chi. Genetics 179, 727-735.

Wallace, D.C., Fan, W.W. 2009. The pathophysiology of mitochondrial disease as modeled in the mouse. Genes Dev. 23, 1714-1736.

Wallace, D.C., Fan, W. 2010. Energetics, epigenetics, mitochondrial genetics. Mitochondrion 10: 12-31.

Wang, Y., Bogenhagen, D.F. 2006. Human mitochondrial DNA nucleoids are linked to protein folding machinery and metabolic enzymes at the mitochondrial inner membrane. J. Biol. Chem. 281, 25791-25802.

Wang, Y., Kaguni, L.S. 1999. Baculovirus expression reconstitutes *Drosophila* mitochondrial DNA polymerase. J. Biol. Chem. 274, 28972-28977.

Wanrooij, S., Goffart, S., Pohjoismäki, J.L., Yasukawa, T., Spelbrink, J.N. 2007. Expression of catalytic mutants of the mtDNA helicase Twinkle and polymerase POLG causes distinct replication stalling phenotypes. Nucleic Acids Res. 35, 3238-3251.

Wenz, T., Luca, C., Torraco, A., Moraes, C.T. 2009. mTERF2 regulates oxidative phosphorylation by modulating mtDNA transcription. Cell Metab. 9, 499-511.

Wernette, C.M., Kaguni, L.S. 1986. A mitochondrial DNA polymerase from embryos of *Drosophila melanogaster*. Purification, subunit structure, and partial characterization. J. Biol. Chem. 261, 14764-14770.

Williams, A.J., Wernette, C.M., Kaguni, L.S. 1993. Processivity of mitochondrial DNA polymerase from *Drosophila* embryos. Effects of reaction conditions and enzyme purity. J. Biol. Chem. 268, 24855-24862.

Williams, A.J., Kaguni, L.S. 1995. Stimulation of *Drosophila* mitochondrial DNA polymerase by single-stranded DNA-binding protein. J. Biol. Chem. 270, 860-865.

Wold, M.S. 1997. Replication protein A: a heterotrimeric, single-stranded DNA-binding protein required for eukaryotic DNA metabolism. Annu. Rev. Biochem. 66, 61-92.

Wong, T.S., Rajagopalan, S., Freund, S.M., Rutherford, T.J., Andreeva, A., Townsley, F.M., Petrovich, M., Loakes, D., Fersht, A.R. 2009a. Biophysical characterizations of human mitochondrial transcription factor A and its binding to tumor suppressor p53. Nucleic Acids Res. doi:10.1093/nar/gkp750.

Wong, T.S., Rajagopalan, S., Townsley, F.M., Freund, S.M., Petrovich, M., Loakes, D., Fersht, A.R. 2009b. Physical and functional interactions between human mitochondrial single-stranded DNA-binding protein and tumor suppressor p53. Nucleic Acids Res. 37, 568-581.

Wredenberg, A., Wibom, R., Wilhelmsson, H., Graff, C., Wiener, H.H., Burden, S.J., Oldfors, A., Westerblad, H., Larsson, N.G. 2002. Increased mitochondrial mass in mitochondrial myopathy mice. Proc. Natl. Acad. Sci. 99, 15066-15071.

Yakubovskaya, E., Chen, Z., Carrodeguas, J.A., Kisker, C., Bogenhagen, D.F. 2006. Functional human mitochondrial DNA polymerase gamma forms a heterotrimer. J. Biol. Chem. 281, 374-382.

Yamanaka, H., Gatanaga, H., Kosalaraksa, P., Matsuoka-Aizawa, S., Takahashi, T., Kimura, S., Oka, S. 2007. Novel mutation of human DNA polymerase γ associated with mitochondrial toxicity induced by anti-HIV treatment. J. Infect. Dis. 195, 1419-1425.

Yang, C., Curth, U., Urbanke, C., Kang, C. 1997. Crystal structure of human mitochondrial single-stranded DNA binding protein at 2.4 A resolution. Nat. Struct. Biol. 4, 153-157.

Yang, M.Y., Bowmaker, M., Reyes, A., Vergani, L., Angeli, P., Gringeri, E., Jacobs, H.T., Holt, I.J. 2002. Biased incorporation of ribonucleotides on the mitochondrial L-strand accounts for apparent strand-asymmetric DNA replication. Cell 111, 495-505.

Yasukawa, T., Reyes, A., Cluett, T.J., Yang, M.Y., Bowmaker, M., Jacobs, H.T., Holt, I.J. 2006. Replication of vertebrate mitochondrial DNA entails transient ribonucleotide incorporation throughout the lagging strand. EMBO J. 25, 5358-5371.

Yoshida, Y., Izumi, H., Torigoe, T., Ishiguchi, H., Itoh, H., Kang, D., Kohno, K. 2003. p53 physically interacts with mitochondrial transcription factor A and differentially regulates binding to damaged DNA. Cancer Res. 63, 3729-3734.

Zhen, L., Zhou, M., Guo, Z., Lu, H., Qian, L., Dai, H., Qiu, J., Yakubovskaya, E., Bogenhagen, D.F., Demple, B., Shen, B. 2008. Human DNA2 is a mitochondrial nuclease/ helicase for efficient processing of DNA replication and repair intermediates. Mol. Cell 32, 325-336.

Ziebarth, T.D., Farr, C.L., Kaguni, L.S. 2007. Modular architecture of the hexameric human mitochondrial DNA helicase. J. Mol. Biol. 367, 1382-1391.

Ziegelin, G., Niedenzu, T., Lurz, R., Saenger, W., Lanka, E. 2003. Hexameric RSF1010 helicase RepA: the structural and functional importance of single amino acid residues. Nucleic Acids Res. 31, 5917-5929.

Zsurka, G., Kraytsberg, Y., Kudina, T., Kornblum, C., Elger, C.E., Khrapko, K., Kunz, W.S. 2005. Recombination of mitochondrial DNA in skeletal muscle of individuals with multiple mitochondrial DNA heteroplasmy. Nat. Genet. 37, 873-877.

Zsurka, G., Baron, M., Stewart, J.D., Kornblum, C., Bös, M., Sassen, R., Taylor, R.W., Elger, C.E., Chinnery, P.F., Kunz, W.S. 2008. Clonally expanded mitochondrial DNA mutations in epileptic individuals with mutated DNA polymerase γ. J. Neuropathol. Exp. Neurol. 67, 857-866.